REAL-TIME SIGNAL ENHANCEMENT OF THE FETAL ELECTROCARDIOGRAM USING DIGITAL TECHNIQUES

A THESIS

Presented to

The Faculty of the Graduate Division

by

Vernon Thomas Rhyne

In Partial Fulfillment

of the Requirements for the Degree

Doctor of Philosophy

in the School of Electrical Engineering

Georgia Institute of Technology

October, 1967

In presenting the dissertation as a partial fulfillment of the requirements for an advanced degree from the Georgia Institute of Technology, I agree that the Library of the Institute shall make it available for inspection and circulation in accordance with its regulations governing materials of this type. I agree that permission to copy from, or to publish from, this dissertation may be granted by the professor under whose direction it was written, or, in his absence, by the Dean of the Graduate Division when such copying or publication is solely for scholarly purposes and does not involve potential financial gain. It is understood that any copying from, or publication of, this dissertation which involves potential financial gain will not be allowed without written permission.

3/17/65
b

REAL-TIME SIGNAL ENHANCEMENT OF THE FETAL

ELECTROCARDIOGRAM USING DIGITAL TECHNIQUES

Approved:

[redacted]

Date approved by Chairman: 10-10-67

ACKNOWLEDGMENTS

While I cannot, in this brief space, give thanks to all of the people who have aided me in these efforts, I would like to acknowledge the special assistance of a representative few. First, I want to thank my advisor, Dr. John B. Peatman, for his help in selecting a problem and his guidance during the course of this research. Second, I want to thank Dr. Aubrey Bush for his assistance in the writing of the thesis, particularly Chapter V, and Dr. F. K. Hurd for his advice concerning the organization of the thesis. Thanks are also due to Dr. Nanette Wenger, Director of Cardiac Clinics at Grady Hospital, for her cooperation, and to Dr. A. G. Hansen, Dr. W. L. Bloom, and Dr. S. L. Dickerson for serving as members of the reading committee for my final oral examination.

The recorded data that was used to evaluate the signal enhancement system was provided by Dr. Edward Hon of the Yale School of Medicine. I would also like to thank Mr. Fred Dixon of the Engineering Experiment Station for the loan of vital tape recording equipment. The hardware used in building the prototype system was purchased with funds from the National Science Foundation's Research Initiation Grant Number GK263, "Time-Oriented Digital Systems Design."

I would also like to thank Mr. Dick Cole, Mr. M. H. Eskew, and the NASA-Langley Research Center for providing educational leave to support my first year of graduate study, and Dr. B. J. Dasher for providing an NDEA fellowship during my second. Finally, I would like to thank my wife, Glenda, for her support, particularly in typing the thesis.

TABLE OF CONTENTS

TABLE OF CONTENTS CONTINUED

LIST OF TABLES

LIST OF ILLUSTRATIONS

LIST OF ILLUSTRATIONS CONTINUED

LIST OF ILLUSTRATIONS CONTINUED

SUMMARY

One of the most fertile areas of biomedical research is prenatal physiology. Scientists and medical researchers have tried to develop techniques and devices with which medical diagnoses can be made even before an individual's birth. Their research has included chemical tests, x-ray technology, sonar-like sounding of the uterus, and other equally varied schemes for checking the health of the developing fetus. Within this climate it is logical that attention should be focused on the embryonic heart, since the electrical signals associated with the beating of this fetal organ propagate through the uterus to the skin of the maternal abdomen.

Each beat of the heart produces an electrical waveform, commonly referred to as a complex, that propagates from the heart muscle through the surrounding tissue. The central peak of this complex, designated as the R-peak, dominates the waveform, while the P and T waves which flank it are much smaller. Diagnosis of heart condition requires that all of these portions of the complex be observable, so that their shape and relative timing may be interpreted.

For over fifty years, medical researchers have been able to detect the fetal electrocardiogram by placing a pair of electrodes upon the maternal abdomen. Diagnosis of the condition of the developing fetal heart could not be made, however, since the noise picked up by the recording system and the mother's own electrocardiogram combined to obscure the low-voltage portions of the fetal complex. Thus, some method of signal

enhancement had to be developed in order to present a clearer picture of the fetal complex to the diagnostician.

Many different techniques for obtaining the desired improvement in signal-to-noise ratio have been tried. Only recently, through the use of coherent averaging, has enhancement sufficient for observation of the low-voltage portions of the abdominally recorded fetal complex been obtained. This technique consists of the additive combination of repeated fetal complexes in such a way that the true signal reinforces itself while the random noise cancels out. The current coherent averaging systems have several shortcomings, and the research reported here has been an effort to develop a new signal enhancement device that will overcome these.

The chief disadvantage of the current signal enhancement systems is the manner in which they calculate the averaged waveform. All of the systems have used a commercially available device that can only compute an equally weighted average over a predetermined number of complexes. The average must then be reset and accumulated again. This type of averaging has two disadvantages. First, the weighting scheme gives equal weight to the oldest complexes and the most recent ones, and thereby "waters-down" short-term changes in the fetal complex. Second, the requirement for periodic resetting of the average gives the user only a sequence of "snapshots" of the average fetal complex, rather than a continuous picture of its variations.

The research reported here details the design of a new averaging device that is closely matched to the requirements of the medical researcher investigating fetal electrocardiography. This new device computes

the average fetal complex in such a way as to give more weight to the more recent complexes, thereby enabling the user to observe short-term anomalies in the fetal waveform. The new device also computes this average without the periodic resetting required by the previous signal enhancement systems.

A prototype of the new system was constructed by using modern integrated-circuit digital components and an inexpensive delay line for data storage. An approximate cost analysis showed that the new system could be manufactured and sold for no more than the cost of previous systems. The effectiveness of this prototype was evaluated by using it to enhance the fetal complexes present in actual abdominal recordings. Also, a theoretical analysis of the averaging process was made, comparing the new technique with other common averaging techniques and showing that, when compared upon the basis of the ability to detect transient changes in the fetal complex, the new system offers a higher gain in signal-to-noise ratio.

The results of this research indicate that the new signal enhancement device should be a useful tool for the prenatal diagnosis of fetal heart condition.

CHAPTER I

INTRODUCTION

One of the most fertile areas of biomedical research is prenatal physiology. Scientists and medical researchers have tried to develop techniques and devices with which medical diagnoses can be made even before an individual's birth. Their research has included chemical tests, x-ray technology, sonar-like sounding of the uterus, and other equally varied schemes for checking the health of the developing fetus.

Within this climate it is logical that attention should be focused on the embryonic heart, since the electrical signals associated with the beating of this fetal organ propagate through the uterus to the skin of the maternal abdomen. For over fifty years cardiologists have attempted to amplify these signals for observation and analysis in the same way that the adult electrocardiogram is studied.

Little success has been achieved because of the electrical environment within which the fetal signals must be detected. The signals from the maternal heart, the skin-potential changes associated with maternal breathing and muscle movement, and the electromagnetic noise picked up by the recording equipment all combine to obscure the essential features of the fetal waveform and hence prevent diagnosis of the fetal heart condition. Many schemes for enhancing the quality of fetal signals available to the diagnostician have been tried. Only recently, however, through the use of coherent averaging techniques, has an improvement in the quality of the fetal signal sufficient for observation

an improvement in the quality of the fetal signal sufficient for observation of its true nature (without the obscuring noise) been achieved. The presently available averaging schemes still have significant drawbacks, and the widespread use of fetal electrocardiography is awaiting the development of more satisfactory signal enhancing equipment.

The research and development efforts detailed herein were aimed at making a significant improvement in the fetal signal enhancement equipment available. Through the use of digital techniques, an improved averaging scheme which will permit observation of the enhanced fetal signals in a manner that is more useful and natural to the medical diagnostician is developed. Because of the characteristics of this new averaging device, it should have application to other research areas wherein aperiodic waveforms with fairly low repetition rates must be combined in order to improve signal-to-noise ratio.

A prototype of the averaging device was built, and experimental evidence showing the signal enhancing performance of this prototype is presented herein. The results indicate that such a device should be a useful tool in diagnosing the condition of the fetal heart.

CHAPTER II

HISTORICAL DEVELOPMENT OF FETAL ELECTROCARDIOGRAPHY

General Background Information

Electrocardiography is the study of heart function through observation of the weak electrical signals associated with the beating heart. These electrical signals are an aggregate of the electrochemical activities of each of the heart's muscle cells as they go through their contraction and relaxation cycle. The muscle cells forming the heart's pumping chambers contract during each pumping cycle, decreasing the chamber volume and forcing blood out. In the normal heart, this electrical activity propagates along well defined neural paths. The rate of propagation varies along differing paths so that the contractions of the upper receiving chambers (atria) and the lower pumping chambers (ventricles) are properly synchronized. These signals propagate away from the heart muscle through the bodily tissue and may be detected by using a pair of electrodes attached to the skin. Typical signal values are in the microvolt range, hence amplification of these signals for visual interpretation is required. The waveform generated by a single beat of a normal heart may be typified by Figure 1. This waveform is called a complex. Each portion of this signal is given an alphabetic label as shown in Figure 1. The dominant portion, the QRS pulse, is the most easily distinguished part of the overall waveform, and it may be observed by using a pair of electrodes placed almost anywhere on the body. Diagnosis of the

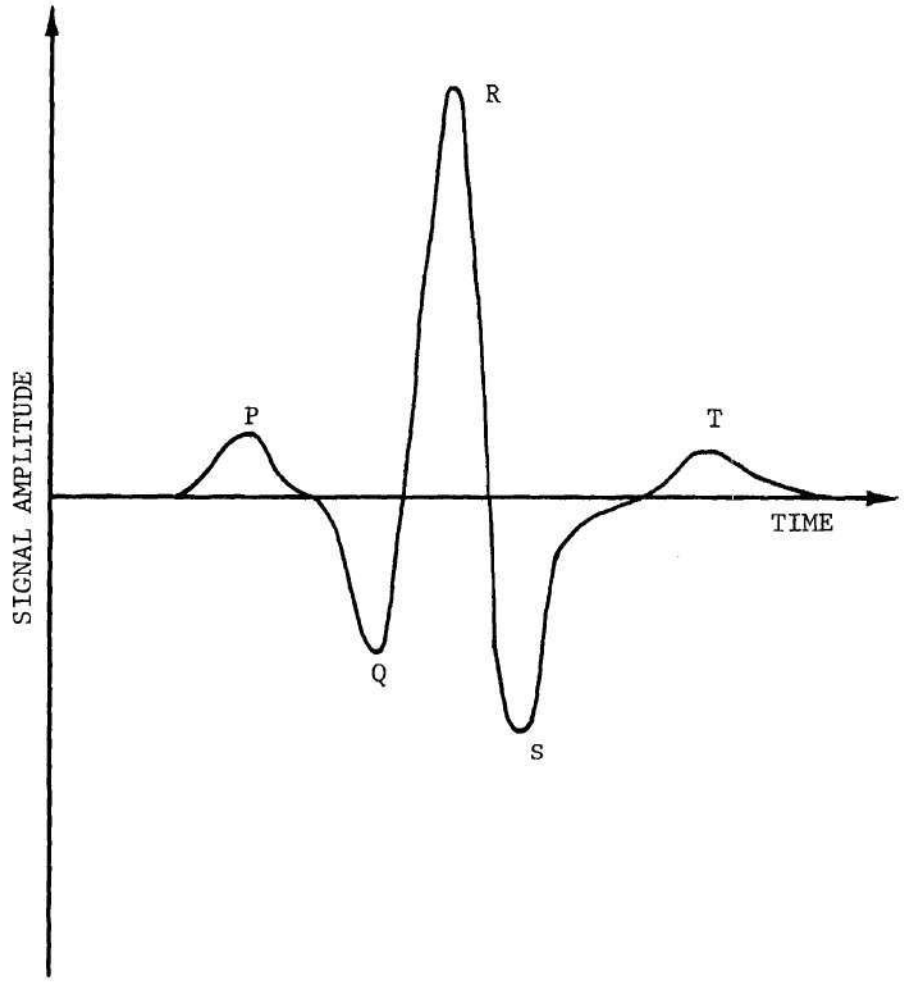

Figure 1. Typical PQRST Complex Produced by a Single Heartbeat

condition of the heart by using the electrocardiogram (henceforth abbreviated EKG) involves observation of the shape of these various portions of the overall complex and the relative timing between them.

The first observation of the fetal electrocardiogram (hereafter referred to as FECG) was made by Cremer over fifty years ago (1). He used a single pair of abdominal electrodes and obtained barely discernible breaks in the maternal record. These breaks occurred at a rate well above the rate of the maternal heart and hence were identified as complexes produced by the fetus. (Note: the normal maternal rate is 70 to 100 beats per minute; the normal fetal rate is 120 to 180 bpm.) Cremer could make no diagnosis as to the condition of the fetal heart from these records since the noise picked up by the equipment obscured all but the slight fetal R-peak. A portion of Cremer's recording is reproduced in Figure 2.

In the period since Cremer's first observation of the FECG, considerable improvement of EKG equipment has taken place. Special fetal EKG equipment has now been developed which, with proper placement of the abdominal electrodes, can pick up a considerably stronger fetal signal. Typical values as measured by such a special FECG system are fetal complexes with an R-peak greater than 15 microvolts, maternal R-peaks above 100 microvolts, and a noise level of about 10 microvolts. Experience reported in the literature has shown that signals no worse than the above typical values can be obtained in over 80 per cent of the cases (2), (3). A typical abdominal recording made with modern equipment is shown in Figure 3.

With the improvement in equipment and the associated improvement

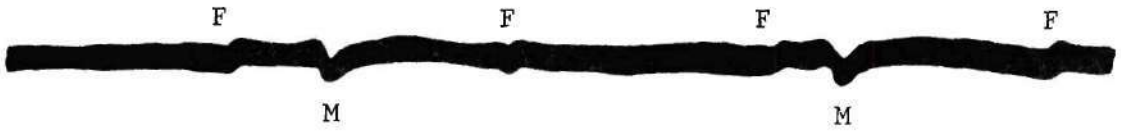

Figure 2. Waveform Observed by Cremer

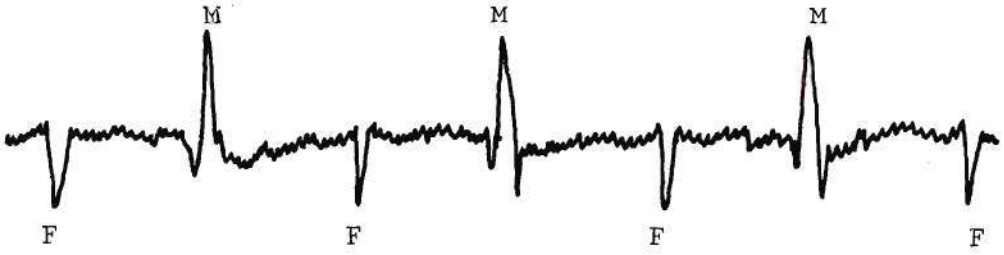

Figure 3. Typical Waveform Observed Using Modern FECG Equipment

in techniques, it is now generally possible to observe enough of the fetal signal to diagnose fetal death (by the absence of any complex at all), multiple pregnancy (by the presence of multiple R-peaks), and the orientation of the fetus in the uterus (by the polarity of the observed R-peaks) without any signal enhancement. It is not possible to diagnose the condition of the fetal heart, however, since the fetal P and T waves have not yet been observed in an unenhanced abdominally recorded FECG. An article which recently appeared in Medical Arts and Sciences states:

> Practical techniques for improving signal-to-noise ratio of abdominally recorded FECG's are essential if fetal electrocardiography is to be used in clinical obstetrics . . . since the greatest single drawback at the present time is inaccuracy as a result of inability to detect low amplitude signals which may be submerged in noise. (4)

Thus, present efforts are aimed at enhancing the fetal signal relative to the maternal signal and the noise until prenatal diagnosis of fetal heart condition can be made. These efforts can be broken into two main categories:

1. Techniques aimed at directly improving the fetal signal by using multiple-electrode configurations or direct attachment of an electrode to the fetus.
2. Techniques aimed at indirectly improving the fetal signal by using signal processing techniques such as filtering, autocorrelation, and averaging.

Direct Signal Enhancement Techniques

Multiple-electrode Schemes

The first attempts at direct improvement involved the use of one or more electrodes in addition to the normal abdominal electrode pair (5),

(6). These additional electrodes were placed well away from the uterus and hence picked up only the maternal complexes. The signals from the various electrodes were combined so as to cancel the maternal complexes in the abdominal records and leave the fetal complexes. This technique proved to be a good method for improving the ratio between the fetal signals and the maternal signals, but the noise which masked the weak P and T portions of the fetal complexes remained. Thus, while the presence of the fetal heartbeat could then be detected more easily, diagnosis of fetal heart condition still could not be made.

Intra-uterine Electrodes

The second direct signal improvement technique was the development of the intra-uterine or direct fetal electrode (7). Here an electrode is placed in intimate contact with the fetus, thereby allowing observation of the fetal complex with little maternal interference. However, the use of such an electrode during the months prior to delivery brings the danger of introducing infection into the uterus, of rupturing the membranes surrounding the fetus, and of injuring the fetus. This technique is generally useful only during the late stages of labor, when the membranes are broken and attachment can be made to the presenting fetus.

Also, despite the reduction in the interference of the maternal complexes, the signal-to-noise ratio usually does not show sufficient improvement to permit observation of the low voltage portions of the fetal complex. The leading American medical researcher in this area, Dr. Edward Hon, has stated:

While there is a marked improvement in the signal-to-noise ratio

> when direct FECG electrodes are used, even then it is not always possible to see the FECG baseline [the fetal P and T waves] clearly. To assess this more adequately, some method of signal enhancement must be used. (8)

Thus, the chief accomplishment of these direct signal enhancement schemes is elimination of the maternal complexes. They usually do not provide an improvement in the ratio of the fetal signal to the noise that is sufficient for observation of the low-voltage portions of the fetal complex. Also, as will be shown later, there are other satisfactory methods of removing the maternal interference from the FECG signals, with the patient instrumentation limited to a single pair of abdominal electrodes.

Indirect Signal Enhancement Techniques

Signal Filtering

The initial efforts at indirectly improving the fetal signal-to-noise ratio involved filtering the signals picked up by the abdominal electrodes. The noise which is present along with the fetal complexes comes from three major sources. One source is the low frequency changes in skin potential associated with maternal breathing and movement. A second source is the high frequency skin noise associated with vibrations of muscle fibers. The third source is electromagnetic energy that is picked up by the body acting much like an antenna.

The latter noise source may be essentially removed by using a shielded recording room. Some of the low-frequency noise may be removed by keeping the patient still and by high-pass filtering (above two to five Hertz). Such filtering is usually included in the EKG amplifiers designed for fetal applications. The remaining noise falls in the same frequency range as the harmonic components of the fetal complexes and

hence filtering cannot be used to separate the FECG. Also, any filter designed to be matched to the expected fetal waveform would distort the shape of the atypical fetal complex. Since observation of the true nature of such an abnormal waveform would be of prime clinical importance, such matched filtering cannot be used successfully.

Autocorrelation Techniques

Favret and Caputo (9) have investigated the use of autocorrelation techniques for the detection of the fetal EKG. Their primary goal has been identification of fetal complexes that are almost totally submerged in noise. Their system involves recording abdominal signals and processing this data through an off-line digital computer. They report that the normal fluctuations in the fetal period and the typical shape of the fetal complex cause a destructive interference in computing the correlogram. They report in the above cited article that " . . . correlation techniques, even with extremely long signals, cannot be expected to provide significantly improved detection performance over visual examination of pen recordings."

Coherent Time Averaging Techniques

Thus, the most promising means of improving the quality of the fetal complex is the use of coherent time averaging. This technique, which has found application in a variety of fields, involves the additive combination of repeated samples of the signal in such a way that the true signal reinforces itself while the noise tends to cancel out. In order to obtain coherent addition of the signal components, the samples must be taken with the same time relationship to the signal, preferably beginning just before the portion of the signal which is to be enhanced. This

is not difficult if the signal is exactly periodic. For the aperiodic case, however, it is necessary to generate a marker pulse which matches the aperiodicity of the signal and is time-locked to it. The marker pulse can then be used to trigger the taking of the sequence of samples and, when they are combined, the signal components present in the samples will reinforce coherently.

The application of coherent averaging to fetal electrocardiography involves three basic operations:

1. Elimination of the interfering effects of the maternal complexes.
2. Indication to the averaging system when a fetal complex is present so that the new complex may be included in the average. (This indication must be timed so that the repeated FECG complexes reinforce each other.)
3. Performance of the averaging operation.

Several researchers (10), (11), (12), (13), have been investigating this field. While their exact averaging systems vary somewhat, they all may be characterized by the general block diagram of Figure 4.

The signals detected on the maternal abdomen are amplified by an FECG amplifier and sent to three places. First, the signals go to a maternal complex detector. This is usually a combination of a filter and a variable threshold detector. The filter is roughly matched to the spectrum of the large maternal QRS pulse and, when a sufficiently large voltage reaches the threshold detector, the detector indicates to the rest of the system that a maternal pulse is present. This maternal complex detector may contain some type of holding circuit so that once set, it

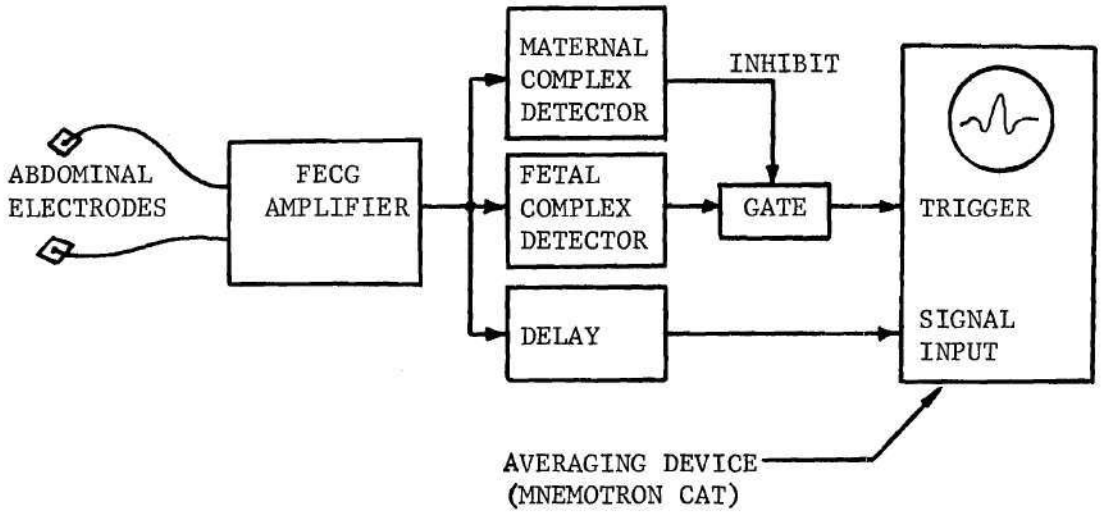

Figure 4. Block Diagram of Current Coherent Averaging Schemes

will remain set for a brief period to assure that the interfering maternal complex has passed before the fetal averaging process resumes.

Second, the signals go to a fetal complex detector which again, in the simplest case, is a filter-threshold detector combination. The threshold of the fetal detector is set somewhat lower than the maternal detector so that the lower amplitude fetal R-peaks will trigger it. (Note that in the rare cases when the fetal signal is as large as the maternal signal, a slight repositioning of the abdominal electrodes will bring about a reduction in the size of the fetal complexes so that discrimination between the fetal and the maternal complexes can then be based upon a difference in amplitude.)

The most elaborate and most effective of the fetal complex detection schemes is that of Offner and Moisand (11), which uses three separate filter-threshold detector combinations and three separate pairs of abdominal electrodes. By waiting until all three detectors sense a fetal pulse, they are able to set the thresholds in each detector very low and still not get many false indications due to noise spikes. This permits their system to operate with fetal pulses of smaller amplitude. It does increase the amount of hardware and the difficulty of instrumenting the patient.

One researcher (14) has studied the use of well-matched filters for the sole purpose of detecting the presence of the fetal R-peak without any threshold detector. His results seem to indicate that such a scheme can do as good a job of indicating when a fetal complex is present in the abdominal signal as the other filter-threshold detection schemes. The matched-filter fetal detection scheme has not yet been incorporated

into any reported averaging system, however.

Whenever the fetal complex detector indicates the presence of a fetal signal, the detector output is used to trigger the beginning of the averaging cycle of the averaging device shown in Figure 4, unless the maternal complex detector also indicates the presence of a maternal pulse. In that case, the maternal complex detector closes the gate shown in Figure 4, preventing the triggering of the averaging device. Thus, only those fetal complexes that are not preceded by a maternal complex will be included in the average.

The delay shown in Figure 4 is necessary so that each fetal complex that triggers an averaging cycle will arrive at the input to the averaging device a short period of time after the triggering pulse. This is equivalent to generating a trigger pulse just prior to the occurrence of each clean fetal complex, even though the fetal complexes occur aperiodically. As a result, the fetal complexes will be averaged coherently. This delaying has been accomplished, in the cases cited, by using a tape recorder with two reading heads as shown in Figure 5. The abdominal signals are recorded on the tape and are first picked up by read head A for input to the maternal and fetal complex detectors. The signals then pass on to read head B a short time later for delayed input to the averager which, if it has been triggered, will include the delayed waveform in its accumulated average.

Shortcomings of Present Signal Enhancement Systems

Through coherent averaging, the first signal-to-noise improvement sufficient for observation of the low-voltage portions of the fetal com-

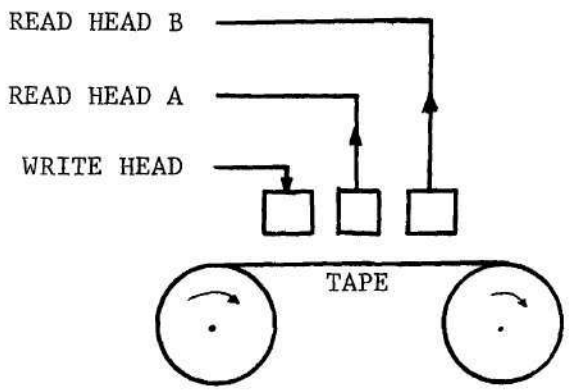

Figure 5. Multiple Read Heads Used for Delay of FECG Signals

plexes has been achieved. Two of the researchers (10), (11), have published averaged waveforms that clearly show the fetal P wave. No one has at this time reported observation of the fetal T wave in an enhanced abdominal recording. The use of coherent averaging with the scalp electrode has brought about signal enhancement sufficient for observation of the T wave, however (10). Despite this improvement in the fetal signal, the presently available systems have drawbacks which prevent their widespread diagnostic use. These drawbacks will be considered in the following paragraphs.

Limitations of the Averaging Method

All of the signal enhancement systems discussed above use the same commercially available device as their averaging computer. This device, the Mnemotron CAT (Computer of Average Transients), is only capable of taking an equally weighted average over a designated number of waveforms. In other words, if it is preprogrammed to average 100 waveforms, it computes the average by taking 1/100th of each waveform and summing them. After computing the average, the CAT must be reset and a new average accumulated over the next 100 waveforms.

Since the signal increases algebraically with each new waveform added into the average, after n waveforms have been averaged the signal strength will be n times what it was originally. The noise, since it is random and uncorrelated, will add in an rms rather than an algebraic fashion. Thus, the total noise will be increased by only the square-root of n. (For a complete discussion of the equally weighted average's effect on signal-to-noise ratio see Chapter V.) After n waveforms have been included in the average, the signal-to-noise ratio of the average will

be $n/\sqrt{n}$ or $\sqrt{n}$ times better than the signal-to-noise ratio of the original data. Despite this desirable improvement in signal quality, there are two inherent limitations in the usefulness of such an equally weighted average.

First, the original (and hence older) waveforms have the same influence on the final average as do the more recent signals. Thus, if there is a change in the configuration of the fetal complex during the averaging period, the effect of the changed waveforms on the overall average will be "watered-down" by the preceding waveforms.

Since observation of such transient changes in the fetal complex is necessary in order to properly diagnose the condition of the fetal heart, this "watering-down" may result in improper diagnosis. Concern about this problem prompted one medical researcher to write:

> While an averaging technique improves markedly the signal-to-noise ratio, averaging may mask transient changes in FECG details. To minimize this possibility it is necessary to use an average weighted in favor of the more recent FECG's. While there is less enhancement of the signal-to-noise ratio, the technique [weighted averaging] permits a more accurate appraisal of short-lived FECG changes. (15)

The second limitation on the averaging technique of the CAT is the requirement that the averaging process be restarted upon completion of the predetermined number of averaging cycles. Hence, rather than seeing a picture of the dynamic changes of the fetal complex, the user can only get a picture of the average configuration at the end of repeated (and possibly somewhat lengthy) time periods. There is no capability for presenting a running average that continuously updates itself to show the more recent configuration of the fetal complex.

Limitations of the Method of Removing the Maternal Complex

While the filter-threshold detector combination previously mentioned is quite satisfactory for detecting the presence of a maternal complex and then closing the gate so as to prevent the starting of the averaging process, this simple technique cannot eliminate maternal complexes coming just after a fetal complex. Such a fetal complex will have already triggered the averaging computation of the CAT when the blanking associated with the presence of the maternal complex takes place. Thus, even though the fetal complex may be distorted by the PQ portion of the maternal complex which precedes the R-pulse, the complex will still be added into the current average. Because of this possible distortion, there is a need to eliminate not only those fetal complexes which are preceded by interfering maternal complexes, but also those that are closely followed by the maternal R-peak.

Other Considerations

Finally, the complexity of the equipment used in these averaging schemes, the tape recorder with its double read heads, the CAT, the filters and threshold detectors, make the acquisition and use of such a system by a normal hospital or research clinic prohibitively expensive.

Goals for the Reported Research

The research which is presented in the following chapters has been an attempt to advance the quality and usefulness of available FECG signal enhancing equipment. It was hoped that the limitations of the available systems could be overcome and that the overall system cost could be reduced.

The general specifications for such an improved signal enhancement system were outlined as follows:

1. The system should be capable of identifying those fetal complexes that are free of an interfering maternal complex coming closely before or after the fetal complex.
2. The system should be able to sample these complexes at a suitable rate and to store the sample values for further processing.
3. The system should be able to compute a running average of these fetal complexes that gives more weight to the more recent complexes.
4. The weighting factor should be variable.
5. The system should display the average fetal complex thus accumulated for interpretation by the user.
6. In addition, hopefully, the system should cost less than previous signal enhancement systems.

CHAPTER III

THE FECG SIGNAL ENHANCEMENT SYSTEM DESIGN

Introduction

The main objective of this research has been to design a FECG signal enhancement system (SES) that will meet the general specifications outlined at the end of Chapter II. To verify the design, a prototype of the SES was constructed. In this chapter, the input and output constraints for the SES are considered, and, based upon these constraints, the design of the SES is presented in a generalized fashion. The subsequent chapter contains a detailed explanation of the operation and construction of the prototype.

Input and Output Constraints

The input data to the SES is typical abdominally recorded EKG signals which have been amplified by a suitable FECG amplifier. Data of this kind, as previously discussed, contains fetal complexes, maternal complexes, and noise. The desired output of the SES is an enhanced view of the fetal complex. This signal enhancement is brought about by using a coherent averaging technique that gives more weight to the more recent fetal complexes. This average is "running" in nature, giving a continuous picture of the enhanced fetal complex which does not require periodic resetting of the average.

Computer Simulation

As an aid to good system design, the operation of the SES upon

typical FECG data was simulated on a digital computer. The simulation consisted of the generation of FECG data and the programmed operation upon this data in the same way that the SES would operate when constructed. In this way, various system designs were evaluated without having to construct and modify different pieces of hardware. This simulation, in addition to providing a degree of confidence that the hardware would work, pointed up several problems that were not at first obvious and permitted several hardware saving shortcuts to be found.

A sample of the data generated by the simulation program is shown in Figure 6, along with the enhanced fetal complex that was obtained by the most effective of the various SES designs that were tried. The upper trace shows the relative sizes of the simulated fetal and maternal complexes and the simulated noise level. The lower trace, shown at an expanded time scale, is the enhanced fetal complex. The success of the enhancement, particularly the recovery of the fetal T wave, is a result of the fact that the fetal complex, as simulated, had exactly the same configuration from beat to beat. In a more realistic situation, the beat-to-beat changes in the fetal complex would reduce the degree of signal enhancement. A more detailed discussion of the computer simulation program is given in Appendix I.

General Discussion of SES Operation

As a result of the computer simulation, the general system design of the SES was developed. This design was changed somewhat during the construction of the prototype, and a block diagram of the final SES is shown in Figure 7. A generalized discussion of this system follows, with

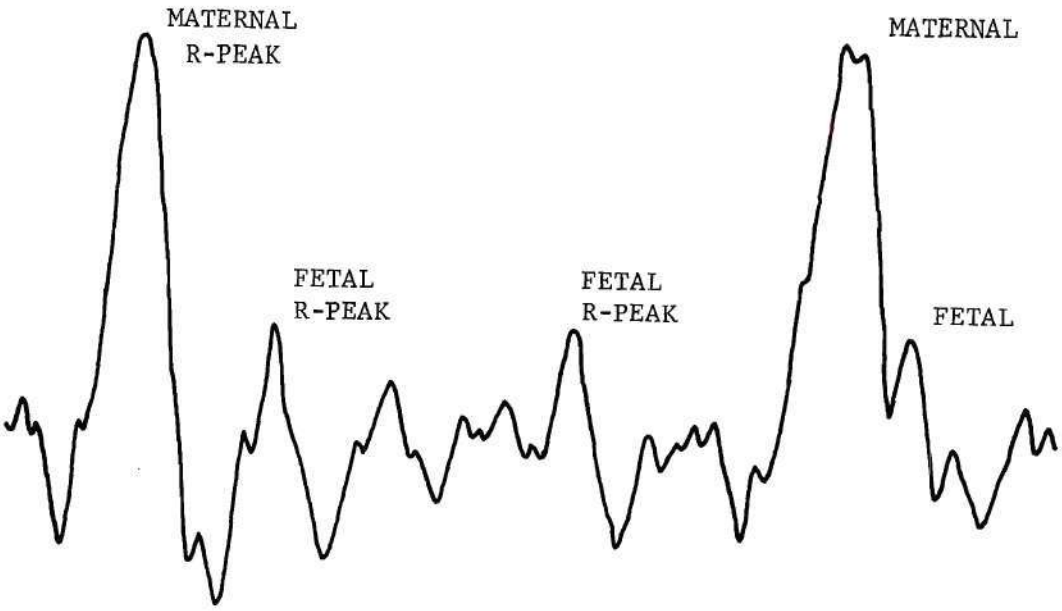

a. Computer-generated FECG Data

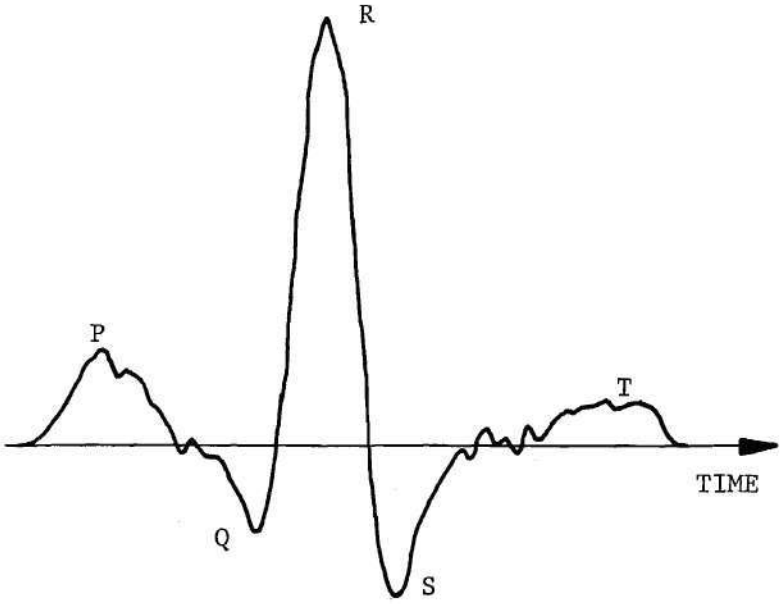

b. Enhanced Fetal Complex Produced by Computer Simulation

Figure 6. Computer Simulation of FECG Signal Enhancement System

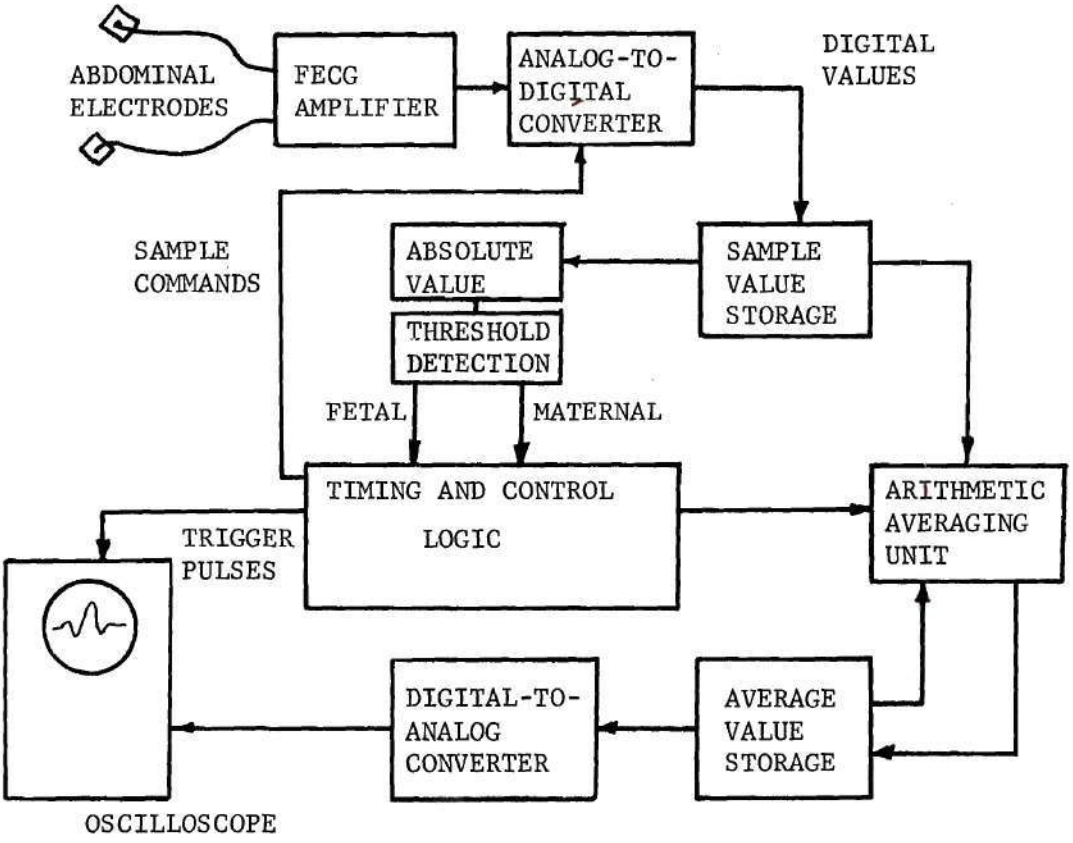

Figure 7. Block Diagram of SES

the details of the prototype left to Chapter IV.

Input and Conversion

Initially, a pair of electrodes is properly placed upon the maternal abdomen and will therefore pick up the maternal complexes, the fetal complexes, and noise. These signals are amplified by a suitable FECG amplifier, which will also do some high-pass filtering (passing frequencies above two to five Hertz) in order to help stabilize the baseline of the signals. The output signals from this amplifier will have a peak amplitude of several volts, rather than the microvolt signal amplitude picked up directly by the electrodes.

This signal is presented to an analog-to-digital converter (ADC), which generates a digital code, usually referred to as a code word, or simply a word, that represents the magnitude and sign of the input signal. This process takes place every two milliseconds. It is initiated by the "Sample Commands" which come from the timing and control portion of the SES. This sampling period corresponds to a sampling rate of 500 samples per second, which is well above the Nyquist rate of 90 samples per second that was computed by Favret and Caputo (9) based on their spectral analysis of typical FECG complexes. This rate is also convenient for use with the two-millisecond digital delay line that was used to form a recirculating memory in the prototype.

At the completion of each conversion cycle of the ADC, the coded sample, or sample word, that has been generated is transferred from the ADC to the sample value storage area of the SES memory.

Detection of the Fetal and Maternal Complexes

The final version of the SES uses a threshold detection scheme to

identify the fetal and maternal complexes that are present in the abdominal signals. Several other schemes for doing this were considered, e.g., a rate-tracking system that estimated the fetal and maternal rates and predicted the occurrence of the next beat based upon the previous rates. However, the threshold detection scheme, when simulated, worked as well as any of the others; since it can be implemented with the simplest digital hardware, this scheme was used.

To accomplish this threshold detection, each sample word is added to the three samples that were taken just before it (to reduce the effects of noise). The sum of the four samples is passed through an absolute value circuit that converts the digital code word for any negative sum to a positive code word representing the same magnitude. This absolute value is then compared to two different digital thresholds by the threshold detection circuit shown in Figure 7. The two thresholds are set by switches.

The lower threshold is set above the expected peak noise level and, thus, will be crossed only by a sum of samples that were taken from a fetal or a maternal R-peak. The upper threshold, which may be called the maternal threshold, is set above the fetal R-peak, and therefore will be crossed only when a maternal R-peak has been sampled. The setting of these thresholds is illustrated in Figure 8, along with the logical meaning of their being crossed.

It can be seen from Figure 8 that whenever the absolute value of a sum is greater than the lower threshold, either a fetal or a maternal complex is present in the input signal. If the subsequent sums of samples continue to increase until the upper threshold is crossed, then the com-

LOGICAL MEANING OF THE THRESHOLD CROSSINGS

UPPER THRESHOLD	LOWER THRESHOLD	MEANING
NOT CROSSED	NOT CROSSED	NEITHER COMPLEX PRESENT
NOT CROSSED	CROSSED	FETAL COMPLEX ONLY PRESENT
CROSSED	NOT CROSSED	CANNOT HAPPEN
CROSSED	CROSSED	MATERNAL COMPLEX PRESENT

Figure 8. Threshold Detection of the Fetal Complex

plex that was detected was maternal in origin. If the sums of samples reach a peak that is less than the upper threshold, then a fetal complex is present.

The Sampling Aperture

In order to completely characterize each fetal complex, a group of consecutive samples must be taken and stored. This group of samples should be centered about the fetal R-peak and should include a number of samples before and after the fetal R-peak that is sufficient to include the fetal P and T waves. Only those fetal complexes that do not have a maternal complex present anywhere within this aperture should be included in the averaged waveform.

The necessary width of the sampling aperture was estimated to be 110 milliseconds. This estimate was made by doubling the value of 55 milliseconds given by Larks for the typical fetal QRS duration (2). This aperture would require at least 28 samples prior to and 28 samples after each fetal R-peak since the samples are taken two milliseconds apart. The memory capability of the final version of the prototype was limited to 47 words, which is less than the 56 words required to completely cover the necessary aperture about the fetal R-peak. As a result, the prototype was constructed so that the 47 word sampling aperture could be shifted to cover more of the period before the fetal R-peak or more of the period after the fetal R-peak. Thus, the user can choose his area of interest and view an enhanced picture of the electrical behavior of the fetal heart in that portion of the fetal complex.

The proper locating of the sampling aperture is accomplished within the sample value storage area of the SES memory. In this storage area

the last 47 consecutive samples are always stored in a "push-down" fashion. This means that the storage of each new sample value causes the removal of the oldest value from the storage area. Whenever the lower threshold of the threshold detector is crossed, the operation of the sample value storage area is changed. The push-down storage cycle continues, but a count of the number of samples that are stored following the threshold crossing is made. This count is reset to zero each time a sum of samples is greater (in absolute value) than any of the previous sums. Once the peak of the input waveform is reached, the count will no longer be reset.

This count, and the push-down operation of the sample value storage area, continues until the count reaches one of two selectable upper limits. In the prototype, these limits are 37 (AFT Aperture) and 21 (CENTER Aperture). Thus, the AFT Aperture will include ten samples taken before the crest of the fetal R-peak and 37 samples taken after it, thereby covering a period of 74 milliseconds following the center of the fetal complex. The CENTER Aperture will include 26 samples taken prior to the fetal R-peak and 21 taken after it. By selecting one of the two upper limits, the user chooses the portion of the fetal complex that is covered by the 47 samples that are stored in the sample value area of the SES when the count reaches the limit. At that time the push-down operation of the sample value storage area is stopped and the new group of samples is ready for inclusion in the averaged waveform.

If the upper threshold is crossed during the sampling aperture, thereby indicating the presence of a maternal complex in the input data, all of the samples stored in the sample value storage area will be dis-

carded and a new sampling aperture started. The SES will take samples to fill the push-down register and then begin its threshold comparison again, looking for a crossing indicative of the fetal R-peak.

This restarting process will happen if a maternal complex is detected either during the period after a fetal R-peak has been detected and the last portion of the sampling aperture is being stored, or during the period before the detection of a fetal R-peak. Thus, any maternal complex whose R-peak is within the sampling aperture on either side of a fetal R-peak will cause that fetal complex to be omitted from the average. This double-sided detection is not available in any other reported FECG signal enhancement system.

Formulation of the Average

Whenever the samples making up the last portion of the aperture can be stored without the detection of a maternal complex, the fetal complex that is characterized by the samples stored in the sample value storage area is used to compute a new average. This average is computed in such a way that the newer complexes have more weight upon the average than do the older complexes.

A complete mathematical analysis of the weighted averaging process is presented in Chapter V. For reference, however, the high lights of this analysis are presented below.

A variable weighting factor is defined, represented by the symbol M. (In the prototype, the weighting factor was limited to integral powers of two from two to 256.)

Each new average is composed of (M-1)/M times the old average plus 1/M times the new complex, or:

$$\text{Ave}_{new} = \frac{(M - 1)}{M} \text{Ave}_{old} + (1/M)\ \text{Complex}_{new} \quad . \qquad (1)$$

The repeated complexes add algebraically due to the time-locked coherence with which the sampling apertures are taken, and the signal present after n complexes have been included in the average may be shown to be:

$$S_n = S[1 - (1 - 1/M)^n] \quad , \qquad (2)$$

where S is the true signal level (assumed constant throughout the n complexes).

The noise present along with the complexes that are averaged will add only in an rms sense and, after n complexes have been averaged, may be shown to have accumulated to:

$$N_n = N\left[\frac{1 - (1 - 1/M)^{2n}}{(2M - 1)}\right]^{1/2} \quad , \qquad (3)$$

where N is the noise level (also assumed constant).

The maximum signal-to-noise ratio that may be obtained by averaging with a particular value of the weighting factor can be found by taking the ratio of Equation (2) to Equation (3) as the number of samples included in the average approaches infinity, as:

$$\left.\frac{\text{Signal}}{\text{Noise}}\right|_{\substack{\text{After}\\\text{Averaging}}} = (2M - 1)^{1/2} \times \left.\frac{\text{Signal}}{\text{Noise}}\right|_{\substack{\text{Before}\\\text{Averaging}}} \quad . \qquad (4)$$

Equation (4) shows that the larger the weighting factor, M, the better the improvement in the signal-to-noise ratio. (Note that if M equals one, there is no improvement.) Equation (4) implies that any de-

gree of signal-to-noise improvement can be obtained by making the weighting factor large enough. It must be remembered that this equation was developed by assuming that neither the signal (i.e., the fetal complex) nor the noise changed during the infinite averaging interval. This should be statistically valid for the noise. In the case of the fetal complex, however, such long-term stability does not occur. Significant transient changes in the shape of the fetal complex do appear from time to time. When they do appear, the literature indicates that such changes will usually persist for 20 to 30 successive complexes (10). For diagnostic purposes, there is a need to show these transient changes in the fetal waveform, as well as to provide signal-to-noise enhancement.

These two requirements will influence the setting of the weighting factor during a particular medical experiment. Should the user desire to see the short-term changes in the fetal complex, he should keep the value of the weighting factor fairly low. Then, the amount of each of the older complexes that is included in the average will be decreased more rapidly with the inclusion of each newer complex, allowing the more recent fetal complexes to have a greater influence upon the averaged waveform. This is shown in Table 1, which uses Equation (2) to calculate the number of fetal complexes that make up 50 and 90 per cent of the averaged waveform for various weighting factors. The effect of decreasing M is clearly shown; for example, at M = 64, one half of the average is the result of the most recent 46 fetal complexes, while at M = 16, the same amount of weight is given to the 11 most recent complexes. Thus, the lower values of M, by making the average more and more the result of the most recent complexes, allow the observation of these short-term changes

Table 1. Effect of Weighting Factor on Number of Complexes Included in the Average

Weighting Factor (M)	Number of Samples Making up 50 Per Cent of the Average	Number of Samples Making up 90 Per Cent of the Average
1	1	1
2	1	4
4	3	8
8	6	18
16	11	36
32	23	76
64	46	153

in the shape of the fetal complex. As a consequence, however, these weighting factors give lower values of signal-to-noise enhancement.

Should more signal-to-noise improvement be desired, the weighting factor can be made larger. Then, if the shape of the fetal complexes is relatively stable over the larger number of complexes that makes up the average, a signal-to-noise improvement on the order of that given by Equation (4) should be achieved. There is an upper bound on this signal-to-noise improvement, however, which is reached when the number of complexes that are included in the average becomes so large that the long-term changes in the fetal complex over the averaging period are significant. Then, since the fetal complexes included in the average are not identical, the signal-to-noise improvement given by Equation (4) cannot be attained. The larger number of complexes included in the average will also have the effect of "watering-down" the short-term changes in the fetal complex.

By adjustment of the weighting factor, however, the user can obtain a variable trade-off between signal-to-noise improvement and dynamic response. For any value of M, still, the system will compute the averaged waveform in a running manner without the requirement for periodic resetting.

The Arithmetic Averaging Unit

The weighted averaging process described above is performed by the arithmetic averaging unit shown in Figure 7. This particular circuit is diagrammed in more detail in Figure 9. When a sequence of sample values characterizing a fetal complex that is free of maternal interference has been stored in the sample value storage area, the control section

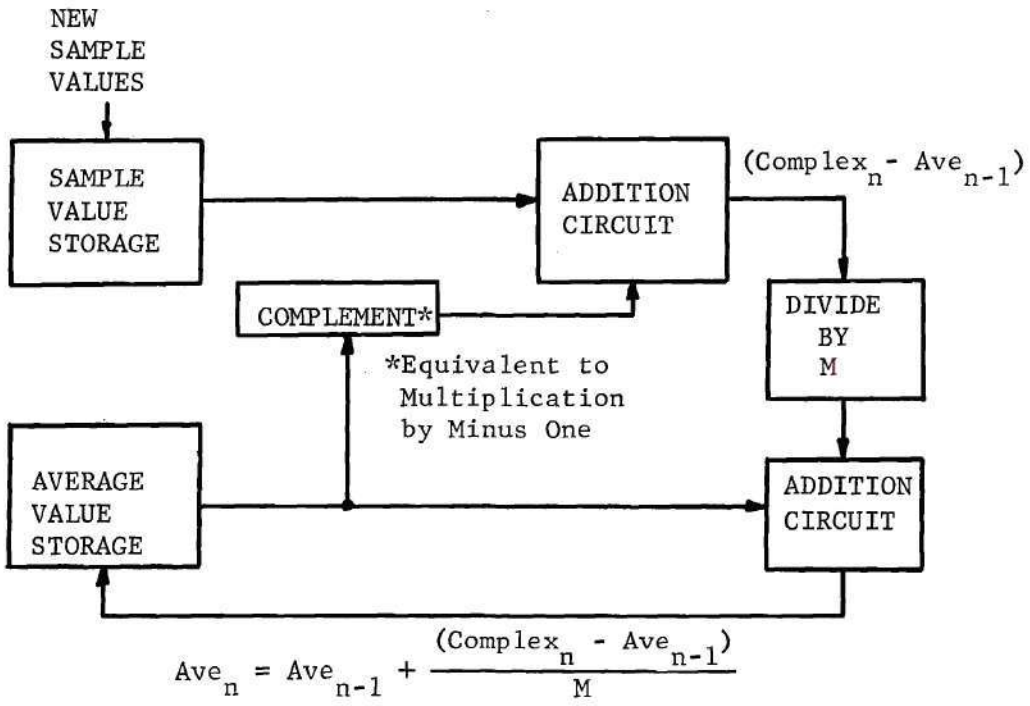

Figure 9. Computation of the Averaged Complex

of the SES starts the averaging process.

Like the sampled fetal complex, the averaged waveform is stored as a sequence of average sample values that correspond to average values of this waveform taken every two milliseconds. This sequence of average sample values is stored in a separate portion of the SES memory that is referred to as the average value storage area. During the averaging process, each of the sample values corresponding to a sample of the new complex is combined with a corresponding average sample value from the averaged waveform. Since there are 47 sample values corresponding to each waveform, the averaging process shown in Figure 9 is actually repeated 47 times as each new complex is included in the average.

Each sample of the new complex is brought from the sample value storage area, paired with the value of the average waveform with which it is to be combined. The digital word representing the sample value taken from the average waveform is complemented (a digital process that is equivalent to multiplication by minus one), and the two sample values are added, giving a sum, defined here as DELTA, of:

$$\text{DELTA} = \text{Complex}_n + (-1)\ (\text{Ave}_{n-1}) \quad . \tag{5}$$

This sum is divided by the weighting factor, M, and the quotient, DELTA/M, added to the sample of the average waveform that was used to compute DELTA originally. This sum gives the <u>new</u> value of the average waveform at that point as:

$$\text{Ave}_n = \text{Ave}_{n-1} + \text{DELTA}/M$$

$$= Ave_{n-1} + (1/M)\ (Complex_n - Ave_{n-1})$$

$$= Ave_{n-1}\ (1 - 1/M) + (1/M)\ Complex_n$$

$$= [(M - 1)/M]\ Ave_{n-1} + (1/M)\ Complex_n \quad . \qquad (6)$$

This is the desired average. (Compare with Equation (1).)

As each new average word is calculated, it is stored in the average value storage area, replacing the previous average word. In this manner, the 47 words which characterize the new averaged waveform are computed from the old average words and the sample words which were taken from the most recent fetal complex.

The SES then returns to its sampling of the input signal, continuing this sampling process until the threshold detection circuit can again identify a fetal complex that should be included in the average. During the period between averaging cycles, the sequence of values that makes up the averaged waveform remains unchanged in the average value storage area.

Display of the Averaged Waveform

Once each sampling time (every two milliseconds) this sequence of average values is read from the average value storage area and passed to a digital-to-analog converter (DAC) for conversion to a voltage corresponding to their digital value. The output voltage from the DAC is displayed upon an oscilloscope, renewing itself every two milliseconds and changing whenever a new complex is included in the average. Typical output waveforms generated from FECG data by the prototype in both the CENTER and AFT settings are shown in Figure 10. The step-like discontinuities that are present in the upper trace correspond to the sequence of digital

a. AFT Aperture

b. CENTER Aperture

Figure 10. Typical Output Waveforms of the SES

values which represent the average waveform. The lower trace has been smoothed by a low-pass filter. This display process is covered in more detail in the following chapter.

CHAPTER IV

DETAILED DISCUSSION OF THE PROTOTYPE

Introduction

The previous chapter explains, in a general fashion, the design of the digital signal enhancement system which evolved from the computer simulation. The next step in the research effort was the construction of a working model of the signal enhancement system so that the effectiveness of the system could be evaluated by using it to process some actual FECG data. The construction of this prototype was also useful in that it brought to light some of the practical problems associated with transferring the general system design to actual digital hardware.

This chapter contains a detailed description of the prototype. Each of its logical subsystems is covered in the appropriate detail, and the interactions between these subsystems as the prototype performs the signal enhancement process are explained. The limitations of the prototype are explained, and some recommendations for hardware improvement are made. The chapter concludes with a discussion of the cost of constructing the prototype.

The Hardware Used to Construct the Prototype

The prototype was constructed with Fairchild and Motorola integrated circuit components of the following types:

1. J-K Flip-flops (DC reset only), Fairchild type μL923 and Motorola type MC790P.

2. Dual-input NAND Gates, Fairchild type μL900.

3. Inverting Buffer Amplifiers, Fairchild type μL914.

4. High-gain Operational Amplifiers, Fairchild type μL709.

5. High-speed Analog Comparators, Fairchild type μL710.

The last two items were used in the construction of the analog-to-digital converter used by the prototype. One of the comparators was also incorporated into the output sensing circuitry of the digital delay line that is used by the prototype as a memory. The symbols which represent each of the digital elements listed above (Items 1, 2, and 3) are shown in Figure 11. The two logical voltage levels for all of the digital components were zero volts and +3.6 volts.

The hardware of the prototype was constructed by mounting these components on plug-in printed circuit cards. Usually, each separate card was designed to carry some special-purpose logical subsystem such as a shift register or an adder. The printed circuit cards were fabricated in the printed circuit facilities of the Electrical Engineering Department.

In addition to the specially fabricated printed circuit cards, a small number of general purpose logic cards (Systems Engineering Laboratories Series 8500 Micrologic Modules) were used. With a single exception, these consisted of digital components like the first three types listed above, which were mounted on general purpose printed circuit cards. The exception was the type of flip-flop used; the general purpose cards contained J-K flip-flops having both a DC set and a DC reset capability.

The storage required by the prototype was provided by constructing a recirculating memory with a Computer Devices Corporation digital delay

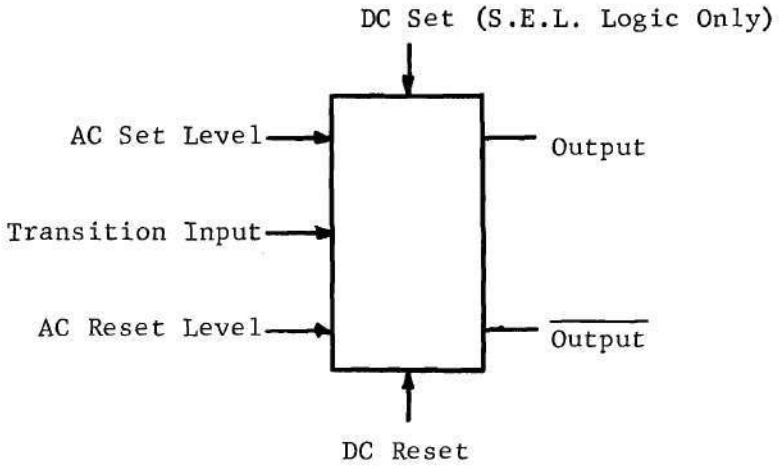

a. Symbol for J-K Flip-flop

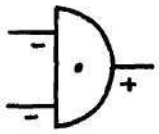

b. Symbol for NAND Gate when used as an AND Gate

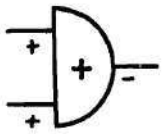

c. Symbol for NAND Gate when used as as OR Gate

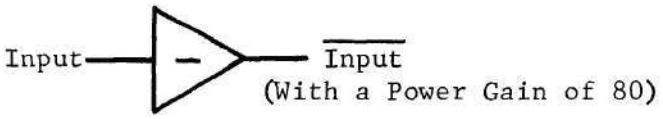

d. Symbol for Inverting Buffer Amplifier

Figure 11. Symbols used in Circuit Diagrams of Chapter IV

line. The driving and sensing circuitry for this delay line was developed as a part of the prototype design and is detailed in Appendix II. The operation of the recirculating memory is explained below.

The Recirculating Memory of the Prototype

As was mentioned in Chapter III, the SES must be able to store both the sequence of sample values representing each fetal complex that is free of maternal interference and the sequence of sample values representing the accumulated average waveform. Since the operation of the memory portion of the prototype may be considered with relative independence from the rest of the prototype circuitry, it is presented here, with the discussion of the operation of the prototype to follow.

The use of a digital delay line to store information is a relatively simple process. The input data, represented by a series of digital words, with each word corresponding to a particular piece of numerical information, is input into the delay line in synchronism with some precisely controlled clock signal. In the case of the prototype, each of these digital words corresponds to a particular sample value, with one sequence of words corresponding to the sample values taken from a fetal complex and another group of words corresponding to the sequence of values that represents the averaged waveform.

These words are represented in some binary code (two's-complement code in the case of the prototype) and the bits that make up each word are put into the line one after the other. Each bit that is put into the delay line appears at the delay line output terminals a fixed amount of time later. This delay, referred to as the propagation time of the delay

line, is a characteristic of the construction of the line. The delay process of the line is explained in Appendix II. The propagation time of the delay line is adjusted so that the binary information that comes out of the sensing circuit is properly synchronized with the clock signals.

The data may then be recirculated to the delay line input circuit and sent back through the delay line. In this way, a number of bits equal to the propagation time of the delay line divided by the clock rate at which bits are put into and taken from the line may be stored. In the case of the prototype, the delay line has a delay of 2000 microseconds and the input rate is one million bits per second. Thus, the delay line of the prototype will store 2000 bits. Each word stored by the prototype is 20 bits long; therefore, the memory capability of the delay line is 100 words, since 100 words of 20 bits each total to 2000 bits. The choice of the 20 bit word-length will be explained later.

In the prototype, the recirculation path of the memory is closed through two external registers, A and B, as shown in Figure 12. These registers are used whenever a new word is inserted into the memory and whenever the averaging calculation of the prototype takes place. The logical signal labeled COINC is used to change the input connection to Register B. The data coming out of the delay line is shifted into Register A, and, during the normal operation of the memory, the gating signal COINC allows the data to shift right on through Register B and back into the delay line input circuit. The signal COINC is formed by the logical combination of two other signals, LAD and SAMP, whose exact functions will be explained later in this chapter.

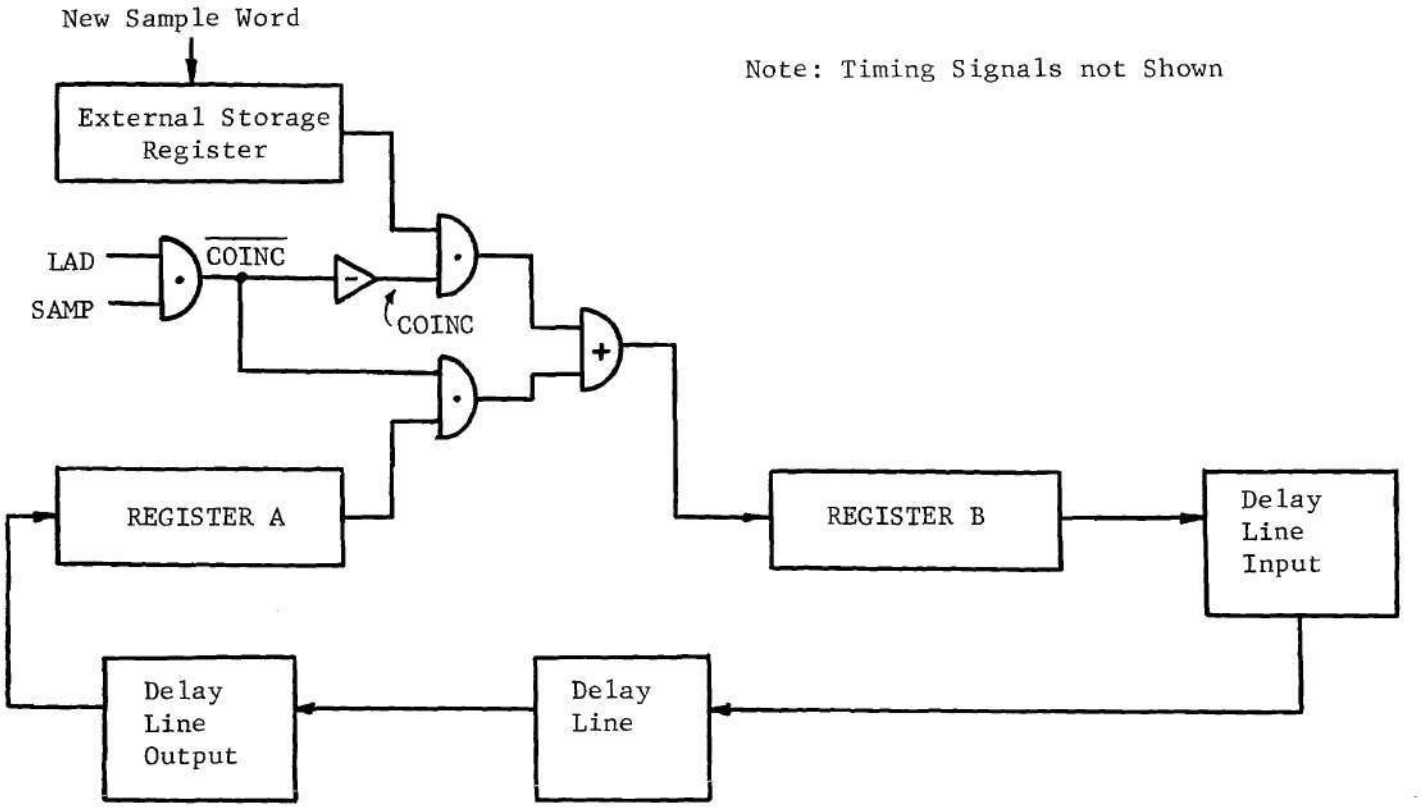

Figure 12. Recirculating Memory of the Prototype

Both Register A and Register B are 20 bits long, thereby providing for the storage of two additional words outside of the delay line. This increases the storage capacity of the prototype to 102 words (2040 bits). As was shown in Chapter III, the storage required by the prototype is:

1. At least 47 words corresponding to the sequence of samples taken from a fetal complex.
2. At least 47 words corresponding to the accumulated average waveform.

This is a total of 94 words, which is within the 102 word capability of the memory used by the prototype.

When a new word is to be inserted into the memory, the word is first shifted into the external storage register shown in Figure 12. The timing and control circuits of the prototype then wait until the stored word that is to be replaced by the newer word has been shifted out of the delay line and into Register A. At that time, the signal COINC is used to change the input connection to Register B so that the data from the external storage register, rather than Register A, will shift into Register B. During the next 20 clock pulses, the new word is shifted from the external storage register into Register B, and the old word is shifted out of Register A and is lost. The control circuit then returns the recirculation path to its normal condition. The new word is shifted from Register B into the delay line and is recirculated along with the other words that were already stored in the memory.

The Timing Circuitry of the Prototype

The prototype has four operating modes. The first is the Reset

Mode, a static mode which the system will be in whenever the main control switch is in the Reset position. When the control switch is placed in the Start position, the digital clock oscillator that provides timing pulses to control the system is started, and the prototype will automatically enter Mode Zero, one of the three dynamic modes that the prototype can be in. Then, in response to the timing and control signals generated as the prototype performs the signal enhancement process, the prototype will transfer back and forth between the operating modes. After an explanation of the timing circuitry of the prototype, the system operation in each of these modes will be explained in detail.

The timing circuits of the prototype are shown in Figure 13, accompanied by a representative timing diagram in Figure 14. When the main control switch is manually placed in the Start position, it provides a DC set signal to the CLOCK ENABLE flip-flop. This flip-flop, when set, provides an enabling level to the crystal-controlled clock oscillator which generates two sequences of narrow, positive-going pulses named T_A and T_B. These pulses occur at the rate of one million pulses per second, and T_A is delayed by one-half of the clock period (0.5 microseconds) relative to T_B. The circuit diagram of the clock oscillator is shown in Appendix II.

The two sequences of pulses are inverted by a pair of inverting buffer amplifiers. This inversion provides the T_A and T_B signals in a negative-going form, in addition to giving power gain. The negative-going T_B signal is used to shift bits into and out of the delay line and through the recirculating registers, A and B. Thus, each pulse of T_B corresponds to the entry of one data bit into and the exit of one data bit from the

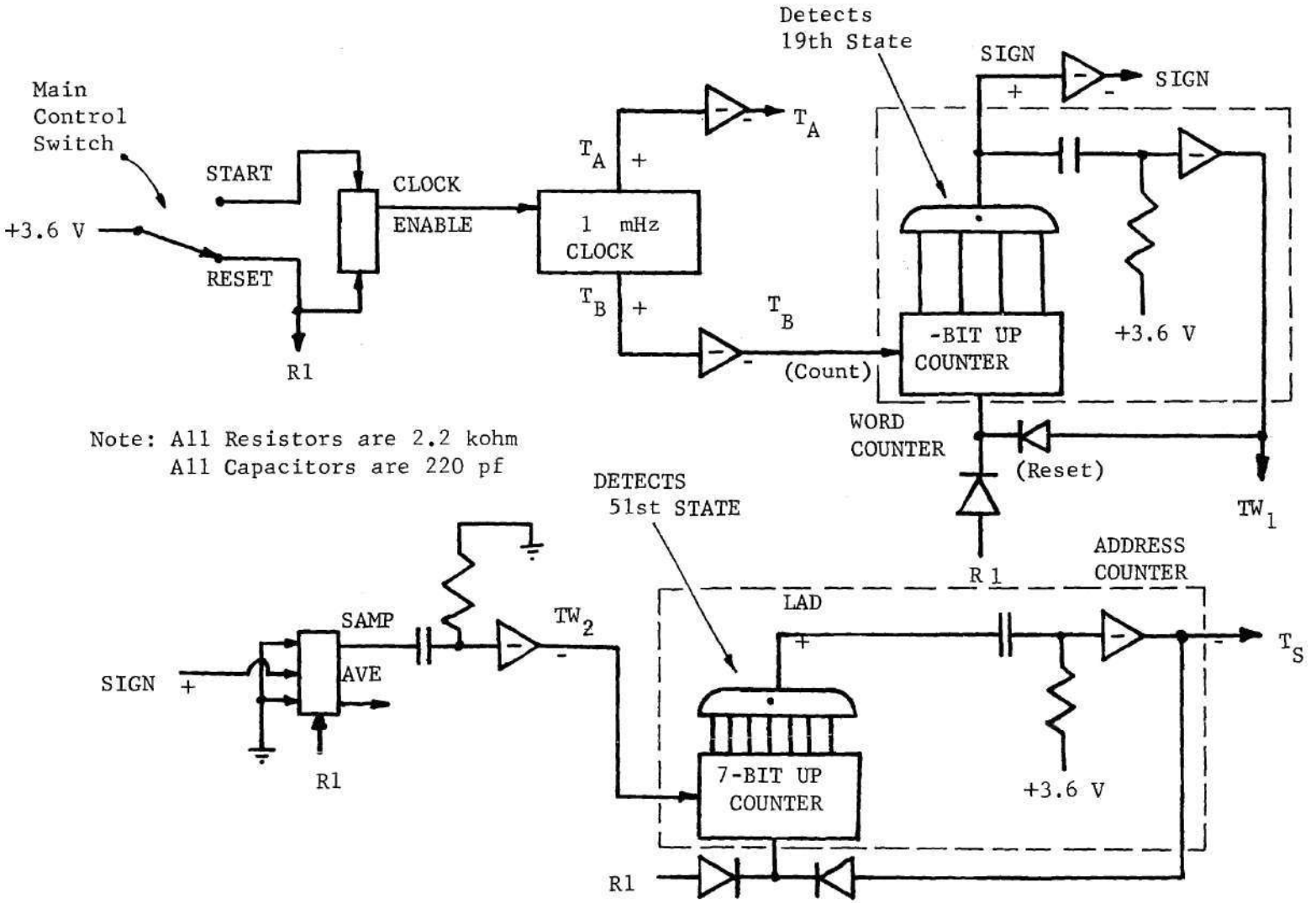

Figure 13. Timing Circuitry of the Prototype

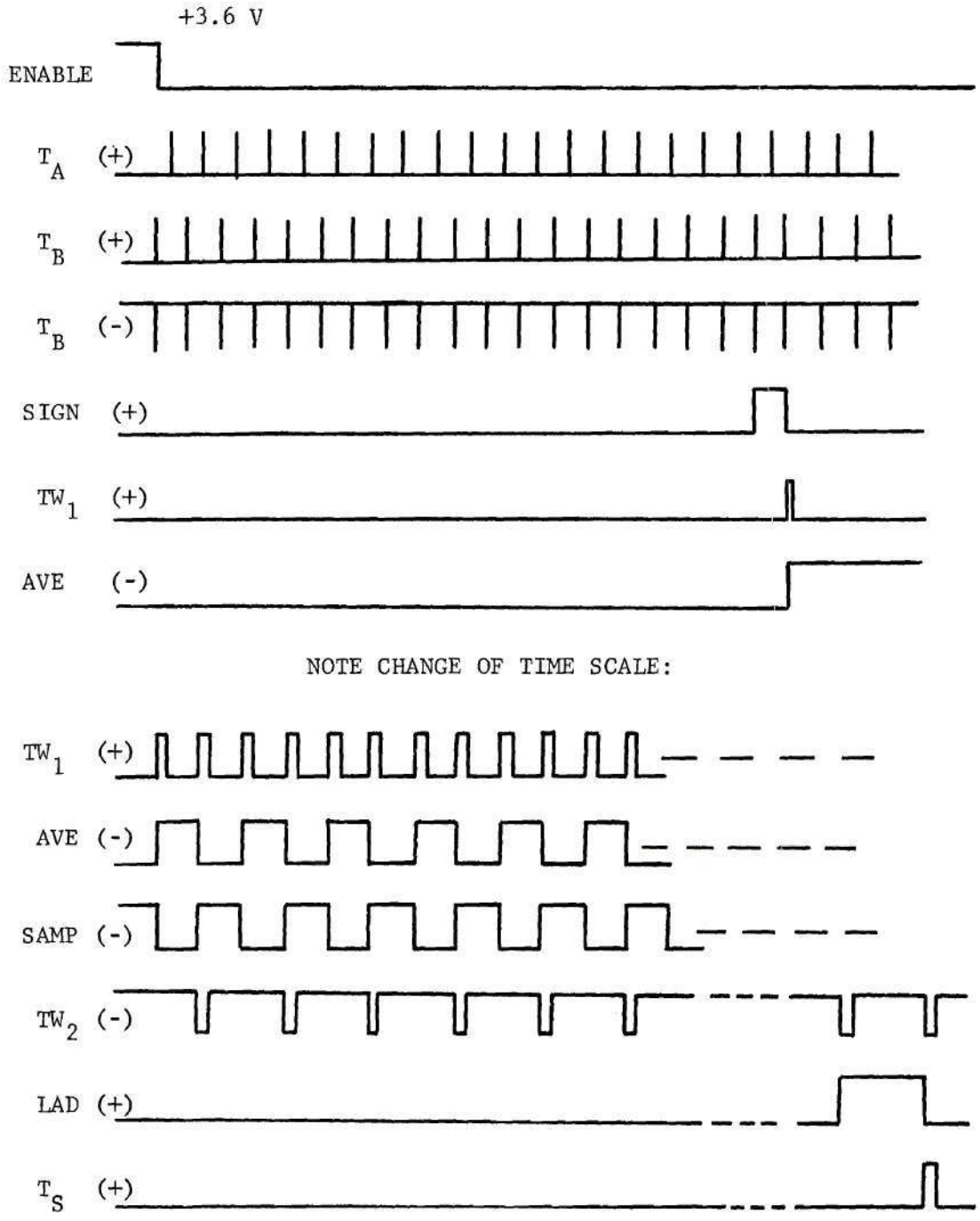

Figure 14. Timing Diagram of Circuitry shown in Figure 13

delay line.

Since each word that enters or leaves the delay line is 20 bits long, the sequence of pulses, T_B, is passed through a divide-by-twenty counter whose output pulses, named TW_1, will occur at the rate at which whole data words enter and leave the delay line. For this reason, the divide-by-twenty counter is referred to as the word counter. This counter is a five-bit binary counter that counts upward from zero toward 31. A gate detects when the counter reaches the 19th state and indicates this by making its output signal, named SIGN, transfer from zero volts to +3.6 volts. When the next T_B pulse counts the word counter to the 20th state, SIGN will return to zero volts, and that negative transition will be coupled through an R-C differentiation circuit and an inverting buffer amplifier to make one of the narrow, positive-going TW_1 pulses. This pulse will reset the word counter to zero, making the 20th state a transitional or momentary state. In this way, one TW_1 pulse is generated for each 20 T_B pulses given to the word counter.

As was mentioned previously, the words stored in the memory correspond to samples of the fetal complexes and the averaged waveform that have been coded in the two's-complement binary code. This code was chosen because of its usefulness in the serial arithmetic operations which the prototype uses in calculating the weighted average. This code uses one of the 20 bits that make up each word to represent the sign of the particular sample, leaving the remaining 19 bits to represent the magnitude of each sample value.

When these words are inserted into the memory of the prototype, they are shifted in with the least significant bit of their magnitude

field first and their sign bit last. This orientation is also for convenience during the arithmetic computations that the prototype performs. This explains the designation of the output of the gate that senses when the word counter reaches its 19th state as SIGN, since this logical signal will indicate when the last bit of each word is being shifted into or out of the delay line. This last bit is always the sign bit of the word.

The sample words which represent a new fetal complex and the words which represent the averaged waveform are interleaved when they are inserted into the memory of the prototype. Thus, the words that come out of the delay line have alternating meaning; a sample word from a new complex comes out every other word time, with a sample word from the averaged waveform in between. The arrangement is made in such a way that when the prototype begins its averaging calculation, each sample of the new fetal complex is stored in the memory of the prototype just after the sample of the averaged waveform with which it is to be combined. Thus, during the averaging calculation, when a particular average word has been shifted completely into Register A, the sample word that is to be combined with it will be the next word to shift out of the delay line output.

In order to keep track of which type of word is being shifted out of the delay line at any time, the signal SIGN is used to trigger a flip-flop. The set output of this flip-flop has been named SAMP, and the timing circuitry is synchronized so that when the SAMP flip-flop is set, one of the sample words from the fetal complex is being shifted from Register A into Register B. Conversely, when the flip-flop is reset, the word

being shifted into Register B is not a sample of a fetal complex; rather, the word will be one of the samples of the averaged waveform. Because of this, the output from the reset side of the flip-flop is renamed AVE, rather than merely using $\overline{\text{SAMP}}$ as the signal name.

The positive-going transitions of the signal SAMP are coupled through an R-C differentiation circuit and a buffer amplifier, generating a sequence of narrow, negative pulses named TW_2. These pulses indicate when a pair of words (one from a new fetal complex, one from the averaged waveform) has been shifted from the delay line into Registers A and B.

In order to keep up with which of the 51 pairs of words is coming out of the delay line at any time, the TW_2 pulses are used to step the address counter of the prototype. This counter is a seven-bit counter that counts up from zero toward 127. In the same way that the word counter is reset, a gate detects when this counter reaches the 51st state and, through the use of an R-C differentiation circuit and an inverting buffer amplifier, resets the counter to zero when the next TW_2 pulse steps the counter to the 52nd state. The output of this gate is called LAD, for Last ADdress. The LAD signal indicates when the last pair of words has been shifted into Registers A and B. The reset pulses to the address counter correspond to a complete recirculation of the data stored in the memory of the prototype and are named T_S.

The various pulse rates generated by the timing portion of the prototype are:

$$T_A = T_B = 1.00 \text{ mHz}.$$

$$TW_1 = T_B/20 = 50 \text{ kHz}.$$

$$TW_2 = TW_1/2 = 25 \text{ kHz.}$$

$$T_S = TW_2/51 = 491 \text{ Hz.}$$

The rate of T_S corresponds to a period of 2.04 milliseconds. This is a result of the two millisecond delay of the delay line plus the additional time required to shift a data bit through Registers A and B. Each of these timing pulses is provided to the rest of the prototype in both the positive-going and the negative-going form.

Operation in the Reset Mode

When the system is manually placed in the Reset Mode, the signal R1 is clamped to +3.6 volts. (See Figure 13.) In this mode, the digital clock is stopped and all registers, counters, and control flip-flops are held in their initialized state by coupling R1 into their DC reset inputs. When the main control switch is manually placed in the Start position, the CLOCK ENABLE flip-flop is set, allowing the system clock to start, and the mode register shown in Figure 15 is used to automatically transfer the system to Mode Zero. The signal CLOCK ENABLE also enables the setting of the MD_A flip-flop. After the switch is moved to the Start position, the first T_S pulse, coming 2.04 milliseconds later, will set the MD_A flip-flop shown in Figure 15. The set output of MD_A is logically combined with the reset output of the MD_B flip-flop, $\overline{MD_B}$, to form $M_0 = (MD_A \cdot \overline{MD_B})$. The signal M_0 indicates that the prototype is in Mode Zero.

Operation in Mode Zero

The function of this mode is to clear the delay line memory of

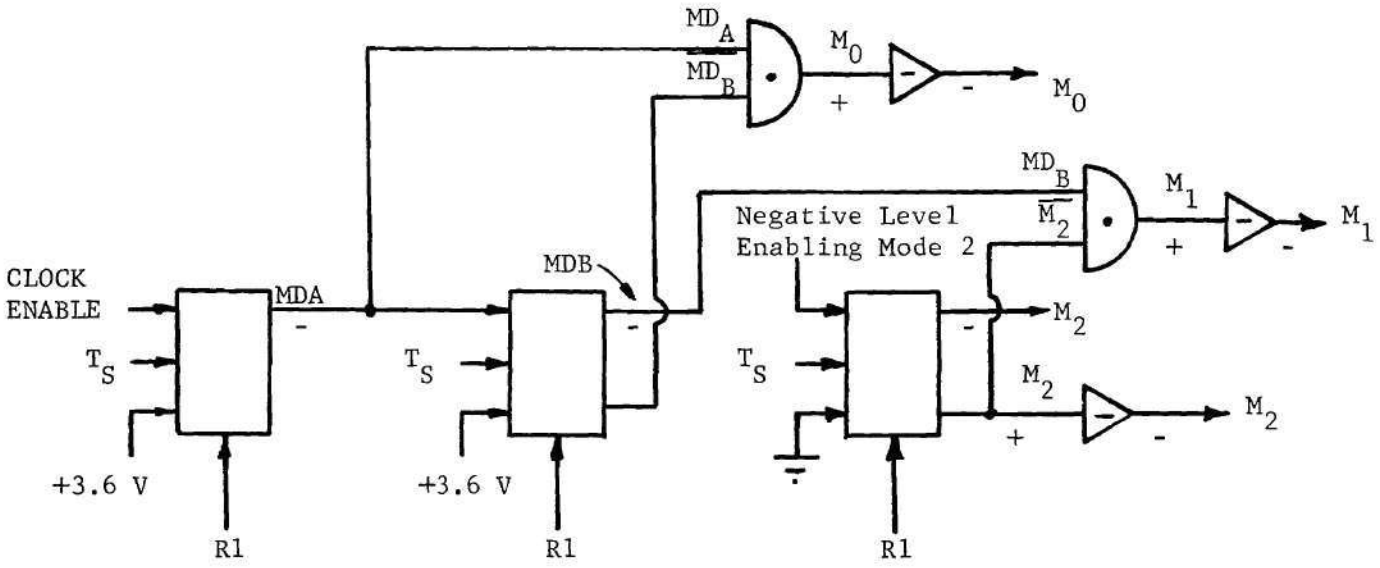

Figure 15. Mode Register of the Prototype

the prototype by filling all of the words in the memory with the digital code for zero (10000000000000000000). To do this, the normal recirculation path from Register B to the delay line input is not enabled. Rather, the input to the delay line is provided by the circuit shown in Figure 16, which couples SIGN into the delay line input when the prototype is in Mode Zero. Since the signal SIGN has a logical value of zero except when a sign bit should be shifting into or out of the delay line, this logical circuit will shift 19 zero-bits followed by a one-bit into each word location of the delay line memory. After 2.04 milliseconds, the second T_S pulse will set the MD_B flip-flop, turning off the signal M_0 and turning on the signal M_1. The M_1 signal indicates that the prototype is in Mode One.

Operation in Mode One

The prototype will be in Mode One for most of its operating period, for this is the mode in which the system samples the input signal and, by using threshold detection, identifies those fetal complexes that are free of distortion due to a nearby maternal complex. When in this mode, the analog-to-digital converter is used to sample the input signal and convert the samples into digital words representing the value of the samples.

The Analog-to-digital Converter

The analog-to-digital converter used by the prototype is of the successive approximation type; it is block diagrammed in Figure 17. The major items making up this type of an analog-to-digital converter are the storage register (Register C), the digital-to-analog converter (DAC), the

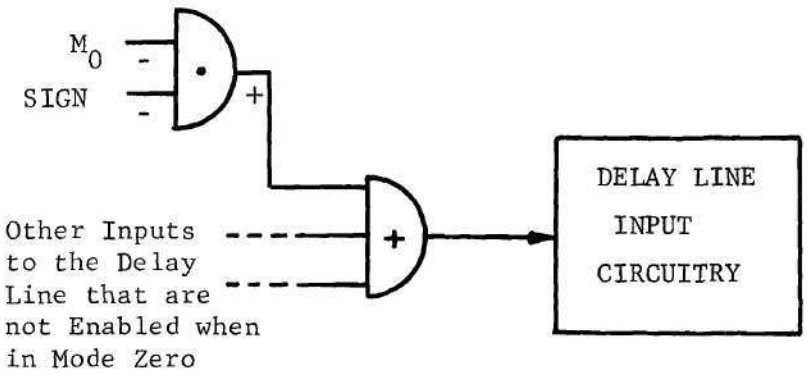

Figure 16. Delay Line Input Circuitry when in Mode Zero

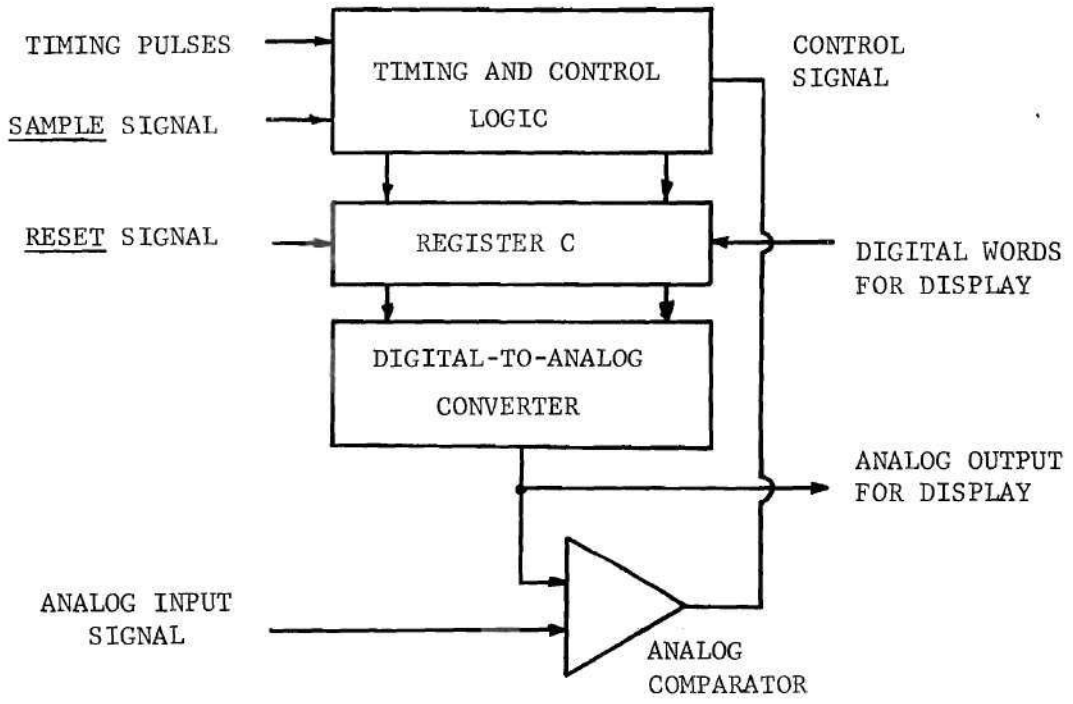

Figure 17. Block Diagram of Analog-to-digital Converter

analog comparator, and the timing and control circuitry. The digital word stored in Register C will provide input signals to the DAC so that, at any time, the output voltage from the DAC will have a magnitude and sign that correspond to the magnitude and sign of the word in Register C.

The conversion process is started by giving a RESET signal to Register C and then giving a SAMPLE signal to the timing and control logic of the ADC. The control circuit then systematically inserts digital values into Register C. By using the analog comparator to compare the output of the DAC to the analog input signal, the particular digital word that most closely represents the input signal value is found. At the end of the conversion cycle, the new digital word is transferred from Register C to the external storage register (Figure 12) for subsequent insertion into the memory. This frees the DAC for the remainder of the period between conversion cycles.

In the prototype, the same DAC is also used to display the averaged waveform. This is accomplished by shifting the sequence of average words into Register C as they come out of the delay line. The analog output voltage of the DAC is displayed on an oscilloscope that is triggered by the SAMPLE commands. During the first portion of each sweep (44 microseconds in the case of the prototype), the output voltage of the DAC is stepped up and down by the successive approximation process of the conversion. This portion of the display is blanked out by using the external cathode connection of the oscilloscope. The analog output during the rest of the period between samples (1996 microseconds for the prototype) will correspond to the sequence of values that are shifted into Register C to display the averaged waveform. Such an output waveform was shown

in Figure 10.

The circuitry of the analog-to-digital converter that is used by the prototype is shown in detail in Figure 18. This ADC converts the analog input signal to an eleven-bit word that is in the two's-complement code. The eleven-bit word uses one bit to represent the sign of the sample, leaving ten bits to represent the encoded magnitude. Thus, the input voltage is quantized into plus or minus 1024 (two to the tenth power) levels.

The DAC is of the ladder decoder type, and converts the two's-complement code word that is stored in Register C into a positive or negative analog voltage of the proper magnitude. The circuit diagram for this ladder decoder is given in Appendix II.

When the prototype is in Mode One, the T_S pulses are used to generate the SAMPLE commands. This results in a sample and convert operation every 2.04 milliseconds. The rate at which the conversion can be made is limited by the time required for the DAC output to settle each time the code word in Register C is changed. In the case of the prototype, the settling time of the DAC limited the conversion rate to one change of Register C every four microseconds, or 250 kHz. This rate is provided by dividing the rate of the T_B pulses by four, giving a pulse rate of 250 kiloHertz, labeled $T_B/4$ in Figure 18.

Each SAMPLE pulse sets the T_0 flip-flop. The negative transition associated with T_0 being set is coupled through an R-C differentiation circuit and an inverting buffer amplifier to generate a narrow positive pulse, R2, that resets both Register C and the eleven-bit shift register that is part of the ADC timing and control circuitry.

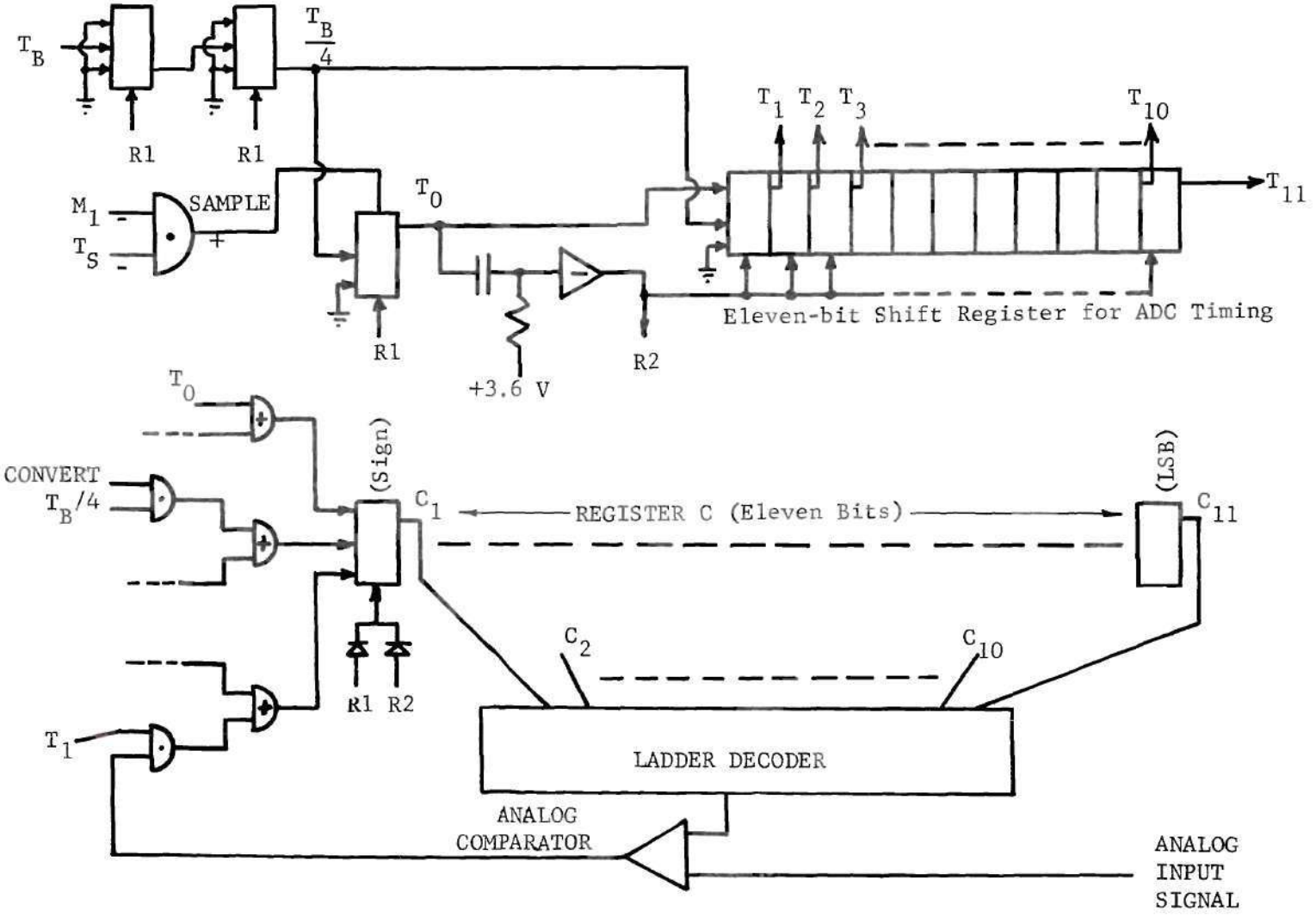

Figure 18. Detailed Block Diagram of the Analog-to-digital Converter

The first transition of $T_B/4$ that comes after the SAMPLE signal will reset the T_0 flip-flop. It will also set the first flip-flop of the eleven-bit shift register, labeled T_1. Since T_0 provided an enabling level, the $T_B/4$ signal will also set the sign bit in Register C, labeled C_1, making the contents of Register C be 10000000000, the two's-complement code for zero. During the conversion cycle the signal CONVERT is used to switch the $T_B/4$ pulses to the transition inputs of all of the flip-flops that make up Register C.

During the period when the T_1 flip-flop is set, the output voltage of the DAC settles to zero volts. If the analog input signal is more positive than the DAC output, the output signal from the analog comparator will prevent the resetting of the C_1 flip-flop. The next transition of $T_B/4$ will shift the one-bit in the eleven-bit shift register to the right, turning off T_1 and setting the T_2 flip-flop. The T_1 signal will have enabled the C_1 flip-flop to be reset unless the analog comparator inhibited the resetting. Thus, if the analog input signal is positive, the sign bit of Register C will remain set; otherwise, the sign bit is reset, indicating a negative sample value.

The T_1 signal will also set the flip-flop of Register C that represents the most significant bit, C_2. This will cause the output of the DAC to settle to a new voltage. When the next $T_B/4$ transition takes place, T_2 is set and the C_2 flip-flop will either be reset or left set, depending upon the output from the analog comparator.

The remaining timing pulses, T_3 through T_{11}, will be generated as the one-bit is shifted through the eleven-bit shift register. Each of these timing pulses will set one of the bits in the magnitude portion of

Register C. This bit will be reset by the next timing pulse if the comparator indicates that it makes the analog output of the DAC too positive. At T_{10}, the least significant bit is being determined, and the external storage register that will hold the converted word is reset as shown in detail in Figure 19. This external storage register was first shown in Figure 12. The last timing pulse, T_{11}, gates the digital word from Register C into the external storage register.

During this transfer, the eleven-bit words generated by the ADC are expanded into twenty-bit words. These additional bits are used to expand the magnitude area of the coded word, as shown below.

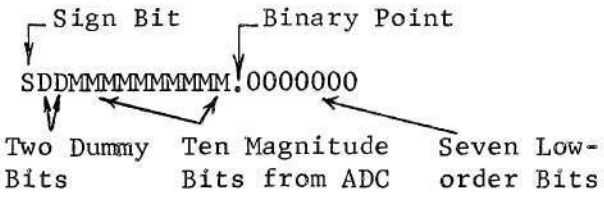

The two's-complement magnitude of the code word will be unchanged provided that the two high-order dummy bits are filled with a logical value opposite to that of the sign bit, $\overline{\overline{C_1}}$. This is accomplished by the gating circuitry shown in Figure 19. The two high-order dummy bits are required by the threshold detection scheme, as will be discussed later in this chapter. The seven low-order dummy bits are initially filled with zeros, and are necessary to prevent the loss of accuracy during the averaging calculations which the prototype performs. These bits are used to carry the fractional magnitudes that arise during the averaging computations of the prototype, and are discussed more fully later within Chapter IV.

The transfer of the converted word frees Register C. During the

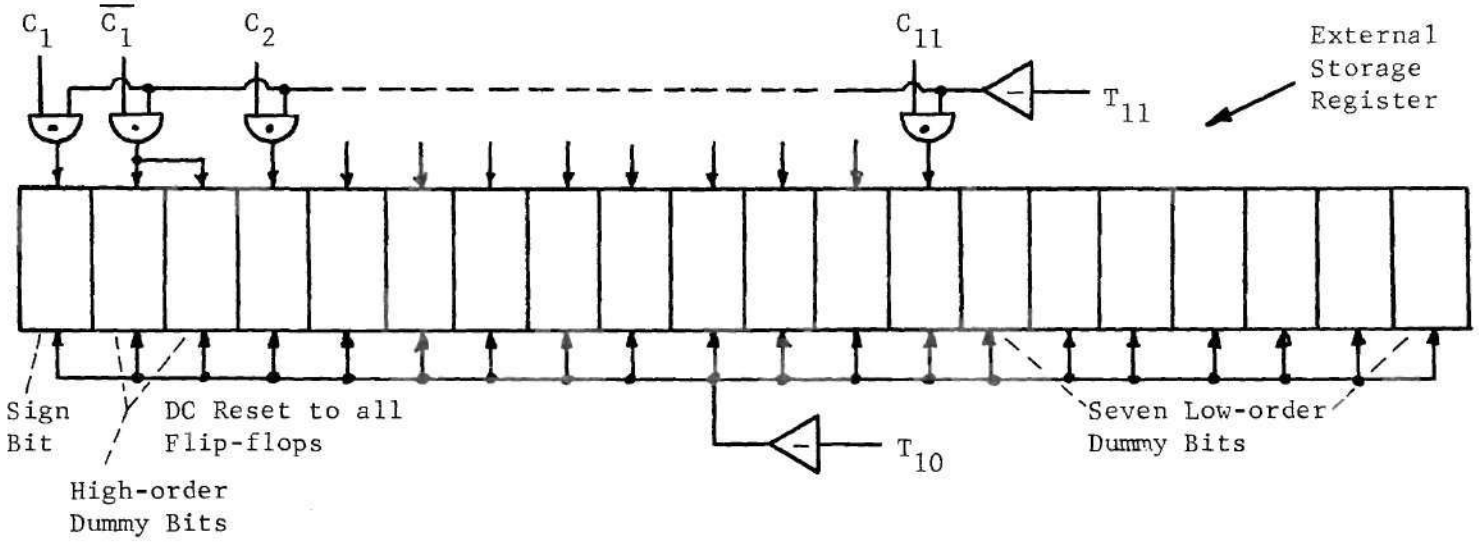

Figure 19. Parallel Transfer of the Converted Word

remainder of the 2040 microseconds before the next conversion, Register C is used to display the accumulated average waveform, in conjunction with the DAC and an oscilloscope. This is accomplished by waiting until each of the words that makes up the average waveform has been shifted out of the delay line and into Register A. At that time, the word is transferred in a parallel fashion into Register C. The circuitry for this is shown in Figure 20.

The signal T_{AD} is formed by the logical combination $(M_1 \cdot SAMP \cdot SIGN)$ and will only be present when the last bit (sign bit) of an average word is being shifted into Register A. At that time, the bits labeled A_0 and A_3 through A_{12} are switched to the enabling inputs of Register C by the T_{AD} signal. These are the sign bit, A_0, and the ten most significant magnitude bits, A_3 through A_{12}, of the code word, with the dummy bits, A_1 and A_2, and the seven low-order magnitude bits, A_{13} through A_{19}, not included in the transfer. The signal T_{AD} also switches a single T_B pulse to the transition inputs of all of the flip-flops of Register C, thereby transferring the bits present at the enabling inputs into these flip-flops. The DAC then settles to the analog voltage that corresponds to the digital code word in Register C.

The waveform that is generated at the DAC output is smoothed to eliminate its step-like discontinuities (resultant from the sequence of discrete values that represent the average waveform) by using a low-pass filter. If the time scale of the DAC output were equivalent to real time, a filter of about 50 Hertz would do. In the case of the prototype, the DAC output corresponds to 94 milliseconds of real time that are presented every 1.88 milliseconds. This is an increase in the time

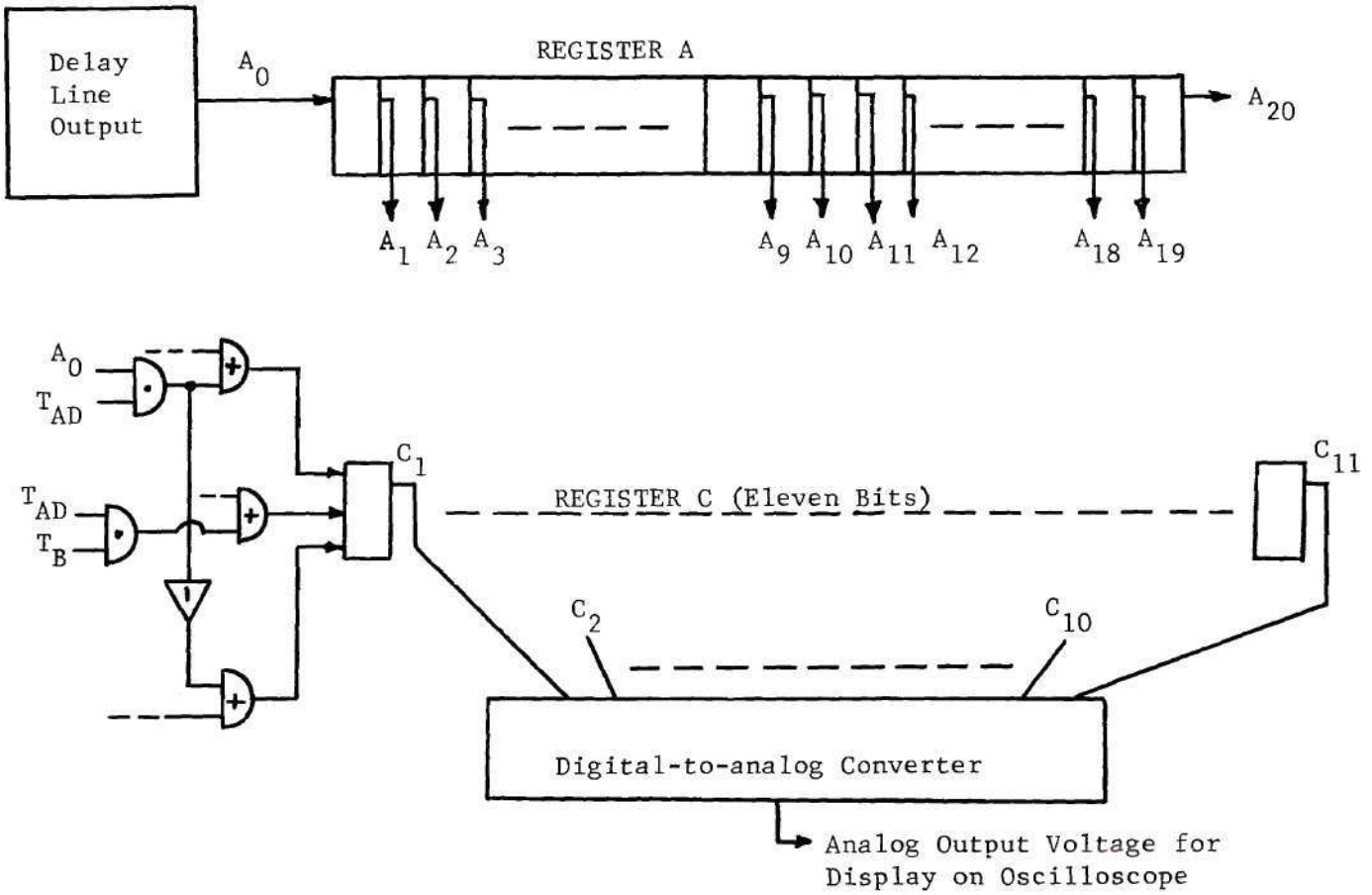

Figure 20. The Display of the Average Waveform

scale of 51, so that a filter with an upper cutoff frequency of 51 × 50 = 2550 Hertz is used.

During the display of the averaged waveform, the ladder decoder (Appendix II) that is used by the prototype as its DAC generates narrow transient spikes at certain transition points between successive average words. These transients result from the fact that the transistor switches that control the ladder decoder network have a longer turn-off time than turn-on time. When the bits of a new word are shifted into Register C, the one-bits in the new word turn on the transistor switches of the ladder decoder that correspond to their binary weights; the zero-bits of the new word turn off the rest of the transistor switches.

Due to the longer turn-off time of the transistor switches, the transistors that were turned on by the previous word in Register C will remain on briefly after the transistors that are turned on by the new word do turn on. During this brief overlapping period, the ladder decoder output will be the voltage represented by the code word formed by combining all of the one-bits in the two successive words. This value may be quite different from the values of either of the actual code words.

These transients are most noticeable when successive average words are near zero, e.g., one word equal to plus zero (10000000000) and the following word equal to minus one (01111111111 in two's-complement code). Then, even though the two successive words are only one quanta apart, their combination during the transient period will be 11111111111, the code word for plus full-scale (+1023). The transient spike would reach from the baseline to the top of the oscilloscope screen in this case.

Because of their extreme narrowness, these transients appear much

like impulse functions to the low-pass smoothing filter used to present a continuous version of the averaged waveform. Hence, even with a properly chosen low-pass filter, these impulse-like discontinuities cause distortions of the smoothed output waveform. These distortions appear as "bumps" in the waveform corresponding to the time-domain response of the low-pass filter when driven by an impulse. In order to eliminate the effect of these discontinuities, a sample-and-hold circuit has been constructed, and is used to sample the output of the DAC. These samples are taken during the period between transitions and thus do not show the effect of the transitional spikes. The output of the sample-and-hold circuit is then filtered in order to give the continuous waveforms that are seen in Figure 10 and Chapter VI. The circuit diagram of the sample-and-hold circuit is shown in Appendix II.

The Storage Cycle of Mode One

When the prototype is in Mode One, the data words that are stored on the delay line are recirculated in two different ways. The words that represent samples of the average waveform are recirculated without a change in address. They are shifted into the delay line and, 2000 microseconds later, emerge from it and are shifted through Registers A and B and back into the delay line. This recirculation path is shown in Figure 21.

As was stated above, the SAMP/AVE flip-flop is controlled so that AVE is present whenever one of the average words is being shifted from Register A into Register B. This word will shift out of Register B during the following word time; the SAMP signal will be present at that time. As shown in Figure 21, the SAMP signal is used to allow each average word

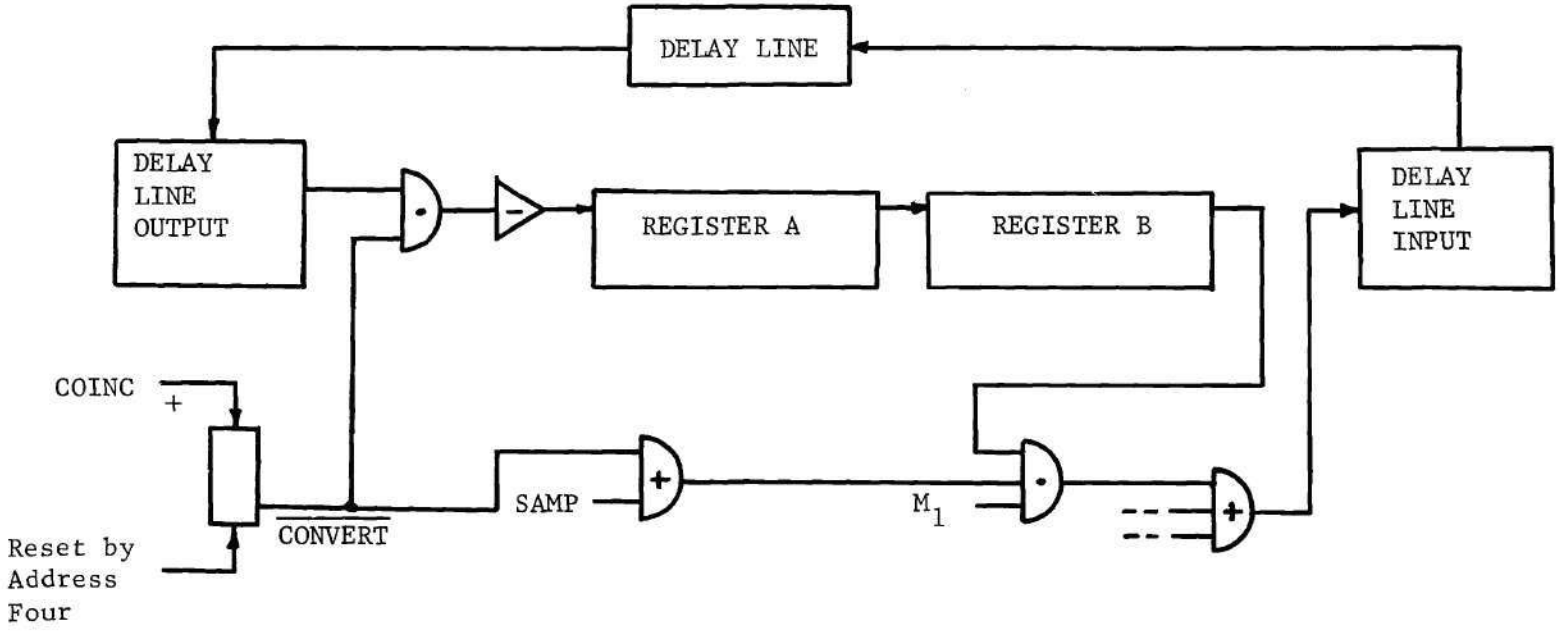

Figure 21. Delay Line Input when in Mode One

to shift into the delay line as it is shifted out of Register B. The samples of the new complex, which shift out of Register B between the average words, are not shifted into the delay line, since SAMP is not present at that time. Whenever the signal CONVERT is present, however, the output of Register B is shifted into the delay line. This is required during the entry of each new sample of the fetal complex (computed by the ADC) into the memory, and will be explained below.

The flip-flop that is used to generate the CONVERT signal that indicates when the ADC is in operation is also shown in Figure 21. This signal is used to block the data coming out of the delay line during the conversion process of the ADC. The ADC and the delay line output sensing circuit share a common power supply in the prototype, and, due to transients introduced during the ADC conversion cycle, the delay line output circuit would occasionally make an erroneous decision. The CONVERT signal, by blocking the delay line output, prevents any information from being taken from the line.

The CONVERT flip-flop is set by the COINC signal which is generated as the last sample word is shifted out of Register B just prior to each T_S pulse. Thus, CONVERT is present for 20 microseconds prior to the start of each conversion cycle (started by T_S). The CONVERT flip-flop is reset when the address register reaches address number four. Since the address counter is reset to zero by T_S and counts up as each pair of words is shifted out of the delay line, address four will be reached 160 microseconds after each T_S pulse (four pairs of words $\times$ 40 microseconds per pair). The blanking out of these four pairs of words reduces the storage capability of the prototype from 51 to 47 pairs of words, which

is the number required by the prototype for storage of the samples of the average waveform and the new fetal complex.

While the average words are circulated without change in address, the sample words from the fetal complex are stored in a "push-down" manner so that only the more recent samples are kept in the memory. In order to accomplish this, the delay line recirculation loop is shortened, as far as the sample words are concerned, by the circuitry shown in Figure 22. When the signal AVE is present, a sample word from a fetal complex is being shifted from the delay line into Register A. The previous sample word has passed through Registers A and B and would normally be shifting into the delay line. In Mode One, however, the sample words are passed directly from the delay line output to the delay line input, bypassing the two twenty-bit registers. This, in effect, advances each sample word by one address during each recirculation of the delay line. The oldest sample value is shifted from address four into address three, one of the address locations that is blocked by the CONVERT signal. This word will be lost when it emerges from the delay line output.

The most recent sample of the fetal complex will be moved from address 50 (the last address) to address 49. At that time, the new sample word that the ADC has calculated is inserted into the just vacated address 50 by the circuitry shown earlier in Figure 12. This new word had been transferred to the external storage register at the end of the ADC conversion cycle (Figure 19). The signal LAD is present during the time when the last pair of words is being shifted out of Registers A and B. When LAD and SAMP are both present, the last sample word will be shifting out of Register A and into Register B. This same word will have already been

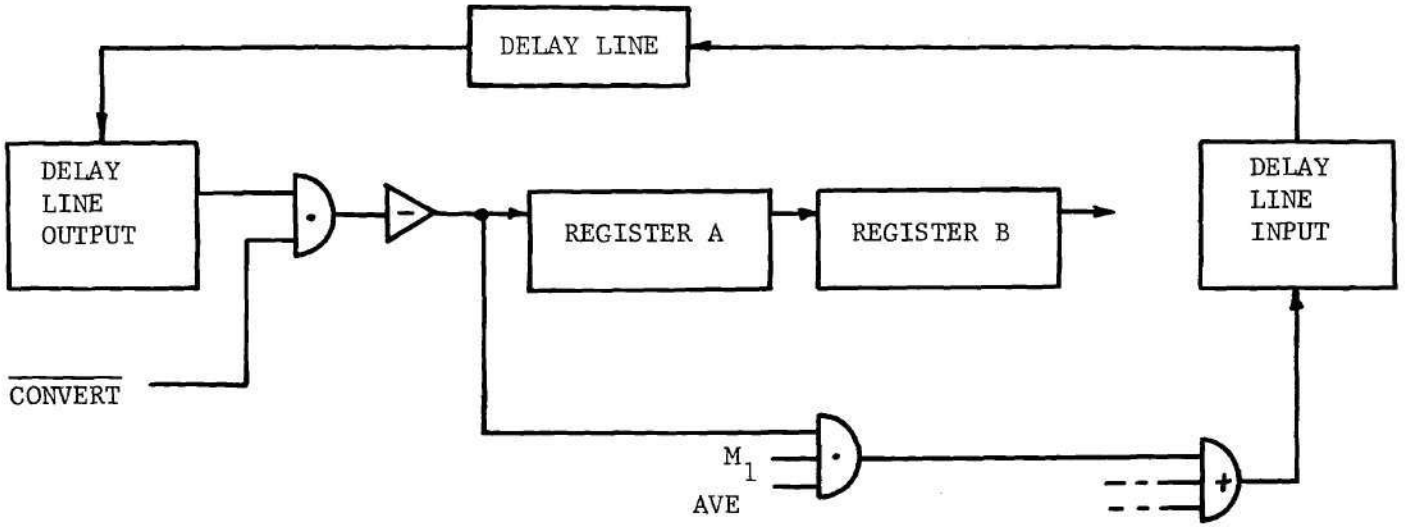

Figure 22. Delay Line Input when in Mode One

shifted into the delay line by the direct path shown in Figure 22, taking address 49.

The coincident presence of LAD and SAMP is used to produce the signal COINC, which switches the input of Register B between Register A and the external storage register. Since COINC is present, the new sample word is shifted into Register B, taking the place that was occupied by what had been the most recent sample value from the fetal complex. Normally, the path from Register B to the delay line is blocked, as far as the sample words are concerned, whenever the prototype is in Mode One. The newest word is shifted on into the delay line, however, since the signal CONVERT is present. (See Figure 21.) The CONVERT flip-flop is always set by COINC.

In this way, the 47 most recent samples of the fetal complex are stored in the sample word of the word pairs addressed from four through 50. The oldest of these is always in address four; the most recent is always in address 50.

The Threshold Detection System

The threshold detection system for locating the fetal peak and the maternal peak is shown in Figure 23. The clock pulses to the serial adder and its output shift register are combined with SAMP (when not in Mode Two) so that addition occurs only when the sample words from the fetal complex are appearing serially at the upper input to the adder. At the start of a delay line revolution, the SUM flip-flop is reset by T_S, thus switching the SIGN signal to the lower input of the adder. Since SIGN is a serial representation of the digital code for zero, the adder output will be the sum of each sample word and zero, i.e., the sample word

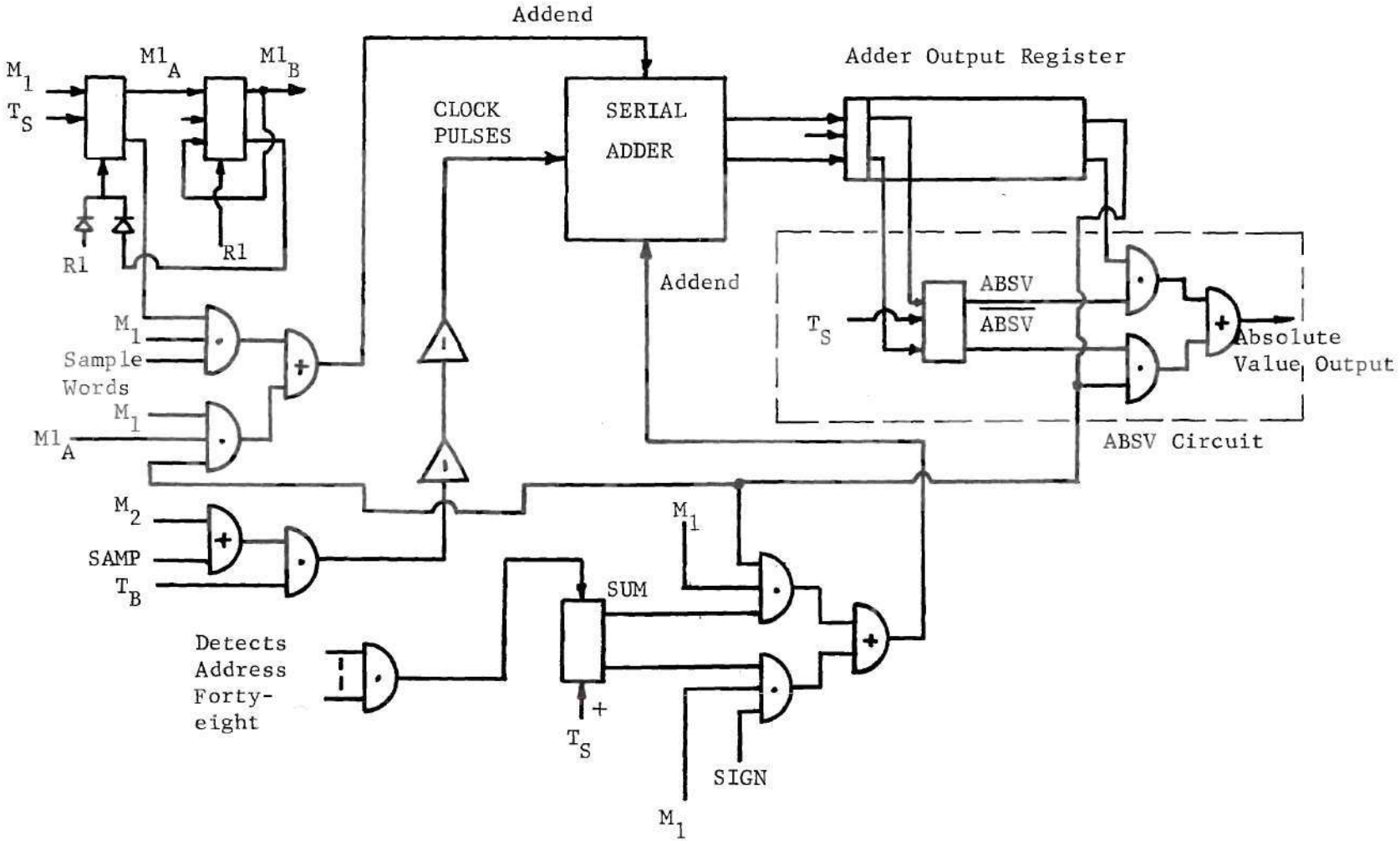

Figure 23. Summation/Absolute Value Circuit for Threshold Detection

itself. Each sum is shifted into the adder output register as it leaves the adder.

When address 48 is reached, the SUM flip-flop is set and the adder operation changes. At that time the 49th sample word is added to the word stored in the adder output register, which is sample number 48. The sum of these two is then stored in the adder output register and sequentially added to samples number 50 and 51 by the closed loop addition circuit. Then, when T_S resets the SUM flip-flop at the end of address 51 (the last address), the adder output register contains the summation of the four most recent samples. The two high-order dummy bits are used during this summation since the sum of the four words may be four times the maximum value for one word. The two high-order magnitude bits of the expanded words will carry this increase in magnitude.

The T_S pulse also sets the $M1_A$ timing flip-flop and, if the sign of the summation word stored in the output register is negative (indicated by a zero sign bit in the adder output register), then the T_S pulse sets the ABSV flip-flop to generate the absolute value of this word for threshold comparison. The signal $M1_A$ will be present until $M1_B$ is set by the next TW_2 pulse (which will come two word times later), as shown in the timing diagram of Figure 24. During $M1_A$, the absolute value of the summation of the four most recent sample words is shifted out of the output register of the adder by way of the ABSV circuit. If the ABSV flip-flop is set, all of the bits of the sum are inverted by the ABSV logic as they shift out. This converts any negative sum to its one's-complement positive form. Since the sum is originally in the two's-complement code, an error equal to one low-order bit is introduced by this simple complement-

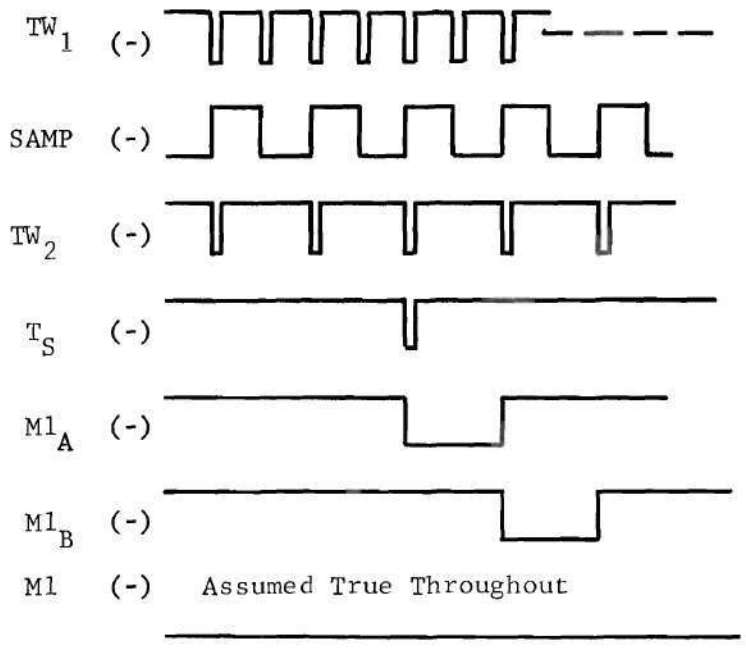

Figure 24. Timing Diagram of Circuitry of Figure 23

ing method. There are exact schemes for doing this complementation, but since the error introduced by this approximation is so small, the simplest hardware scheme was implemented in the prototype.

As the absolute value of the sum is shifted out of the ABSV circuit, it is added back into the serial adder. The other addend is zero again, since the SUM flip-flop was reset by T_S. At the end of $M1_A$, therefore, the adder output register will contain the absolute value of the summation of the four most recent sample values. This summation is compared to the two thresholds in order to identify the fetal and maternal R-peaks.

The sum of four samples, rather than individual sample values, is used for the threshold comparison in order to avoid a problem that was uncovered during the computer simulation. As was explained in Chapter III, once the lower threshold is crossed, the system continues to examine the input sample values until a peak value is reached and then takes more samples until a sample counter reaches one of two possible upper limits. Because of this, the peak of the input signal will always have the same position within the 47 sample aperture that is thus taken about the fetal R-peak. In the simplest threshold detection scheme, this peak will always be the largest value among the 47 values stored on the delay line. This largest value will in general be located near the true fetal R-peak, and, as the computer simulation showed, will usually have a value as large or larger than the true amplitude of the fetal R-peak. This is a result of the simple threshold detection scheme. Whenever the true fetal R-peak is diminished by noise, the fact that it is reduced makes it a poor candidate for the peak value. Rather, a nearby sample value

that has a larger magnitude due to additive noise will be selected as if it were the true peak of the fetal complex. Thus, when each group of 47 sample values is included in the average, the value at the location of the peak sample will almost always be larger than the fetal R-peak, and no negative cancellation of the noise will result at this single point. This led to "spiking" of the average waveform as shown in Figure 25.

This spiking effect is avoided by using the summation of four sample values for comparison with the threshold. As explained above, each new sample value is added to the last three sample values and their sum used for the threshold comparison. This diminishes the effect that the noise can have on recognizing the center point of the fetal complex and eliminates the spiking effect.

The threshold comparison and sampling aperture locating circuitry is shown in Figure 26. When the prototype first enters Mode One, the ENAB flip-flop is reset and the combination ($\overline{\text{ENAB}}\cdot$M1) enables the counting of the six-bit up counter. This counter is stepped by T_S so that it counts once every sampling time (2.04 milliseconds). This counter will count upward, but will be reset when it reaches an upper limit that is detected by the LAD2 gate in the same way that the word and address counters were reset. The upper limit is set by the CENTER/AFT switch shown in Figure 26. When in the AFT position, this switch connects the 32-bit from the counter directly into the LAD2 gate. Thus, since the 4-bit and the $\overline{\text{1-bit}}$ are always connected to that gate, the counter will be reset when it leaves the 36th state whenever the AFT aperture is selected.

When the selection switch is placed in the CENTER position, the LAD2 gate is connected to the 32-bit when the ENAB flip-flop is reset

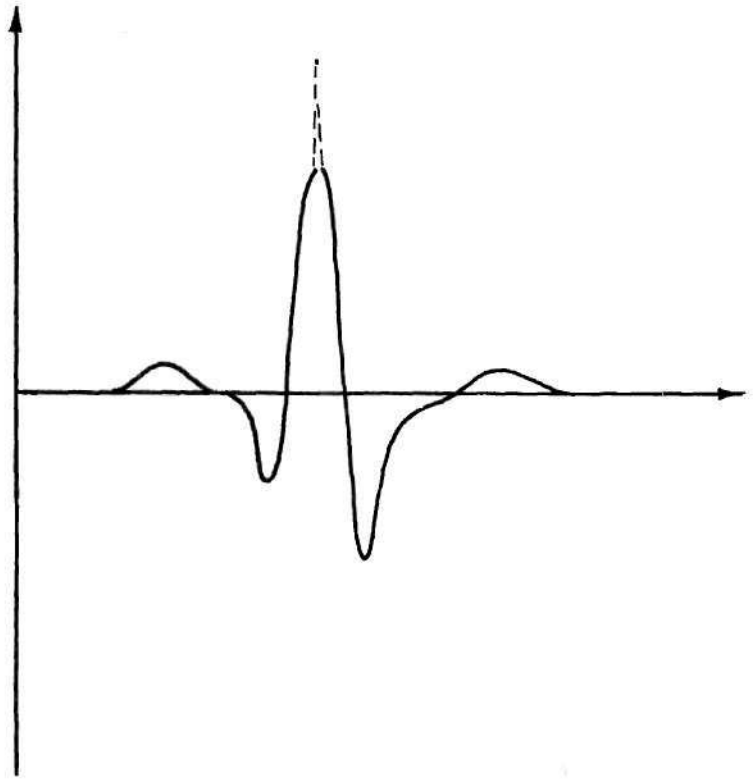

Figure 25. Illustration of the Spiking Effect

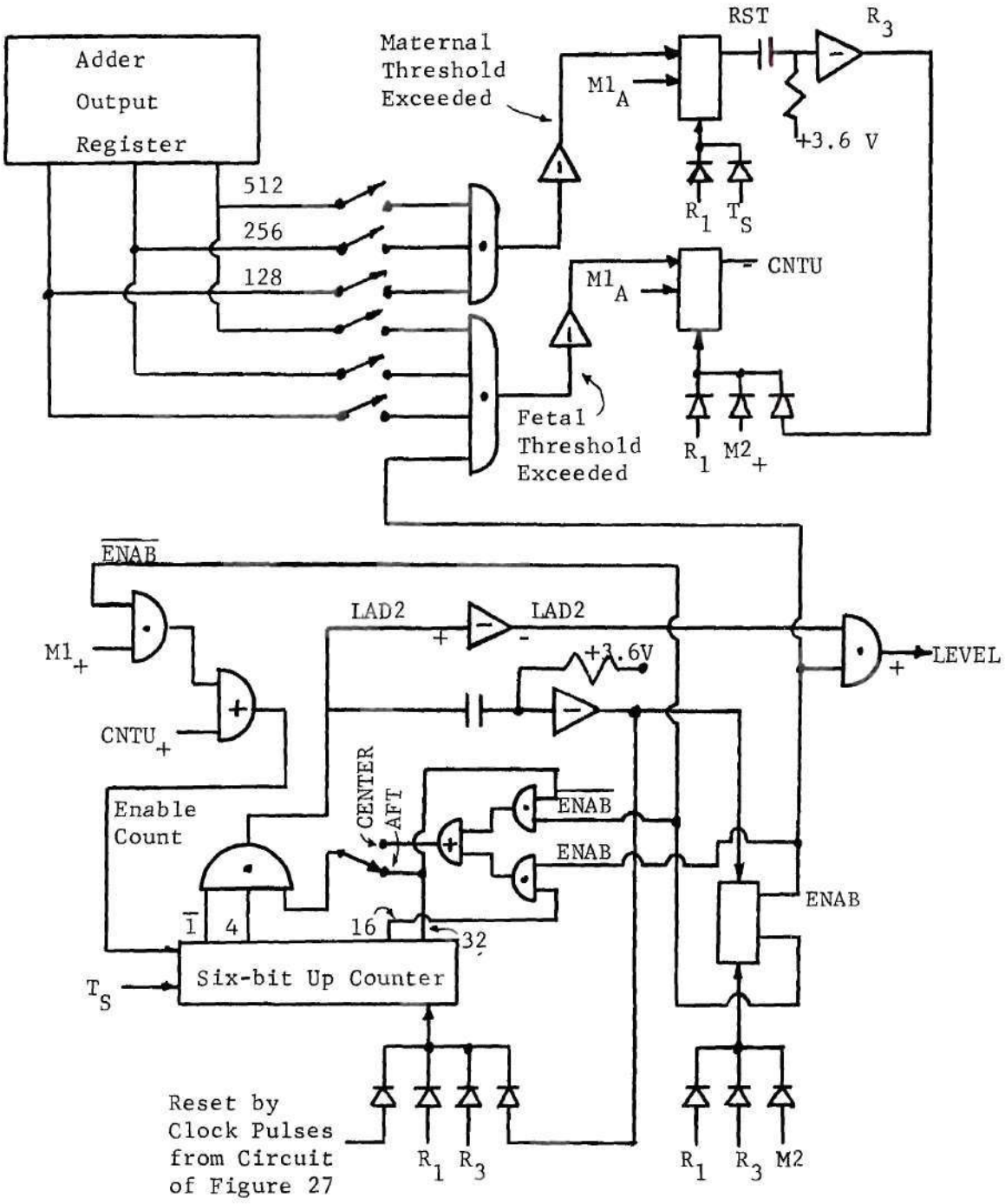

Figure 26. Fetal and Maternal Threshold Detection Circuitry

and to the 16-bit when the ENAB flip-flop is set. Thus, the upper limit on the count is 37 prior to the setting of the ENAB flip-flop and 21 after it is set. Thus, whenever the prototype enters Mode One, 37 samples are taken prior to the generation of the LAD2 signal, whether the CENTER or the AFT aperture is selected. The falling transition of the LAD2 signal, generated as the six-bit counter leaves the 36th state, is coupled through a differentiation circuit and an inverting buffer amplifier to generate a reset pulse which returns the counter to the zero state. This reset pulse also sets the ENAB flip-flop, thereby turning off the enabling signal that allows the six-bit counter to count. This counter will remain in the zero state until the circuitry shown at the top of Figure 26 detects a crossing of the lower threshold.

The fetal detection gate is disabled by the ENAB signal while the first 37 samples are taken and stored. This initial group of samples partially fills the 47 addresses within the push-down sample storage area of the memory of the prototype before the detection of a fetal peak by the lower threshold detector is enabled. Thus, a sufficient number of samples is always included ahead of any fetal peak that is detected so that the sampling aperture will be full. When the ENAB flip-flop is set after the first 37 samples are taken, the fetal detection gate will be enabled, and will indicate whenever the summation stored in the adder output register at the end of the $M1_A$ signal contains the high-order bits corresponding to the switch closures at the gate input. Normally, only the most significant bit switch is closed, making the fetal threshold equal to one-half of full scale, since any summation with the most significant bit present will make the gate output true. The gain of the FECG

amplifier (or the tape recorder) is then adjusted so that the fetal complexes present in the input signals to the prototype will cross this threshold. When the lower threshold is exceeded, the CNTU flip-flop is set at the end of $M1_A$.

Once CNTU is set, the six-bit counter will again be enabled for counting. It will try to reach its maximum state, but will be reset if the upper threshold is crossed or the fetal waveform increases above the value that first crossed the lower threshold. Whenever the maternal threshold gate indicates that the upper threshold has been crossed, the RST flip-flop will be set at the end of $M1_A$. The maternal threshold is usually set at 87.5 per cent of full scale, corresponding to the three most significant bits being present in the summation. When RST is set (indicating a crossing of the upper threshold), it generates R3, resetting CNTU, ENAB, and the six-bit counter, and thereby returning the SES to the state it was in upon first entering Mode One. The system will proceed to take 37 more samples and then look for a fetal peak as before. RST is reset by the following T_S pulse.

The resetting of the six-bit counter by the increasing fetal waveform is accomplished by the comparison circuitry shown in Figure 27. During $M1_A$, as the absolute value of the summed sample words is shifted from the ABSV circuit, the logical combination of $(T_B \cdot SAMP \cdot M1_A)$ provides clock pulses to perform a serial comparison between this sum, as it shifts out of the ABSV circuit, and the value stored in the comparison register. This register is initially set to the zero code. At the end of $M1_A$, the AGRB flip-flop will be left in a set state if the sum is greater than the value in the comparison register. As stated above, during $M1_A$ the sum is

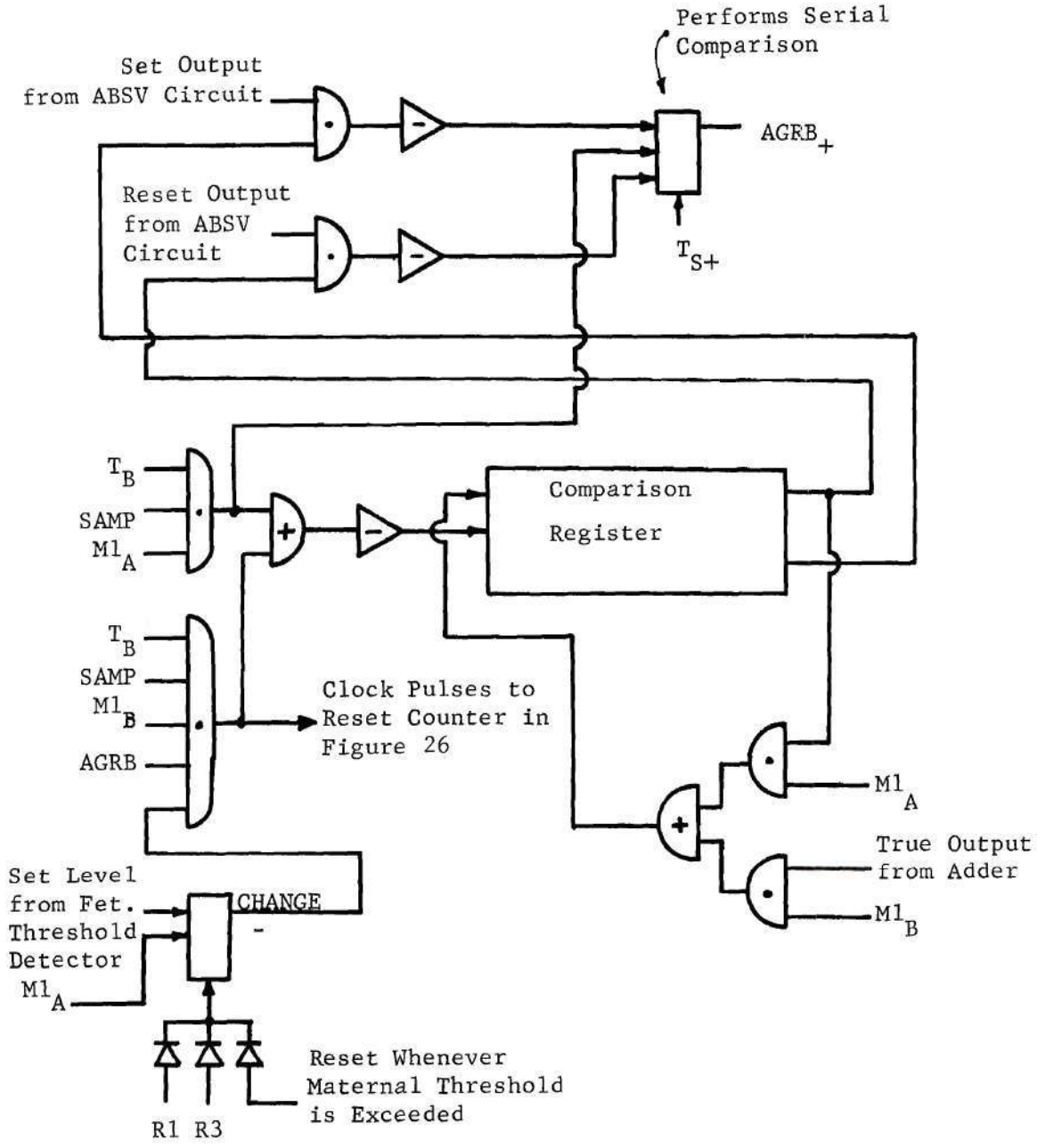

Figure 27. Comparison Circuitry for Threshold Detection

recirculated through the adder and will be back in the adder output register. The value in the comparison register will also have been recirculated back into that register during $M1_A$.

When the fetal threshold gate indicates a crossing of the lower threshold, the same logic that set CNTU will set the CHANGE flip-flop, and during $M1_B$ the value in the adder output register will be shifted into the comparison register if the AGRB flip-flop is still set. If not, the value in the comparison register will be left unchanged. If the sum is greater than the value in the comparison register, the shift pulses that move the sum from the adder output register into the comparison register during $M1_B$ will also reset the six-bit counter of the previous figure.

Thus, each time a summation of samples is greater than any previous sum, the six-bit counter is reset and the new sum stored for comparison with subsequent sums. Only after a peak has been reached will the six-bit counter be allowed to reach its maximum count. Since this counter is stepped by T_S (the SAMPLE command to the ADC), each count corresponds to a new sample value being stored in the memory of the prototype. The push-down process continues, so that a number of samples equal to the upper limit determined by the LAD2 gate will be taken following the peak. This limit is 37 for the AFT aperture and 21 for the CENTER aperture (since ENAB is set) as was explained above. Thus, when the AFT aperture is selected, the 47 sample aperture will have 37 samples following the peak and ten samples prior to it. The rest of the 37 samples that were in the storage area prior to the peak will have been "pushed" out of the memory and lost. When the CENTER aperture is selected, the

47 sample aperture has 21 samples that follow the peak and 26 taken prior to it.

When the upper limit of the six-bit counter corresponding to the desired aperture location is reached, LAD2 and ENAB are logically combined to produce the signal LEVEL which will enable the last flip-flop in the mode register (Figure 15) to be set by T_S. This will turn off M_1 and turn on the signal M_2. The CHANGE flip-flop will be reset by R3 (maternal threshold crossed) or by M_2. The AGRB flip-flop is reset by T_S prior to $M1_A$ coming on. Thus, if there is no maternal interference, the system will take either 37 or 21 more samples after the largest group of values of the fetal R-peak and then, with the 47 sample words of the memory located with the desired relationship to this peak, will enter Mode Two.

Operation in Mode Two

The prototype remains in Mode Two for one recirculation of the delay line (2.04 milliseconds) during which time the sample values stored on the delay line are added into the accumulated average. At the end of the delay line cycle, the T_S pulse resets the M_2 flip-flop of the mode register (Figure 15) and returns the prototype to Mode One. Sampling of the input signal then resumes in accordance with the explanation of the operation in Mode One given above.

The basic function of the computational portion of the SES was described in Chapter III. The circuit that the prototype uses to perform this computation is shown in Figure 28. As stated previously, whenever the signal AVE is present, an average word is being shifted from Register

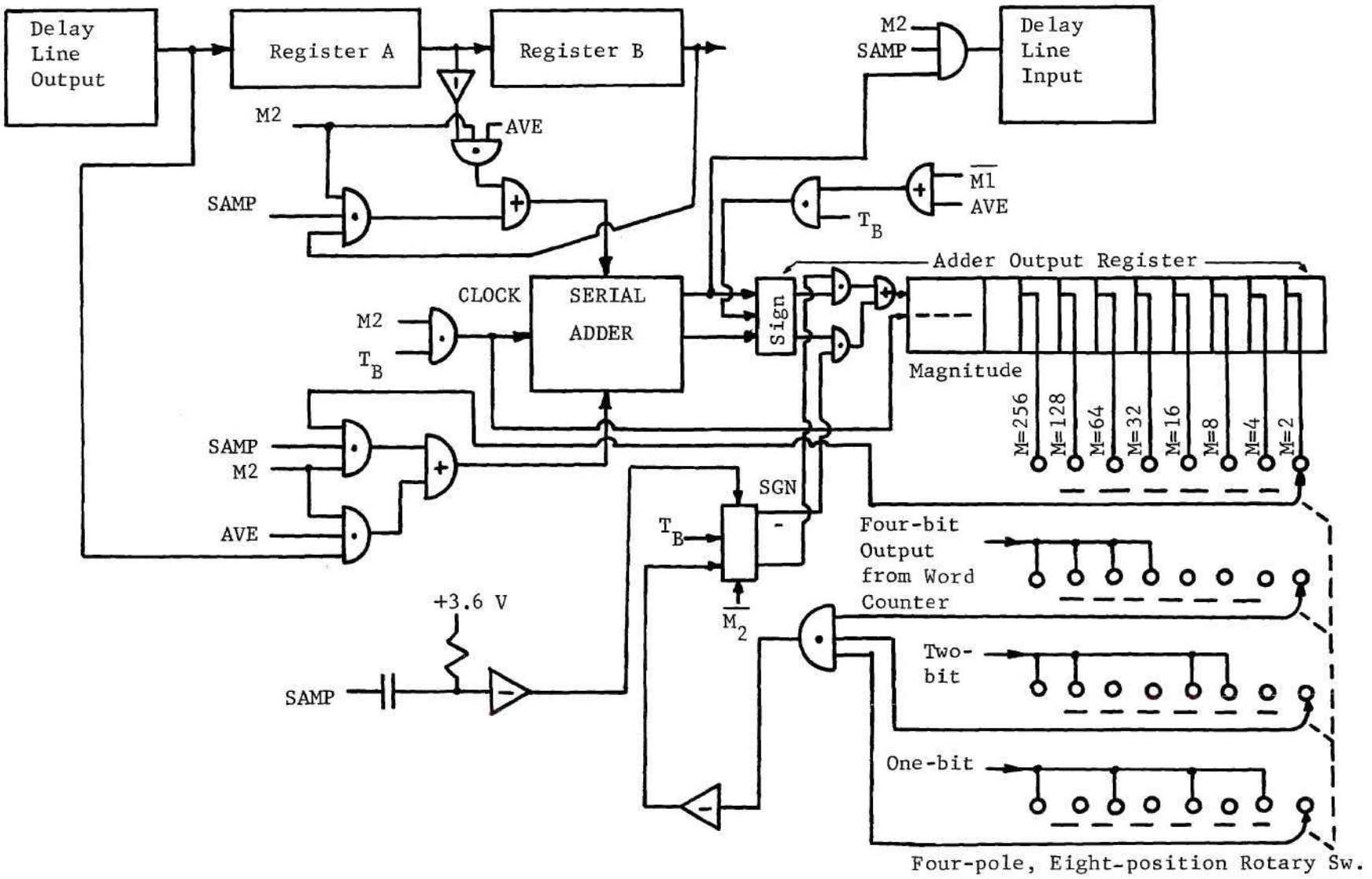

Figure 28. Mode Two Division Circuitry

A into Register B. At this time, when in Mode Two, each average word is logically inverted (equivalent to multiplication by minus one with an error of one least significant bit) and serially added to the sample of the fetal complex which follows it out of the memory. This sample word is taken directly from the delay line output at the same time that the average word is shifting from Register A into Register B.

The sum of these two words, $(Complex_n - Ave_{n-1})$, is shifted into the adder output register. In Mode Two, the adder output register is separated into a sign flip-flop and 19 magnitude flip-flops. The sign bit is clocked separately by logical circuitry that provides shift pulses to it only during AVE time. Thus, during SAMP time, the magnitude bits will shift to the right while the sign bit remains in the same place. This separated shifting process is used to perform the divide-by-M function.

The SGN flip-flop is reset whenever the prototype is not in Mode Two and hence bits are shifted from the sign flip-flop of the adder output register to the magnitude portion with no inversion. At the end of each AVE time when in Mode Two, however, the negative transition associated with the setting of the SAMP flip-flop is differentiated and inverted to generate a positive pulse that sets the SGN flip-flop. The SGN flip-flop, when set, causes a logical inversion of the bits that are shifted from the sign bit portion of the adder output register into its magnitude area. This inversion is a dictate of the two's-complement code, for, as the magnitude area is shifted away from the sign in order to give repeated division by two, the high-order bits must be filled with bits whose logical values are opposite to the sign bit.

Consider the two's-complement code for plus 24:

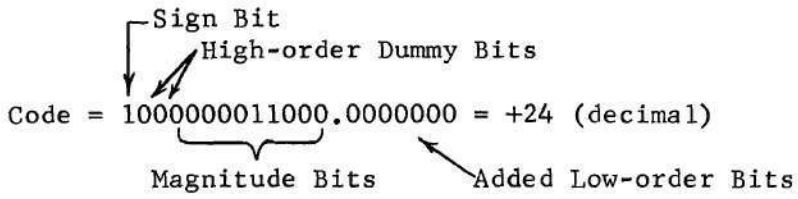

After one shift of the magnitude area the code becomes:

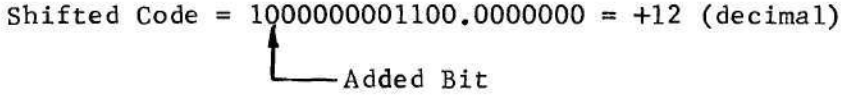

which is equivalent to 12, or one-half of the original value. Note that the high-order bit was filled opposite to the sign bit value. This division process works for either positive or negative numbers.

During this separated shifting process, the additional low-order bits which are added to each sample word are used to prevent the loss of accuracy because of round-off errors. If no low-order bits are added, the accuracy of the computed average words becomes degraded because of this round-off error. As stated above, the division process is used to calculate DELTA/M, where each DELTA word is:

$$\text{DELTA} = (\text{Complex}_n - \text{Ave}_{n-1}) \quad . \tag{7}$$

If the DELTA words are kept at their original ten bits of magnitude, one of the magnitude bits is lost each time a shifting of the magnitude field (corresponding to division by two) takes place. The number of bits that would be lost in a division by M would be $\log_2 M$, e.g., if M is 128, seven bits would be lost.

This loss, if not eliminated by carrying low-order magnitude bits, will introduce a "dead zone" into the calculation of DELTA/M. Whenever a positive DELTA word was so small that all of its bits would be lost during the shifting process, then the apparent value of DELTA/M would be zero. This would mean that the averaged waveform could never get closer to the true value of the fetal complex than the magnitude of this dead zone, since the correcting effect of the DELTA/M factor upon the average waveform would be reduced to zero by the division process. In fact, any positive portion of the fetal complex that was below the dead zone would never be detected at all, since its magnitude would be lost entirely during the calculation of DELTA/M. The size of the dead zone for various values of weighting factor is shown in Table 2. Also, as an indication of the effect of this dead zone upon the recovery of the fetal complex, Figure 29 shows the size of the dead zone for various values of weighting factor relative to the P, R, and T portions of a fetal complex.

The relative sizes of these three waves were taken from one of the few reported fetal waveforms that included a fetal T wave. This waveform was reported by Hon (8) and was observed by coherent averaging of complexes obtained from a direct attachment to the fetal scalp. Figure 30 shows the resulting portions of these waves that would be detected by the prototype at M = 32 and M = 128. Clearly, without the addition of the low-order bits, the dead zone effect would make the prototype unable to detect the low-voltage portions of the fetal complex when the weighting factor was made large in order to get good signal-to-noise enhancement.

For negative DELTA words the division process introduces a some-

Table 2. Effect of Weighting Factor on Width of Dead Zone

Weighting Factor	Width of Dead Zone (Counts)	Width of Dead Zone (Per Cent of Full Scale)
1	1	0.10
2	2	0.20
4	4	0.39
8	8	0.78
16	16	1.56
32	32	3.13
64	64	6.25
128	128	12.50
256	256	25.00
512	512	50.00
1024	1024	100.00*

*All of Fetal Complex Lost in Dead Zone

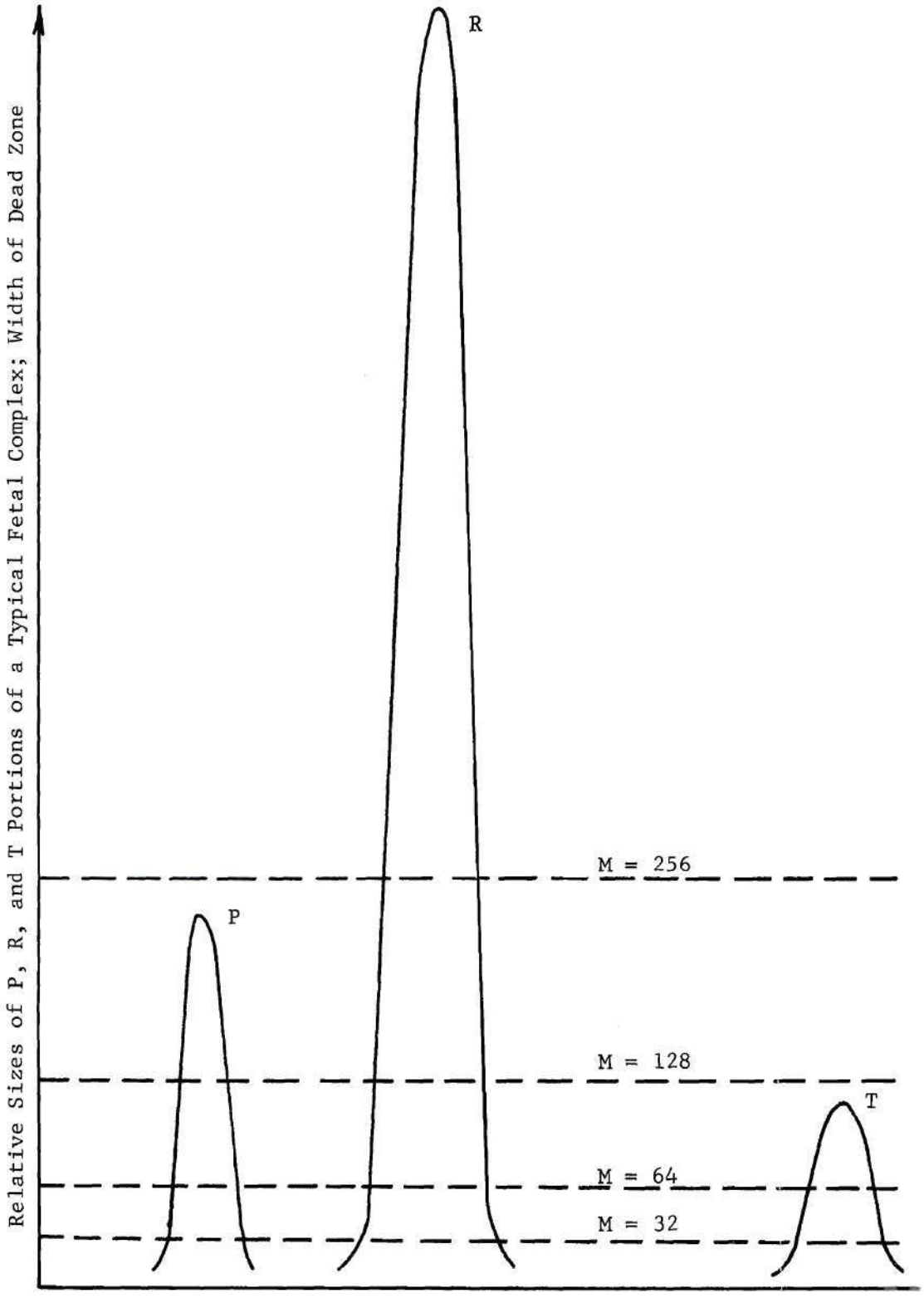

Figure 29. Width of Dead Zone for Various Weighting Factors

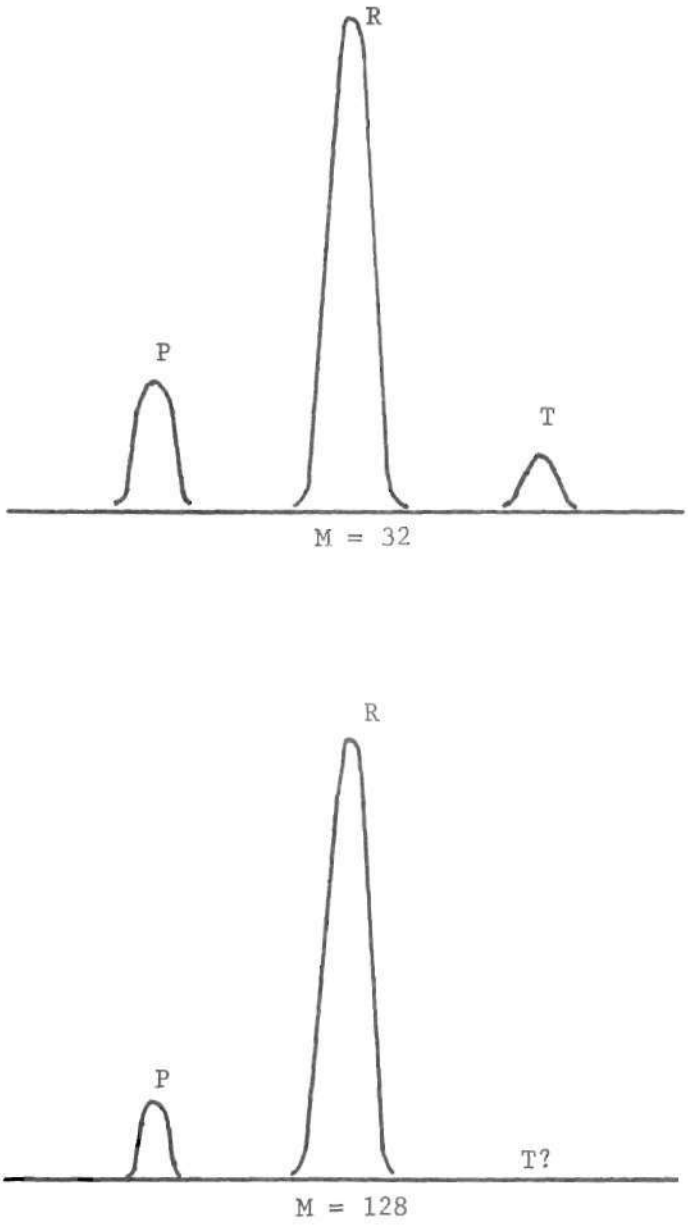

Figure 30. Portions of Typical Fetal Complex Recovered by Prototype

what different effect. For negative numbers the two's-complement code words would become equal to minus one (01111111111) if the significant bits of the magnitude field are completely shifted away. This will prevent the formation of a dead zone, since any negative DELTA word will cause a negative change in the average word no matter how large the weighting factor. The effect of the division process is to decrease the apparent weighting factor, however, since all fractional negative values of DELTA/M are increased to minus one. Thus, for example, when the proper magnitude of DELTA/M should be -3/64, corresponding to a DELTA word of -3 and M = 64, the value of DELTA/M would be calculated as -1. This apparent weighting factor would be <u>three</u> rather than 64. Thus, for small negative signal values, and hence, small negative DELTA words, the weighting factor of the system would not be large enough to accomplish the signal-to-noise enhancement that would be necessary to view the true fetal signal. The additional low-order bits, by allowing the DELTA/M words to take on magnitudes that are less than one, prevent this increase in weighting factor.

The number of bits that must be added to the low-order end of the words is determined by the maximum weighting factor that is to be implemented. In the case of the prototype this was M = 128. Since division by 128 corresponds to shifting the magnitude portion of each DELTA word seven bits to the right, seven additional bits must be added below the ten significant bits of the sample words from the ADC. In general, the number of bits which must be added is equal to $\log_2 M_{max}$, where M_{max} is the largest weighting factor that is to be available. (Note: In the prototype, the division process included M = 256, even though only seven

low-order bits were added. This inclusion of M = 256 did not require any additional hardware within the division portion of the prototype and, because of this, the M = 256 setting was included even though the additional bit was not added to the sample words.)

As the magnitude area of the adder output register is shifted during SAMP time, a rotary switch selects the proper point at which to pick off the quotient resultant from the division process. For example, to divide the code by four, the output is taken from the third stage of the register, as:

Two Additional Bits to be Inserted Here

Code = 1000000011000.0000000 = +24

Output Taken Here = +6

The pick-off point is adjusted to come ahead of the bits that will be lost during the division process. During the shifting process the word counter (Figure 13) counts in accordance with the number of T_B pulses that have occurred. Using the output bits of the word counter, the same rotary switch selects the inputs to a gate that resets the SGN flip-flop at the proper time. The SGN flip-flop then allows the true value of the sign bit to be shifted out after the correct number of dummy bits have been inserted during the division process. In this way a serial division takes place. The divisor is limited to powers of two, however, with a capability ranging from $2^1 = 2$ to $2^8 = 256$ in the prototype.

As the $(Complex_n - Ave_{n-1})/M$ word shifts out of the division circuit, the average word that makes up part of it will be shifting out of Register B. These two words are summed by the serial adder, and the sum:

$$Ave_n = Ave_{n-1} + \frac{(Complex_n - Ave_{n-1})}{M} \quad , \qquad (8)$$

is shifted into the delay line in place of the old average word. This process continues for each of the 47 pairs of average and sample words. At the end of the cycle the system returns to Mode One.

This cycle of modes, Mode One to Mode Two and back, continues as long as the system is operating and can detect the fetal R-peak. The averaged waveform accumulates and is displayed on an oscilloscope as explained above. The enhanced fetal complex may then be seen. The weighting factor can be changed whenever the system is not in Mode Two, and the accumulated average may be reset by using the main control switch whenever desired.

Construction of the Prototype

Figure 31 shows the manner in which the prototype of the SES was constructed. The approximate total hardware requirements are:

Flip-flops	172
Dual-NAND Gates	86
Inverting Buffer Amplifiers	62
Total Integrated Circuits	320.

The approximate cost of each of these components is one dollar. The total system cost is estimated below:

Integrated Circuits	$ 320
Miscellaneous Hardware	500
Power Supplies	500
Delay Line	150
Approximate Total Cost (Excluding Labor)	$1470.

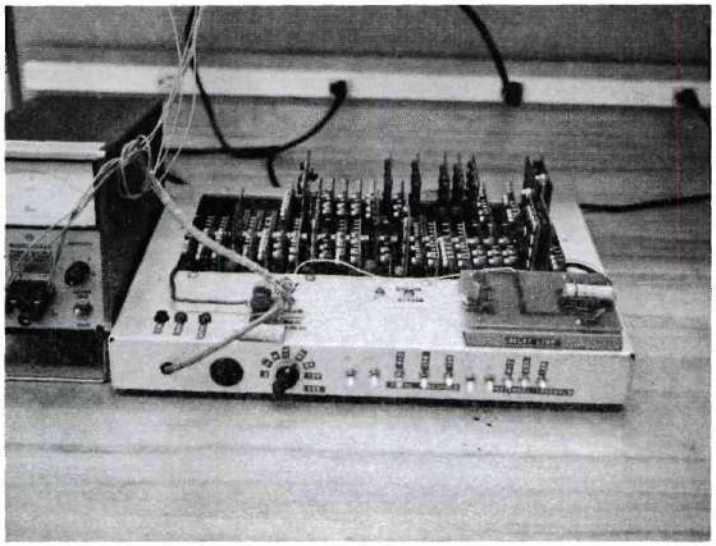

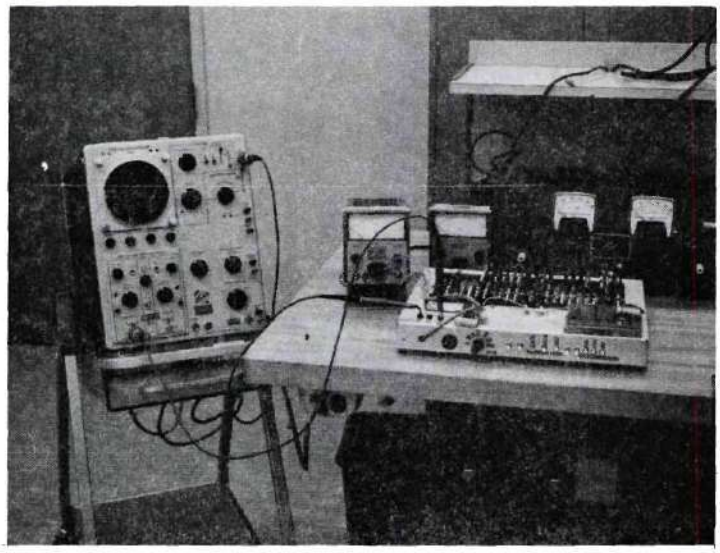

Figure 31. Photographs of Prototype

Since the hardware used by the previous signal enhancement systems costs over 6,000 dollars, it appears that a marketable version of the SES would not cost any more than the previous systems and could be somewhat cheaper.

CHAPTER V

COMPARISON OF COHERENT AVERAGING METHODS

Coherent averaging is a technique for improving the signal-to-noise ratio of repetitive signals that must be detected within a noisy environment. The averaging process consists of combining many repetitions of the signal in such a way that the true signal reinforces itself. The noise, if it is random in nature, will not add at the same rate as the signal, and an improvement in the signal-to-noise ratio will result. There are three major techniques for performing this coherent averaging. The following chapter discusses and compares each of these.

The Equally Weighted, Nonrunning Average

This is the simplest of the techniques in that it requires a minimum of storage and computational capability. Let S(t) represent a repetitive signal that is present along with noise, N(t). If S(t) is exactly periodic, a sampling of the noisy signal can be folded back on itself at the period of the true signal. Let S_i be one of the repetitions of the signal, i.e., one of the fetal complexes in FECG data. The sequence (S_1, S_2, . . .) may then be summed and, if the signals were taken at a rate equal to the repetition rate of the true signal, the true signal will reinforce itself algebraically in the summation. In other words, after n repetitions of the signal have been summed, the true signal present in the summation will be increased to n-times its original strength, as:

$$\text{Signal}_n = S_1 + S_2 + \ldots = n \times S \quad , \tag{9}$$

where Signal_n is the signal present in the summation, n is the number of repetitions, and S is the true signal strength (assumed constant).

The noise, since it is random and not related to the sampling rate, will not add algebraically. Rather, it will add in an rms manner as:

$$\text{Noise}_n = (N_1^2 + N_2^2 + \ldots)^{1/2} = \sqrt{n} \times N \quad , \tag{10}$$

where Noise_n is the noise present in the accumulated signal after n repetitions have been combined, and N is the true noise level (also assumed constant).

The new signal-to-noise ratio is:

$$\left.\frac{\text{Signal}}{\text{Noise}}\right|_{\substack{\text{After}\\\text{Averaging}}} = \frac{n}{\sqrt{n}} \times \frac{S}{N} = \sqrt{n} \times \left.\frac{\text{Signal}}{\text{Noise}}\right|_{\substack{\text{Before}\\\text{Averaging}}} \tag{11}$$

Thus, the signal-to-noise ratio can be improved any desired amount by including a large number of samples in the average.

If the characteristics of the signal are not exactly uniform, however, the signal will change somewhat during a very long averaging period. For this case, typified by electrocardiograph signals, the longer sampling periods are not very informative since the change in the signal characteristics over the period reduces the theoretical effectiveness of such long accumulations. Rather, some compromise is made, and the average is accumulated over a finite number of samples, say X, at which time the enhanced signal waveform may be observed and the accumulation reset and

started again.

The value of X is set depending upon the stability of the signal waveform and the signal-to-noise enhancement desired. The input signal is usually attenuated by 1/X so that the signal strength of the accumulated waveform will be the same as the true signal value. This follows from (9) where:

$$\text{Signal}_X = X \times \frac{S}{X} = S \quad , \tag{12}$$

when the input signals are attenuated by 1/X and the average is only accumulated over X samples.

A schematic implementation of this averaging system is shown in Figure 32. The only information which must be stored is the accumulated average. The only computational capability required is the addition process shown in Figure 32, since the attenuation can be provided by a precision resistive divider.

This sampling and accumulating process is equivalent to convolution of the noisy input signal with a sequence of impulse functions that are spaced by the period of the repeated signal. Such an impulse train is shown in Figure 33. If the signal is not periodic, an adaptive scheme must shift these impulses so that they occur with the same aperiodicity as the signal. Some repeatable characteristic of the aperiodic signal must be used to identify when a particular sample should be taken. In the case of FECG data, the fetal R-peak serves this purpose.

During the enhancement process, the gain in signal-to-noise builds up from one (after only the first sample) to $\sqrt{X}$ at the end of the avera-

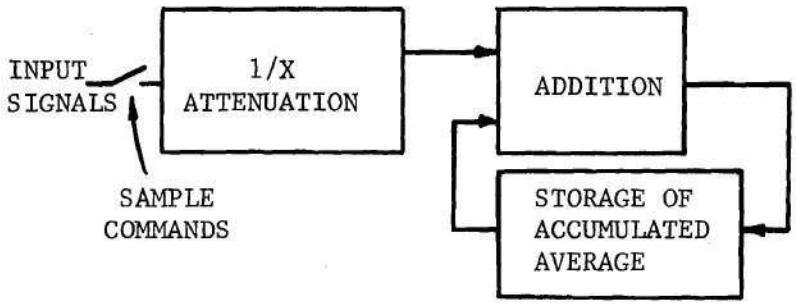

Figure 32. Schematic Implementation of Equally Weighted Averaging System

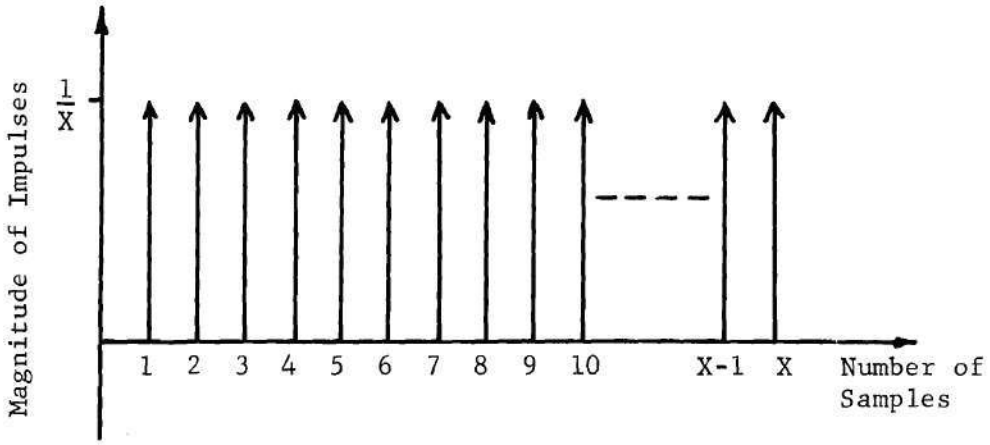

Figure 33. Impulse Train Corresponding to Equally Weighted Averaging

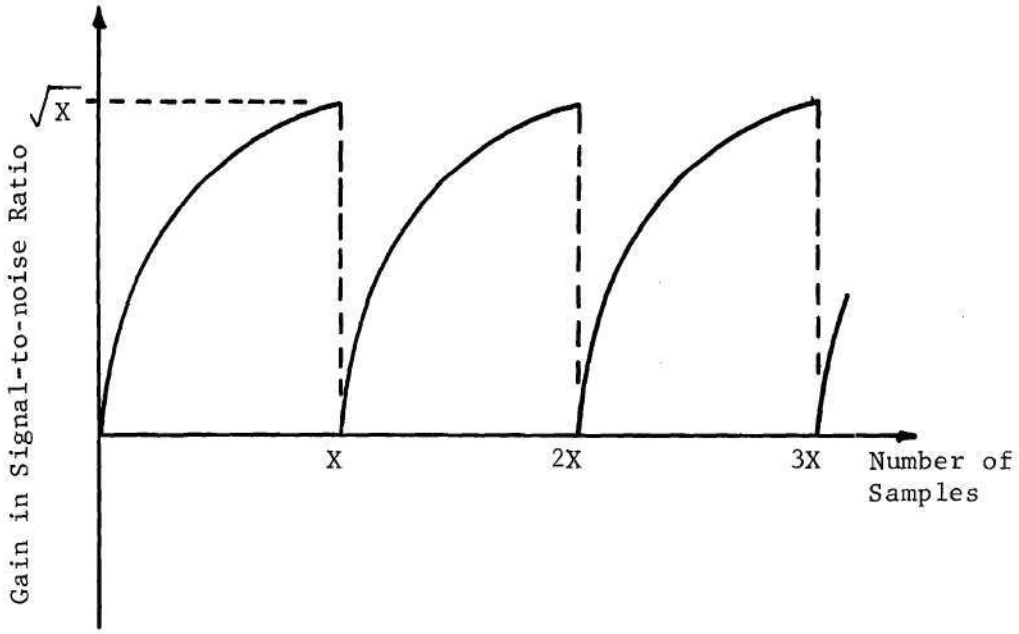

Figure 34. Signal-to-noise Gain of Equally Weighted Average

ging interval. This gain is shown in Figure 34. The resetting of the average at the end of each averaging interval returns the signal-to-noise ratio to its pre-enhanced value. Thus, assuming that the desired signal characteristics are obscured by the noise prior to enhancement, this enhancement scheme can only give a sequence of "snapshots" of the true signal at the end of the averaging interval when the signal-to-noise ratio is high enough. With biological signals of low repetition rate, the time between these snapshots may be fairly long, particularly with the long averaging times necessary for high signal-to-noise enhancement. This prevents the user from seeing the dynamic characteristics of the signal, a necessity for medical diagnosis.

The "Sliding Window" Average

The signal-to-noise enhancement of the equally weighted averaging scheme just described can be achieved without periodic resetting of the accumulated waveform if the data storage capabilities of the signal enhancement system are drastically increased. This is achieved by accumulating the average over the first X samples and then, on each successive sample, adding the new sample into the accumulation and subtracting the oldest sample value from it. In this way, the accumulated signal is always the average of the X most recent samples; hence the name "sliding window" is applied.

The signal-to-noise improvement given by the sliding window scheme builds up to $\sqrt{X}$ and, by adding in the most recent sample and dropping the oldest sample from the average, is maintained at that level. The disadvantage of such an enhancement technique is the increase in the storage

requirements of the system. In addition to the storage of the accumulated average, the system must hold the value of each of the X samples that are combined in the average. This is necessary so that each sample can be subtracted from the accumulated average after X more samples have been taken.

This process can also be compared to convolution with a sequence of X uniformly weighted impulses, without the periodic resetting of the previous system. Here again, the timing of the impulses must be adapted to meet the aperiodicity of the input signal. As shown in the previous section, any desired degree of signal enhancement may be obtained by increasing the number of samples included in the window, provided that the signal remains constant during the averaging interval.

The fetal EKG complex is not uniform in such a long-term sense, however, since significant transient changes in the configuration of this complex do occur. When they do, they will usually persist for 20 to 30 successive complexes (10). To properly highlight these changes, the sliding window should not be so wide as to "water down" changes of this length. This requirement establishes some maximum window length and, as a result, establishes some maximum signal-to-noise enhancement that is achievable without obscuring the short-term changes. In order to improve upon this maximum, an averaging technique that gives more weight to the more recent samples may be used, with the additional advantage that this weighted average can be computed without either the periodic resetting of the equally weighted, nonrunning average or the large storage requirements of the sliding window.

The Weighted, Running Average

As was pointed out in Chapter III, the signal enhancement process can be accomplished by a relatively simple digital system that gives more weight to the more recent repetitions of the signal. The input signal is again sampled and a summation is made such that:

$$\text{Ave}_n = \frac{\text{Signal}_n}{M} + \frac{M - 1}{M} \text{Ave}_{n-1} \quad , \tag{13}$$

where Ave_n is the accumulated average after n samples have been taken, Signal_n is the n^{th} repetition of the signal, and M is a variable weighting factor. The generalized block diagram of such a system was shown in Figure 9.

Considering a summation starting with the first repetition of the signal, assuming a constant signal, S, and random noise of constant level, N:

$$S_1 = \frac{1}{M} S \quad ,$$

$$S_2 = \frac{1}{M} S + \left[\frac{M - 1}{M}\right]\left[\frac{1}{M}\right] S \quad , \tag{14}$$

$$S_3 = \frac{1}{M} S + \left[\frac{M - 1}{M^2}\right] S + \left[\frac{M - 1}{M}\right]^2 \left[\frac{1}{M}\right] S \quad ,$$

where S_1 is the signal component of Ave_1.

Consider S_n:

$$S_n = \frac{1}{M} S\left[1 + \frac{M - 1}{M} + \ldots + \left(\frac{M - 1}{M}\right)^{n-1}\right] \quad . \tag{15}$$

Let $\beta = (M-1)/M$, then:

$$S_n = \frac{1}{M} S[1 + \beta + \ldots + \beta^{n-1}] \quad ; \tag{16}$$

multiplying (16) by β:

$$\beta S_n = \frac{1}{M} S[\beta + \beta^2 + \ldots + \beta^n] \quad . \tag{17}$$

Subtracting (17) from (16):

$$S_n[1 - \beta] = \frac{1}{M} S[1 - \beta^n] \quad . \tag{18}$$

Or:

$$S_n = \frac{1}{M} S\left[\frac{1 - \beta^n}{1 - \beta}\right] \quad . \tag{19}$$

Replacing β by $(M-1)/M$ and simplifying gives:

$$S_n = S[1 - (1 - 1/M)^n] \quad . \tag{20}$$

Since $(1-1/M)$ is less than 1, S_n, the signal component of the average, approaches the true signal strength, S, as n becomes large.

The noise, N, accumulates as follows:

$$N_1 = \frac{N}{M} \quad ,$$

$$N_2 = \left[\left(\frac{N}{M}\right)^2 + \left(\frac{M - 1}{M}\right)^2 \left(\frac{N}{M}\right)^2\right]^{1/2} \quad , \tag{21}$$

where N_1 is the noise component of Ave_1.

Again, letting $\beta = (M-1)/M$:

$$N_n = \frac{N}{M}\left[1 + \beta^2 + \beta^4 + \ldots + \beta^{2n-2}\right]^{1/2} \quad . \tag{22}$$

Or, squaring (22):

$$N_n^2 = \left[\frac{N}{M}\right]^2\left[1 + \beta^2 + \beta^4 + \ldots + \beta^{2n-2}\right] \quad , \tag{23}$$

and, multiplying (23) by β^2:

$$\beta^2 N_n^2 = \left[\frac{N}{M}\right]^2\left[\beta^2 + \beta^4 + \ldots + \beta^{2n}\right] \quad . \tag{24}$$

Subtracting (23) from (24):

$$N_n^2[\beta^2 - 1] = \left[\frac{N}{M}\right]^2\left[\beta^{2n} - 1\right] \quad . \tag{25}$$

Or:

$$N_n^2 = \left[\frac{N}{M}\right]^2\left[\frac{\beta^{2n} - 1}{\beta^2 - 1}\right] \quad . \tag{26}$$

Replacing β by $(M-1)/M$ and simplifying gives:

$$N_n = N\left[\frac{1 - (1 - 1/M)^{2n}}{2M - 1}\right]^{1/2} \quad . \tag{27}$$

Again, as n becomes large:

$$N_n = N\,(2M - 1)^{-1/2} \quad . \tag{28}$$

Thus, since S_n approaches S, the signal-to-noise enhancement that evolves as n becomes very large is:

$$\left.\frac{\text{Signal}}{\text{Noise}}\right|_{\substack{\text{After}\\\text{Averaging}}} = \left[\frac{S}{N}\right]\left[\frac{1}{(2M-2)^{1/2}}\right] = (2M-1)^{1/2} \times \left.\frac{\text{Signal}}{\text{Noise}}\right|_{\substack{\text{Before}\\\text{Averaging}}} \tag{29}$$

This shows that the signal-to-noise enhancement that this system can give is related to the weighting factor, M; the larger the value of M, the greater is the signal-to-noise improvement. The portion of any particular repetition of the signal that is included in the average is decreased by (M-1)/M during each new computation of the average. This process is equivalent to convolution of the input signal with a sequence of exponentially weighted impulses as shown in Figure 35.

The weight of the impulses decreases by (M-1)/M each repetition period in accordance with the dictates of the weighted averaging scheme. When the weighting factor is decreased, the exponential rate of decay is steepened so that the older repetitions have less of an influence on the accumulated average. In this manner, when M is made smaller, more weight is given to the more recent signal waveforms.

The signal enhancement system described in Chapter III is capable of performing this convolution and thereby computing a weighted average of the aperiodic FECG complexes according to the weighting scheme of Equation (13). The threshold detection scheme described in that chapter is an adaptive system that shifts the position of the exponential impulses to correspond to the actual aperiodicity of the FECG complexes. In that way coherent averaging takes place, and the true nature of the complexes

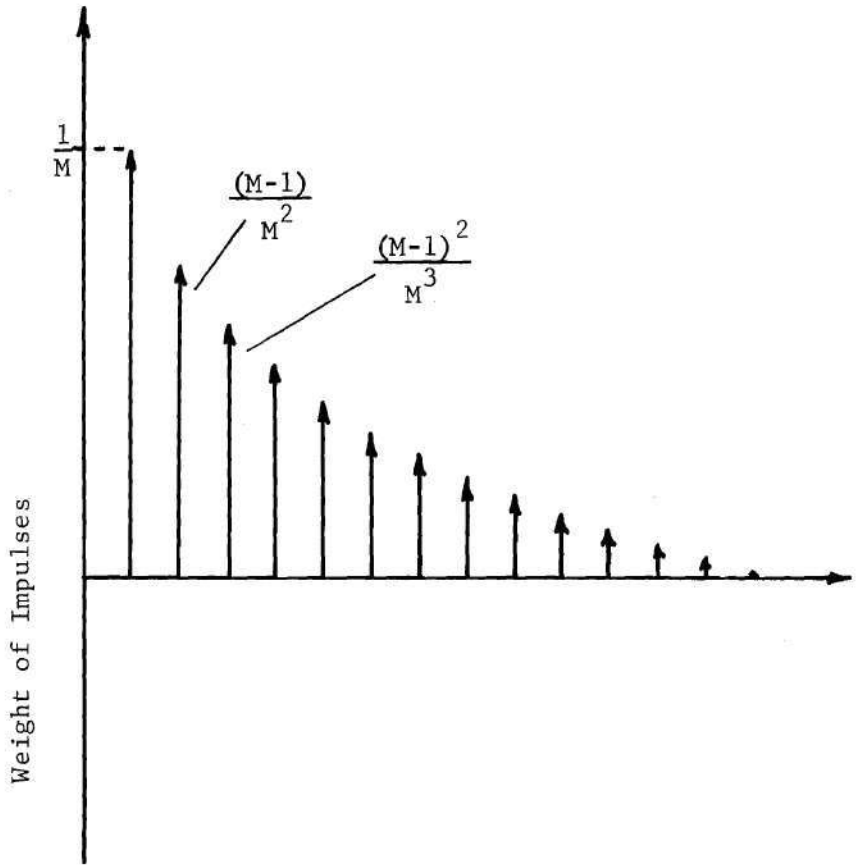

Figure 35. Sequence of Impulses Corresponding to Weighted Average

is clarified.

In order to compare the weighted averaging scheme with the sliding window, it must be remembered that it is desirable to be able to observe short-term changes in the FECG complex that may last no more than 20 successive complexes. Thus, the averaging scheme must not use an averaging period that is so long that these transient changes are obscured.

In order to compare the abilities of the sliding window and the weighted average to detect such transient changes, consider a sequence of repetitive signals, each of signal strength S_a, that have been combined to give an average whose signal strength is A_a. Then, assume that the signal strength changes to S_b for the next 20 repetitions, and require that, at the end of the 20 repetitions, the new average have a signal strength equal to:

$$A_b = \frac{1}{2} A_a + \frac{1}{2} S_b \quad . \tag{30}$$

In other words, the requirement is that the averaging technique allow the repetitive signal to build up to one-half of its true strength after 20 repetitions of the signal have been included in the average.

For the sliding window, the condition of Equation (30) is met when X, the total number of repetitions included in the average, is 40. The resultant signal-to-noise improvement is $\sqrt{40}$ or 6.3.

For the weighted averaging scheme, the necessary weighting factor can be calculated by using Equation (20), which was:

$$S_n = S_b[1 - (1 - 1/M)^n] \quad . \tag{31}$$

The desired result is that after 20 repetitions, the accumulated signal be one-half of the true signal, or:

$$S_{20} = \frac{1}{2} S_b \quad . \tag{32}$$

Thus, from Equations (31) and (32):

$$S_{20} = S_b[1 - (1 - 1/M)^{20}] = S_b/2 \quad . \tag{33}$$

Or:

$$[1 - (1 - 1/M)^{20}] = 1/2$$

$$(1 - 1/M)^{20} = 1/2 \quad . \tag{34}$$

Solving Equation (34) gives M = 29.4. (Note that the closest value for the prototype described in Chapter IV is M = 32.) The signal-to-noise improvement for this value of M may be calculated using (29) as:

$$\text{Gain in SNR} = (2M - 1)^{1/2}$$

$$= (58.7 - 1)^{1/2}$$

$$= (57.7)^{1/2}$$

$$= 7.6 \quad . \tag{35}$$

This is somewhat better than the value of 6.3 given for the sliding window type of enhancement system.

The averaging techniques may also be viewed from a somewhat dif-

ferent point of view. If a known amount of signal-to-noise improvement, say K, is necessary, then K^2 successive signals must be included in the sliding window. The equivalent weighting factor necessary to achieve this gain may be found from (29) as:

$$K = (2M - 1)^{1/2}$$

$$K^2 = 2M - 1$$

$$M = \frac{(K^2 + 1)}{2} \quad . \tag{36}$$

This value of M will give the same value of signal-to-noise ratio improvement as the sliding window which includes K^2 samples.

This equivalency is shown in the graph of Figure 36, which shows the build-up in signal-to-noise ratio for both types of enhancement schemes. The M = 32 case gives the same gain as does the X = 63 sliding window. The gain in signal-to-noise ratio will take longer in the case of the weighted average, since the total gain is only achieved when the number of repetitions included in the average becomes large. The gain of the sliding window is achieved after K^2 signals have been combined. Still, for larger values of gain, K^2 is large and the sliding window also takes a relatively long time to build up to its peak gain.

As a comparison, using the M = 32 case, the equivalent sliding window has 63 samples of the signal, so that it will take 63 repetition periods to achieve its maximum gain of $\sqrt{63}$ or 7.9. The weighted averaging system will be within 90 per cent of this value of signal-to-noise gain after 71 repetitions. The accumulation of the additional eight signals

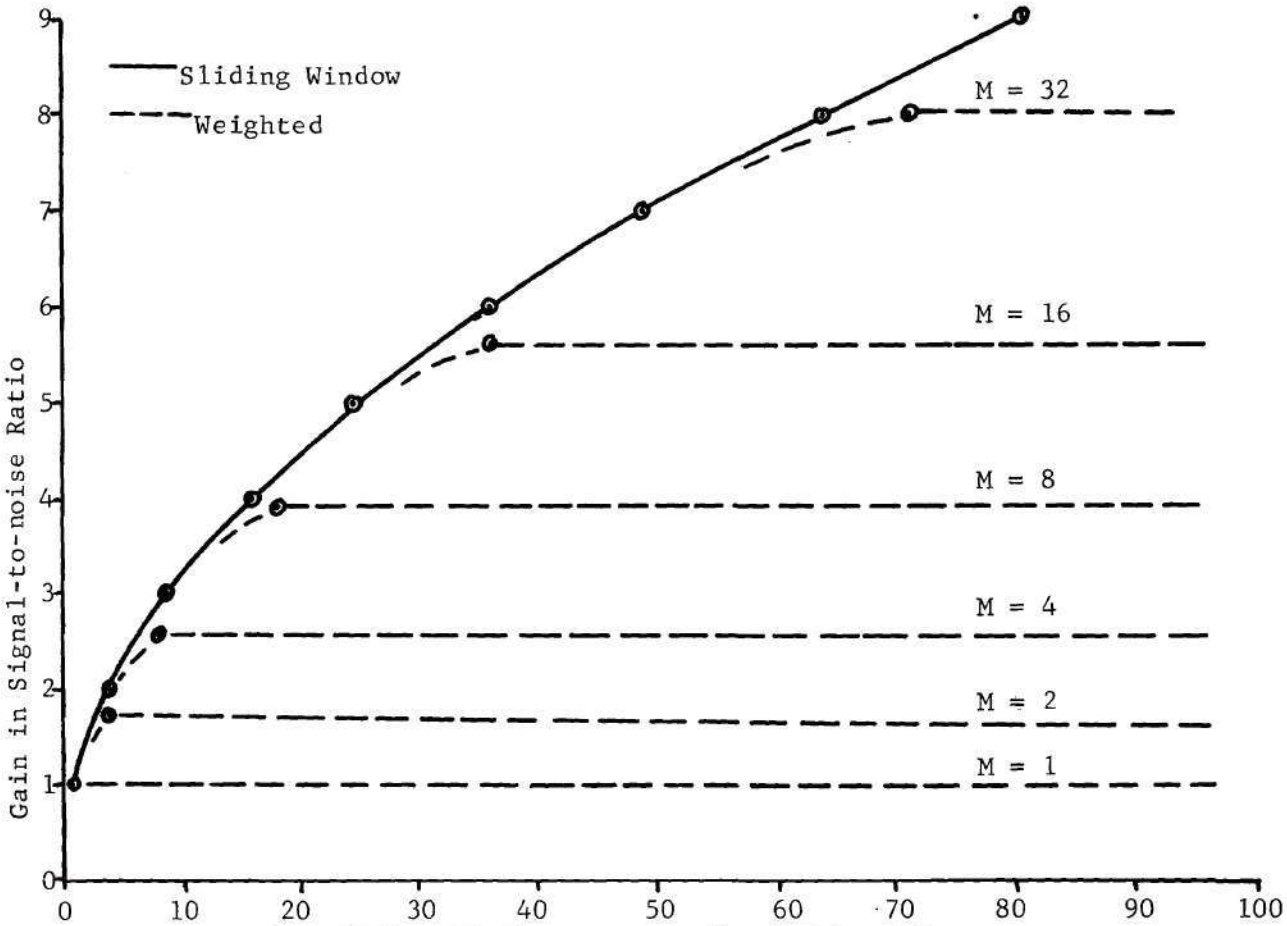

Figure 36. Comparison of Gain of Sliding Window with Weighted Average

required for the weighted averaging scheme should take less than eight seconds, assuming a fetal rate of 150 beats per minute and no worse than 50 per cent interference by the maternal complexes. This slight increase in time should be no trouble, and, considering the drastic reduction in the system storage capability required by the weighted averaging system, is well justified.

As an example of this reduction, using the parameters of prototype of Chapter IV, the storage requirements of the weighted averaging system are 47 average words and 47 sample words, making the total storage requirement equal to:

$$\text{Storage} = 94 \text{ words} \times 20 \text{ bits per word}$$

$$= 1880 \text{ bits.}$$

The sliding window that would give the same signal-to-noise gain as the M = 32 weighted averaging system would require the storage of 62 additional repetitions of the signal with each of these repetitions consisting of 47 sample words, giving a total requirement of:

$$\text{Storage} = 1880 + (62 \text{ repetitions} \times 47 \text{ sample words per repetition} \times 20 \text{ bits per word})$$

$$= 60{,}160 \text{ bits.}$$

This amount of storage is about three times the state-of-the-art capability of a delay line storage system, necessitating the use of a core or drum memory.

Conclusions

It has been shown that, when a comparison based upon ability to

detect transient changes in the FECG is made, the weighted averaging scheme gives a slightly higher signal-to-noise gain than the sliding window, as well as a great reduction in the hardware required to implement the signal enhancement system. The requirement that a suitable signal enhancement system must not obscure transient changes in the fetal waveform that last no more than 20 complexes is shown, based upon recommendations in the medical literature (10). Using this criterion, the optimal value of the weighting factor is calculated to be $M = 32$. These results show that the SES described in Chapter III should provide signal enhancement of the fetal electrocardiogram in a manner more useful to the medical researcher than the other common averaging schemes.

CHAPTER VI

ANALYSIS OF EXPERIMENTAL RESULTS

Introduction

The operation of the prototype was verified in four distinct phases:

1. Computer simulation of the hardware and the data.
2. Operation of the prototype upon simulated FECG signals.
3. Operation of the prototype upon actual FECG data.
4. Operation of the prototype upon experimental signals that were chosen to study particular aspects of its signal enhancement capabilities.

The initial computer simulation has been mentioned in Chapter III, and it is covered in detail in Appendix I. The remainder of this chapter considers the results that were obtained when the prototype was used to enhance the fetal complexes contained in both simulated and actual FECG data and to process other experimental signals.

Results with Simulated FECG Data

Early in the experimental studies, prior to the availability of actual FECG data, a hybrid simulation of data that approximated FECG data was made, and the signals that were generated by this simulation were processed by an early version of the prototype. This version of the prototype did not include the low-order bits that prevent the loss of accuracy during the averaging calculations and, thus, it had the dead

zone effect mentioned in Chapter IV. All of the tests were made with M = 64 or less, and, while the dead zone effect limited the signal enhancement capabilities of the early prototype, the other aspects of the prototype (signal detection by threshold detection, maternal interference, etc.) were demonstrated.

The FECG signals that were processed by the prototype during this portion of the research were generated by using the hybrid simulation system that is diagrammed in Figure 37. The fetal rate was established by the digital clock, which was varied manually throughout the simulation to simulate the aperiodicity of the fetal heartbeat. The rate was kept in the vicinity of 150 beats per minute. Each time a clock pulse was produced, the first 60-millisecond one-shot was triggered. At the end of the 60-millisecond duration of the first one-shot, the second one-shot was triggered, producing a second pulse of the same duration. The outputs of the two one-shots were amplified and inverted once and twice respectively to produce pulses of opposite polarity. These pulses were integrated to produce the up-down ramp shown in Figure 37. The magnitudes of the input pulses were adjusted to make the peak of the ramp equal to ten volts. Some continuous adjustment of potentiometers A and B was required to keep the baseline of the integrator output at zero volts. This baseline would drift since the integral of the positive input pulse was not exactly cancelled by the integral of the negative input pulse.

The up-down ramp thus generated was used to drive a diode function generator to give the output waveform shown in Figure 37. The output waveform was symmetrical, with small P and T waves flanking the R-peak. This simulated fetal complex was summed with two noise signals and a simu-

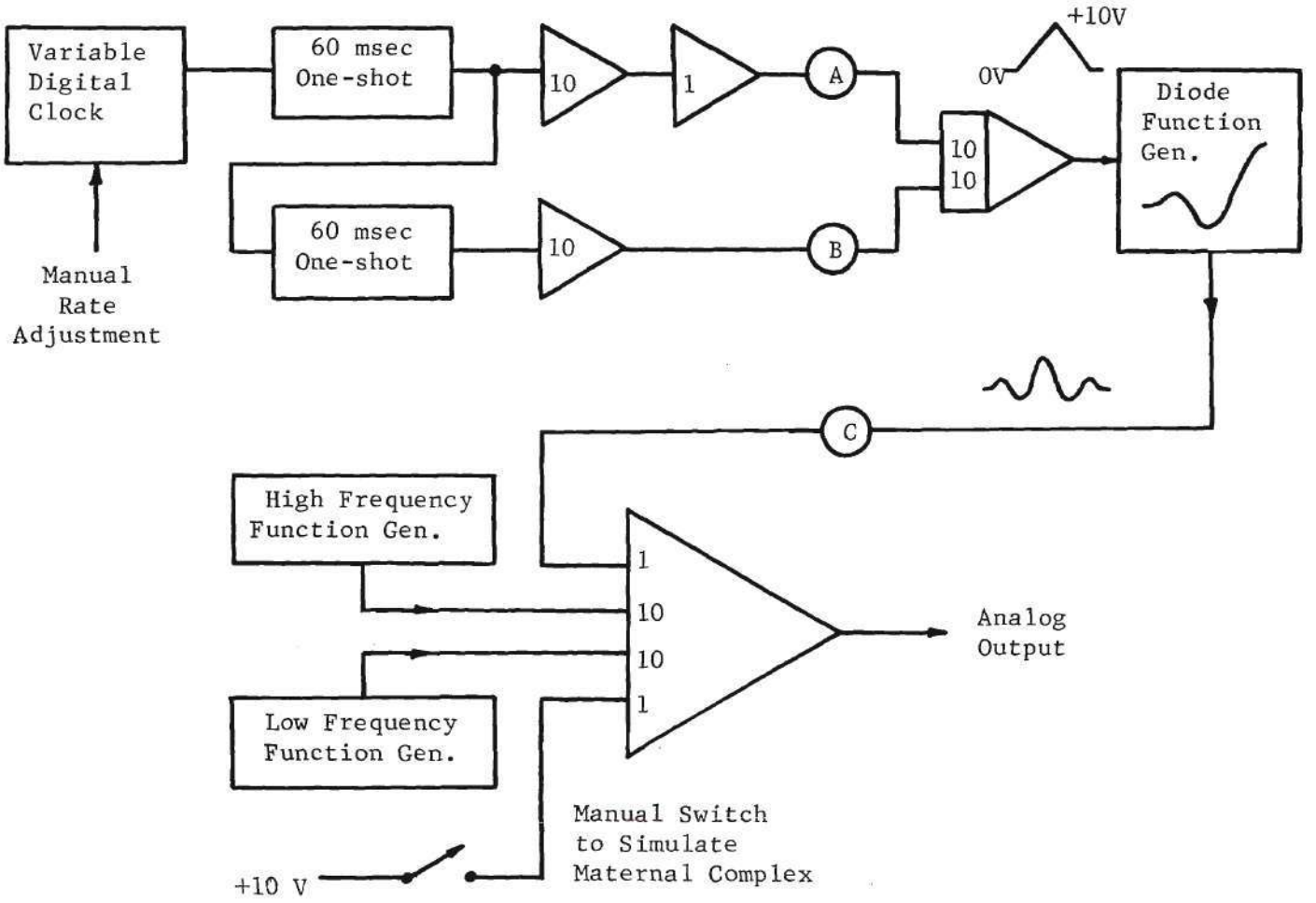

Figure 37. Block Diagram of Analog Simulation of FECG Data

lated maternal signal. The first noise signal was produced by a General Radio White Noise Generator and represented the high frequency muscle noise and electromagnetic noise present in typical abdominally recorded FECG signals. The other noise generator was a Hewlett-Packard Low Frequency Function Generator, which approximated the low frequency muscle noise. The maternal complexes were simulated by manually closing a switch which saturated the output of the final summing amplifier. A portion of a typical simulated signal is shown in Figure 38a. The operation of the prototype was studied by using a variety of signal-to-noise ratios and choices of the weighting factor.

In each case, the amplitude of the input data was adjusted so that the threshold detectors were able to distinguish between the fetal and maternal complexes, and the data was then presented to the prototype. The average fetal complex that was accumulated was photographed and the resultant waveforms for several of these simulated test runs are shown in Figures 38, 39, and 40.

Figure 38a shows a strip-chart recording of several seconds of simulated data. The fetal and maternal complexes are indicated. The prototype was allowed to process on this data for approximately one minute with the weighting factor, M, set at 32. The accumulated average waveform is shown in Figure 38b. The relatively clean baseline and a slight indication of the fetal P and T waves can be seen.

Figure 39 shows a comparison between "theoretical" and actual results. The upper trace of Figure 39 is the fetal waveform that was accumulated after about one minute of processing on data that contained only the simulated fetal complex. The noise and the simulated maternal

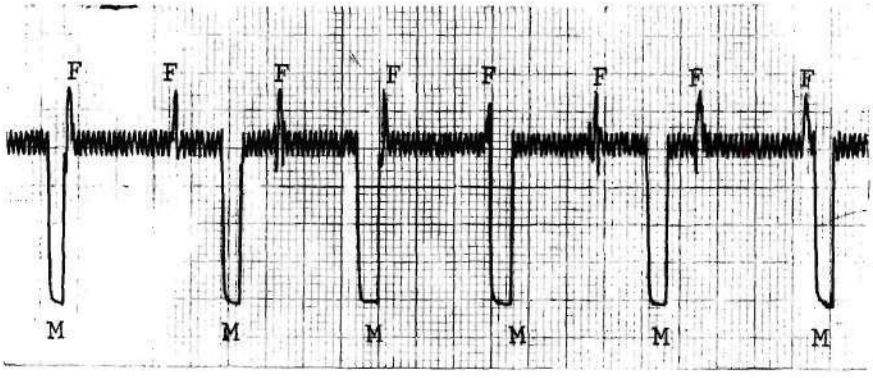

a. Simulated FECG Data

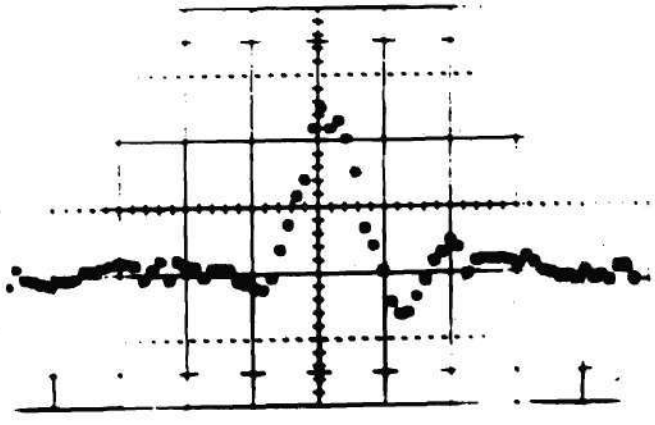

b. Enhanced Fetal Complex, M = 32

Figure 38. Results of Operation of the Prototype upon Simulated Data

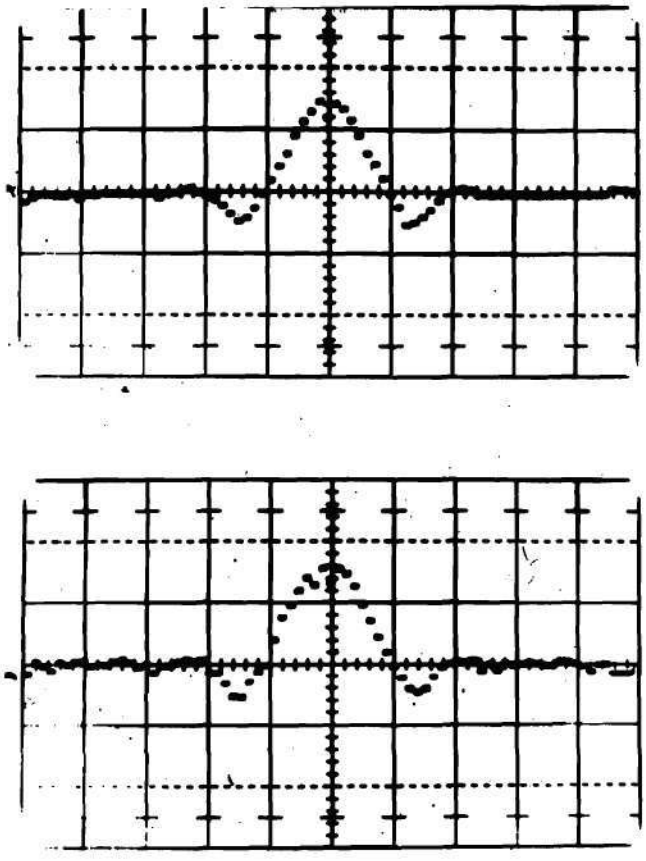

Figure 39. Enhanced Fetal Complexes Obtained from Simulated FECG Data, M = 32

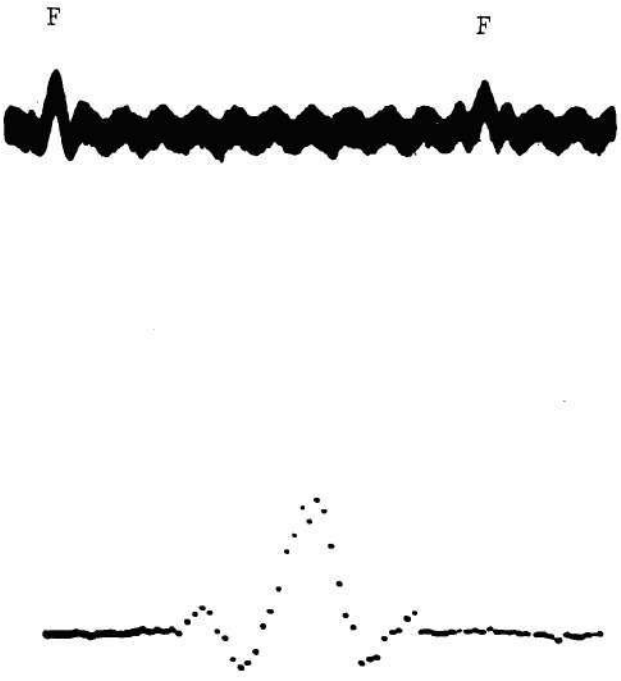

Figure 40. Simulated FECG Data and Enhanced Fetal Complex, M = 64

complexes were not included. The lower trace of Figure 39 shows the fetal waveform that was accumulated from simulated FECG data with noise and the maternal complexes included. The waveform that was accumulated in the presence of noise and maternal complexes is very similar to that accumulated with no interference. The weighting factor was set at 32 in both cases. The close comparison indicated the fidelity of the waveform that was averaged from the noisy data, even with the dead zone of the early prototype. Figure 40 shows another accumulated waveform and the data from which it was retrieved.

The results of operation upon the various simulated data seemed to verify the ability of the prototype to bring a satisfactory representation of the fetal complex out of noisy abdominal recordings when the weighting factor was no larger than 64. The question now was how the system would perform using data as actually recorded from the maternal abdomen.

Results with Actual FECG Data

Obtaining the Data

To completely chronicle the attempts that were made to obtain real FECG data for input into the prototype would require several pages. A brief summary of these efforts follows, however. Initially contact was made with Dr. Nanette Wenger of the Cardiovascular Research Laboratory of Atlanta's Grady Hospital. With her assistance several attempts were made to detect the fetal complex through the use of abdominal electrodes of both the suction-cup type and the stick-on variety. These recordings were attempted with the cooperation of the Grady Department of Obstetrics,

which provided suitable test subjects. The results of these attempts were virtually nil, however, primarily due to the lack of EKG equipment that was specifically tailored to recording the fetal complex and the inexperience of all of the experimenters as to placement of the abdominal electrodes. This placement is very critical, and without proper location of the electrodes, the detection of any fetal signal is improbable.

Next, contact was made with several Atlanta obstetricians who were interested in this area of research, but they were not able to help in recording the FECG. One obstetrician did suggest that Dr. Walter Bloom of the Ferst Research Center at Piedmont Hospital might be of assistance. Despite Dr. Bloom's willing assistance, no FECG records were recorded, due to the same lack of proper FECG equipment that plagued the efforts made at Grady.

Finally, correspondence was sent to the four leading researchers in this field, Dr. Edward Hon of the Yale Medical School, Dr. Saul Larks of the University of Missouri, Dr. Franklin Offner of Northwestern University, and Dr. D. C. Amoss of Drexel Institute of Technology, asking for advice and assistance in obtaining FECG data. Each of these gentlemen was cooperative and offered all the assistance that he could. Dr. Hon, in particular, sent a variety of tape recorded FECG records. In order to process the data that was received from Dr. Hon, the early prototype was modified to include the low-order bits that were discussed in Chapter IV. Representative portions of the actual FECG data have been processed by the improved prototype, and the results are presented in the following section.

Presentation of Results

Figure 41 shows several seconds that typify the data with which the operation of the prototype was studied. The upper trace was recorded by using abdominal electrodes. The lower trace was recorded using a direct fetal electrode attached to the fetal scalp; note the absence of maternal complexes. Approximately 15 minutes of such data was recorded, with the abdominal record and the scalp record in separate channels on the tape. It should be noted that, unlike the earlier signal enhancement systems, tape recording is not a requirement of the SES operation. The signals could be input into the SES directly from the FECG amplifier.

Figures 42 through 45 are time history presentations of the enhanced fetal complexes that were obtained by processing several minutes of the recorded data. The data from the recorder was passed through a 1 Hertz high-pass filter to remove any DC offset voltage, and the gain of the filter was adjusted until the fetal and maternal complexes had the proper relationships to the thresholds of the prototype.

Figure 42 shows that the performance of the prototype is somewhat erratic at M = 8. The significant changes in the averaged waveform occur when the baseline of the FECG data shifts until a group of samples is taken that are above the lower threshold even though the fetal complex is not present. These samples, when included in the average with M = 8, cause significant changes in the accumulated complex.

Figure 43 shows the improvement in signal enhancement that is obtained when M = 32. The baseline of the fetal complex is now clear, along with a trace of the preceding fetal P wave. When M is increased to 128, as in Figures 44 and 45, the signal enhancement is of sufficient quality

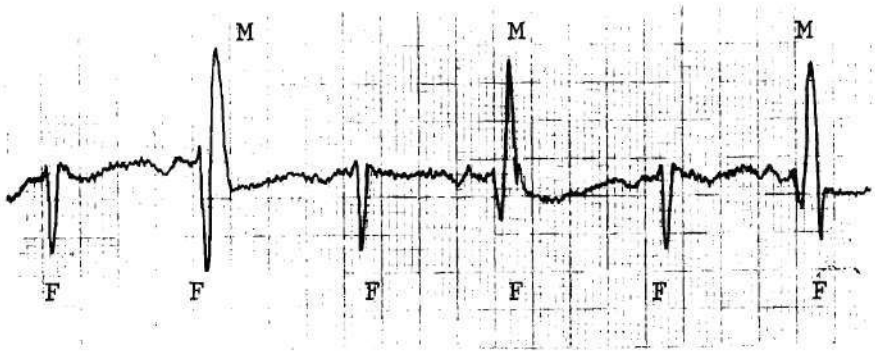

a. Signals Recorded from the Maternal Abdomen

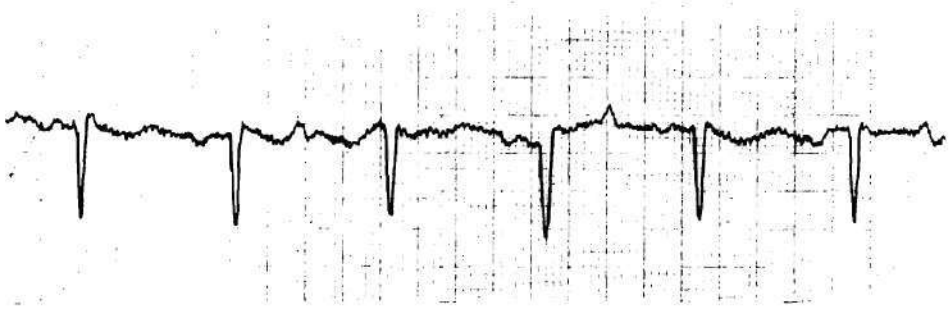

b. Signals Recorded from the Fetal Scalp

Figure 41. FECG Signals as Recorded for SES Processing

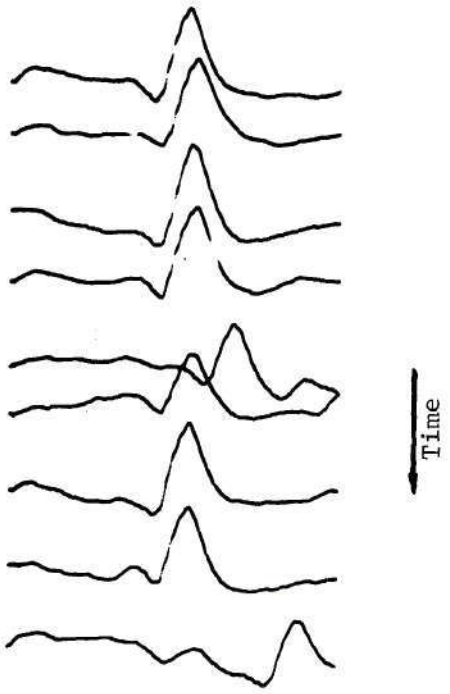

Figure 42. Time History Presentation of Fetal Complexes Obtained from Actual Abdominal Recordings; M = 8, CENTER Aperture, 15 Second Intervals

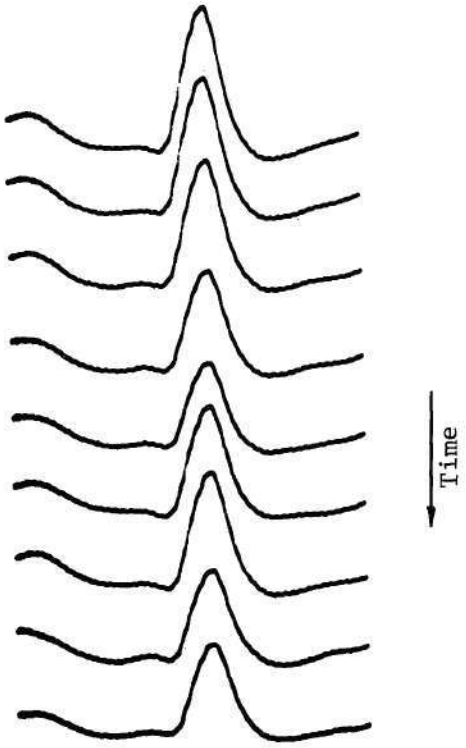

Figure 43. Time History Presentation of Fetal Complexes Obtained from Actual Abdominal Recordings; M = 32, CENTER Aperture, 30 Second Intervals

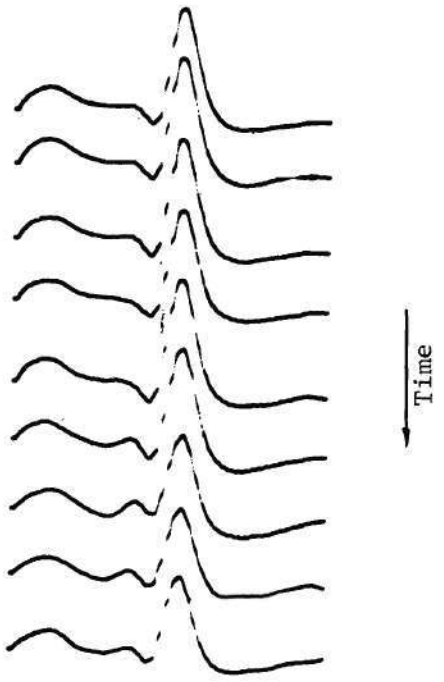

Figure 44. Time History Presentation of Fetal Complexes Obtained from Actual Abdominal Recordings; M = 128, CENTER Aperture, One Minute Intervals

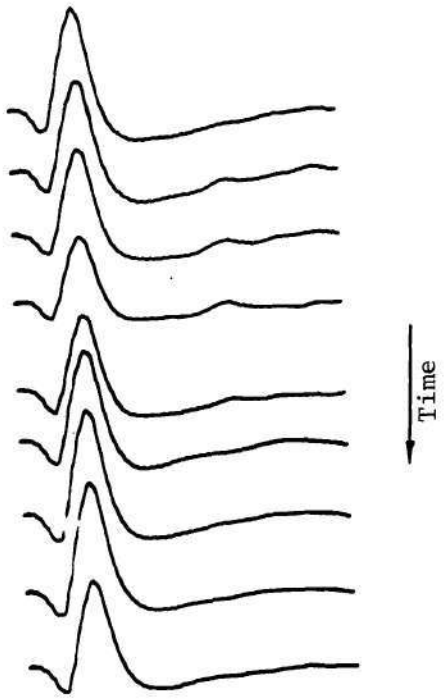

Figure 45. Time History Presentation of Fetal Complexes Obtained from Actual Abdominal Recordings; M = 128, AFT Aperture, One Minute Intervals

to permit an even better presentation of the average fetal complex. In Figure 44, particularly in the lower four traces, the fetal P wave is clearly present. In Figure 45 the trailing fetal baseline is clearly shown, with the upper traces showing a wave, possibly the fetal T wave, that appears and persists for several minutes.

By way of comparison, Figure 46 shows the enhanced complexes that were obtained from the scalp electrode and the abdominal electrodes. These complexes were obtained by processing five minutes of data, first from the tape channel carrying the scalp data, then rewinding the tape and processing the same five minutes of data from the channel containing the abdominal recording. The similarity between the enhanced complexes is evident. The chief difference is that the PQ portion of the complex that is obtained from the abdominal recording is somewhat flatter than the corresponding portion of the complex obtained from the fetal scalp. This flattening seems to agree with the research efforts of Dr. Alan Kahn (16), who has studied the electrical transmission paths from the fetus to the skin of the maternal abdomen. His work suggests the possibility that the capacitive properties of the fetal-maternal interface may attenuate the higher frequency portions of the fetal complex, and thereby may smooth the complex until the fetal P and T waves are difficult to identify. Such a "smoothing" is apparent in Figure 46.

Finally, the magnitude of the data given to the prototype was adjusted so that the maternal complexes present in the abdominal recordings of Figure 41 would be treated as if they were fetal complexes. The averaged waveforms thus generated are shown in Figure 47. Note the opposite polarity of the maternal complex, corresponding to the data shown in

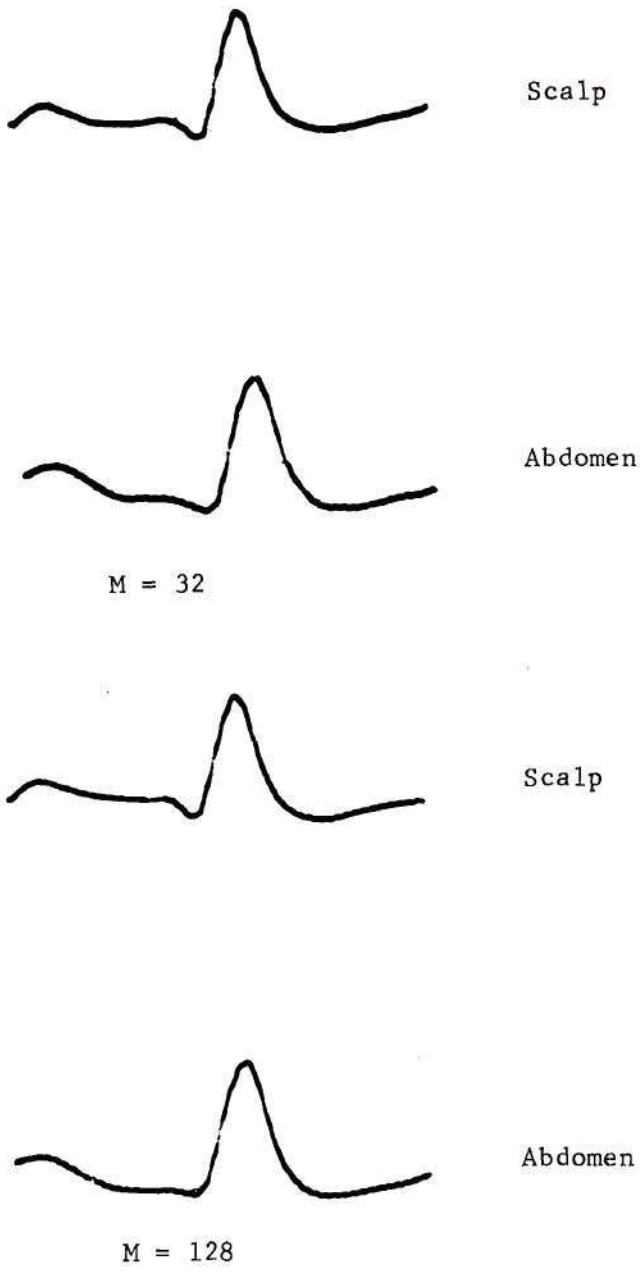

Figure 46. Comparison Between Enhanced Fetal Complexes from Abdominal Recordings and Direct Connection to the Fetus

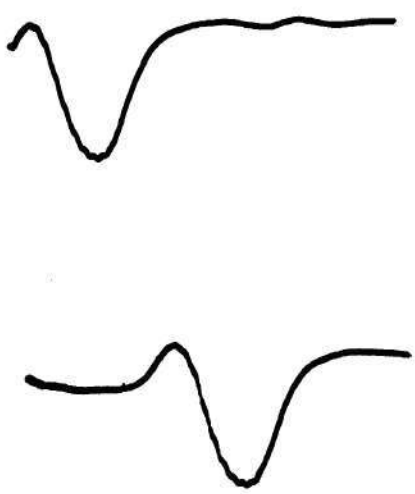

Figure 47. Maternal Complex Obtained from Actual Abdominal Recordings; M = 32, CENTER and AFT Modes

Figure 41.

Results with Other Input Signals

With the aim of verifying that the final prototype was, in fact, properly performing the various operations that make up its signal enhancement process, a variety of known input signals were applied to the prototype and its performance studied. Initially, a DC voltage was applied to the prototype, and by increasing this voltage until the fetal threshold was exceeded, the rate of rise curves shown in Figure 48 were obtained. These curves, recorded at a relatively slow time scale, show the build-up of the average from the initial zero value toward the level of the DC input voltage.

The rate at which this build-up should occur can be calculated from Equation (20), which was:

$$S_n = S[1 - (1 - 1/M)^n] \quad , \tag{37}$$

where n is the number of groups of samples that have been included in the average. The data shown in Figure 48 was recorded in the CENTER aperture setting. When in this setting, the prototype takes 37 samples, then looks for a fetal peak, which will always be apparently present due to the DC input voltage. Then, 22 samples are taken following the "peak," making the time required to fill the aperture equal to 118 milliseconds, since the samples are taken 2.04 milliseconds apart. Thus, Equation (20) may be written as:

$$S_t = S[1 - (1 - 1/M)^{\frac{t}{118}}] \quad , \tag{38}$$

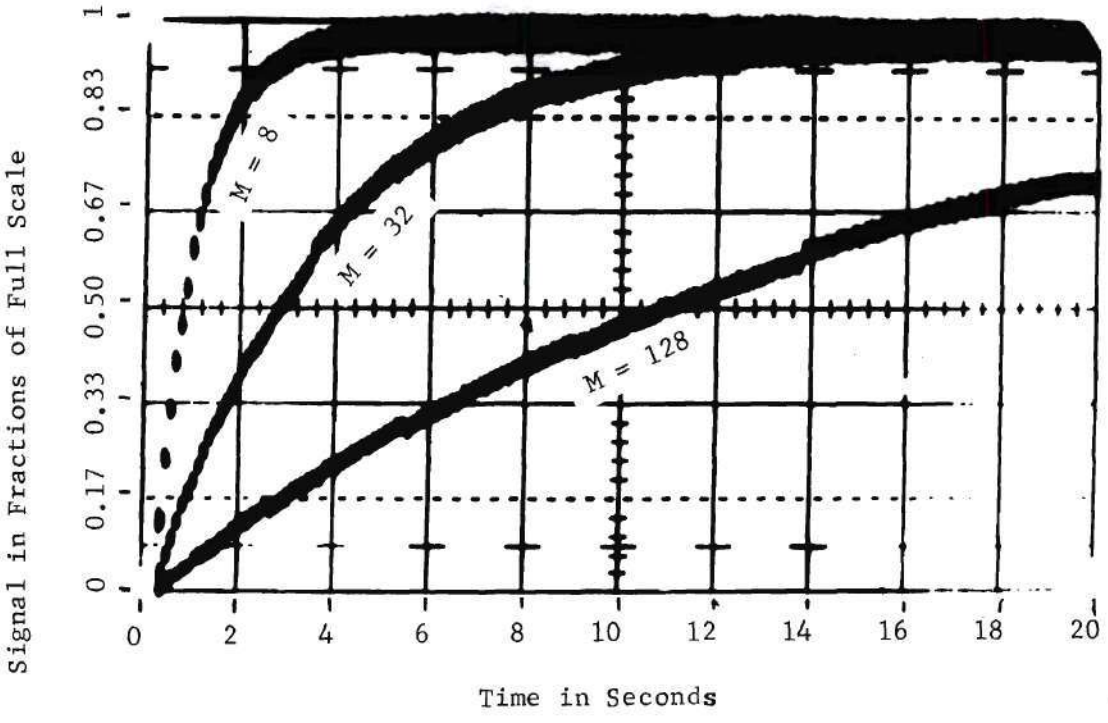

Figure 48. Experimentally Observed Signal Rise Curves

where t is in milliseconds. Using Equation (36), the rate of rise curves shown in Figure 49 were plotted for comparison with Figure 48. The two agreed so closely that replotting them together was not informative since all of the points fell virtually on top of each other.

Next, in order to study the noise suppression characteristics of the prototype, the fetal threshold was set to zero and random noise was used as an input signal. This noise was generated by a General Radio Random Noise Generator. The output from the DAC was blanked by the previously mentioned sampling circuit so that the initial disturbance associated with the analog-to-digital conversion did not appear at the sampling circuit output. The remaining signals, as shown in Figure 50, were measured using a Hewlett-Packard RMS Voltmeter.

While this meter does not read true rms voltage for non-sinusoidal input signals, the measured data was expected to bear some near-linear relationship to the true rms voltage of the accumulated waveforms. Theoretically, the noise was shown to decrease with increasing M according to Equation (28) which was:

$$N_n = N(2M - 1)^{-\frac{1}{2}} \quad . \tag{39}$$

The experimentally measured noise was normalized to the M = 2 figure and plotted in Figure 51, along with the theoretical decrease in noise given by Equation (28). The comparison is surprisingly good, considering the use of a meter that does not read true rms voltage and the non-infinite averaging periods.

These quantitative results showed that the prototype was perform-

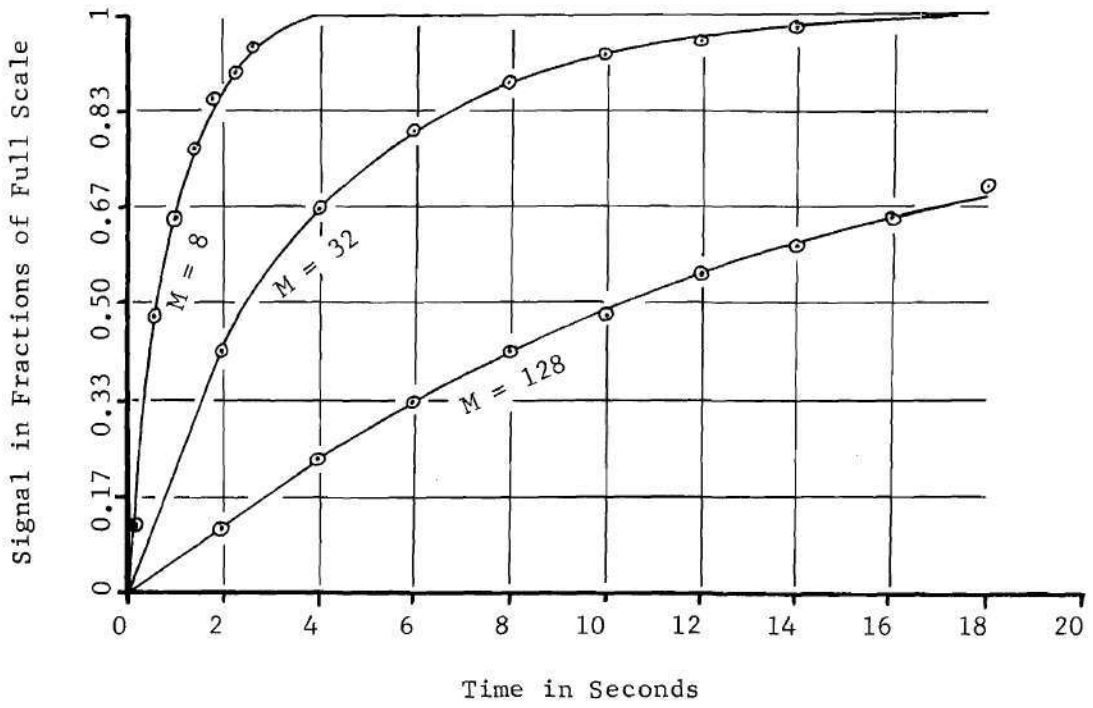

Figure 49. Calculated Signal Rise Curves

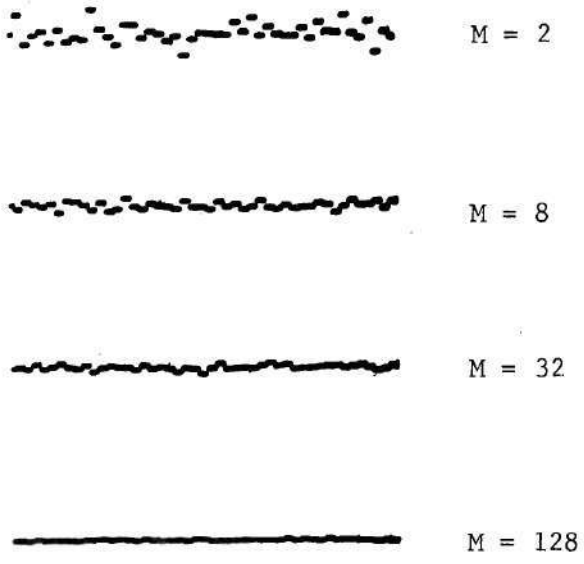

Figure 50. Averaged Signals Observed with Random Noise as the Input to the Prototype

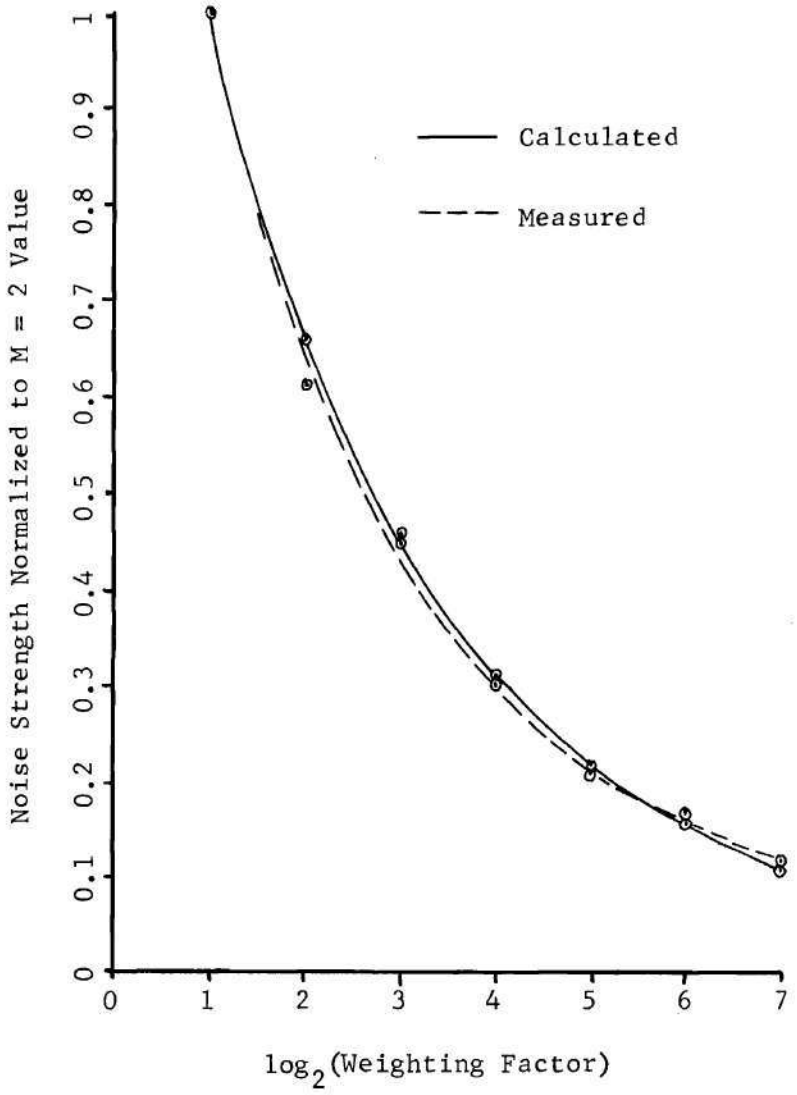

Figure 51. Decrease in Noise with Increasing Weighting Factor

ing the signal enhancement process in accordance with the mathematical analysis shown in Chapter V. In addition, a series of qualitative tests were run using known input signals (triangular waves, damped sinusoidal oscillations, etc.) plus additive random noise. Figure 52 shows the success with which the prototype was able to recover a sinusoidal waveform that was mixed with additive random noise. The superimposed "before" and "after" waveforms are almost identical. These additional signal enhancement results further verified the effectiveness of the prototype.

The results of these tests and the experimental results discussed previously in this chapter verified that the prototype could provide usable signal enhancement of the fetal complexes present in abdominally recorded FECG data. The conclusions drawn from these research efforts and recommendations for further research are presented in the concluding chapter.

a. Input Signal to Prototype

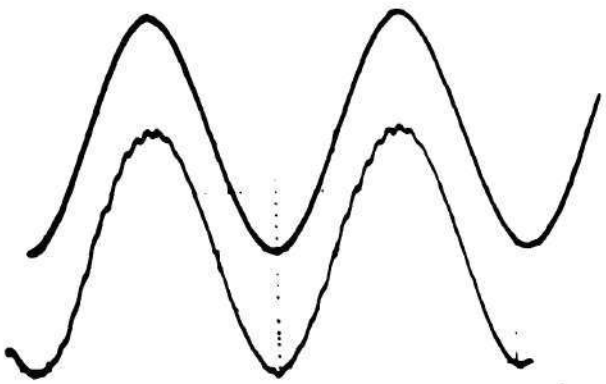

b. Comparison of True Sine Wave with that Recovered by Prototype

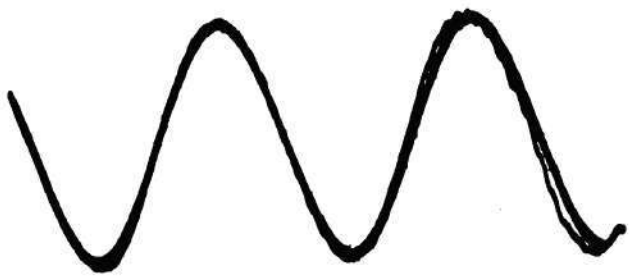

c. True Sine Wave Superimposed upon Averaged Sine Wave

Figure 52. Recovery of Sine Wave from Random Noise by the Prototype; M = 128

CHAPTER VII

CONCLUSIONS AND RECOMMENDATIONS

The central conclusion that may be drawn from the research efforts presented in the previous chapters is that the feasibility of a digital signal enhancement system for use with the fetal electrocardiogram is now well established. A new averaging device has been developed which is well-suited to the enhancement requirements of low frequency, aperiodic signals such as the fetal electrocardiogram. The averaging system used by this device has been analyzed theoretically and, when compared on the basis of ability to detect short-term variations in the configuration of the repetitive input signal, has proven to offer more signal enhancement than other common systems.

A prototype of this averaging device was constructed and evaluated by using it to process abdominally recorded FECG data. The digital design concepts detailed in Chapter IV proved to be satisfactory, for the prototype performed the signal enhancement process well enough for the baseline of the fetal complex to be seen. With the higher weighting factors, both the P wave and the T wave of the fetal complex were observed.

The threshold detection scheme for identifying the fetal and maternal complexes worked well when the FECG signal had clearly defined fetal R-peaks and a fairly stable baseline.

Based upon the cost of the prototype, it appears that a marketable

version of the SES could be produced for no more than the total equipment cost of the current FECG signal enhancement systems.

In addition to verifying the basic concepts of the new digital FECG signal enhancement system, the research has pointed the way to several further areas of study.

First, some means of balancing out the wander in the baseline of abdominally recorded FECG data should be possible. A possible suggestion would be a separate low-pass input channel to the SES. The pass-band for this channel would be adjusted so that the signal received by this channel would be the true baseline, with the fetal and maternal complexes filtered out. This signal could then be digitized and subtracted from the normal sample values calculated by the SES. This technique would therefore normalize the input signals to a zero baseline. Also, a more extensive study of direct high-pass filtering to stabilize the analog baseline might prove fruitful.

Second, subsequent versions of the SES should have a slightly increased memory capacity so that the basic aperture width could be expanded to cover the expected width of the fetal complex.

Third, the use of the SES as an externally triggered averaging device should be investigated. Here, provision could be made for disabling the threshold detection network and, instead, using an external timing signal which would act as the fetal R-peak detector. In this mode the sampling aperture would be located relative to the external signal, rather than the fetal peak. The SES could then be used in conjunction with any of the possible fetal detection schemes, just as the CAT is used now. The SES, however, would provide the researcher with a weighted, run-

ning average that, for FECG applications, is superior to the averaging method of the CAT. Moreover, the SES in this mode should have application in neurology, in electro-encephalography, and in adult electrocardiography.

Fourth, the performance of the SES should be evaluated by using a variety of input signals so as to obtain an understanding of the lower limits of fetal signal-to-noise ratio below which the SES cannot identify the fetal complexes.

APPENDIX I

EXPLANATION OF THE COMPUTER SIMULATION PROGRAM

A simplified flow chart of the simulation program is shown in Figure 53. The program was written in ALGOL for the Burroughs B-5500. The data generation subroutine produces a sequence of digital values that correspond to the sequence of values that would be generated by the analog-to-digital converter of the SES as it digitizes the input signal every two milliseconds. Stored within this subroutine are two sequences of values that correspond to the sample values that would be obtained by sampling a typical fetal complex and a typical maternal complex. These typical waveforms are normalized to have a peak value of unity. This peak value is the R-peak of the waveform.

These waveforms are multiplied by scaling factors which adjust the size of the complexes that are to appear in the simulated data. The subroutine reads these scaling factors from data cards prior to the simulation. The data cards also give the desired fetal and maternal rates and the length of time that these rates and scaling factors are to apply. The subroutine then repeats the properly scaled series of values at the desired rates. Each output value consists of a summation of the value from the fetal complex, the value from the maternal complex, and a noise value.

The noise is generated by a random number generator which produces a Gaussian-like distribution of numbers that are truncated at a peak noise

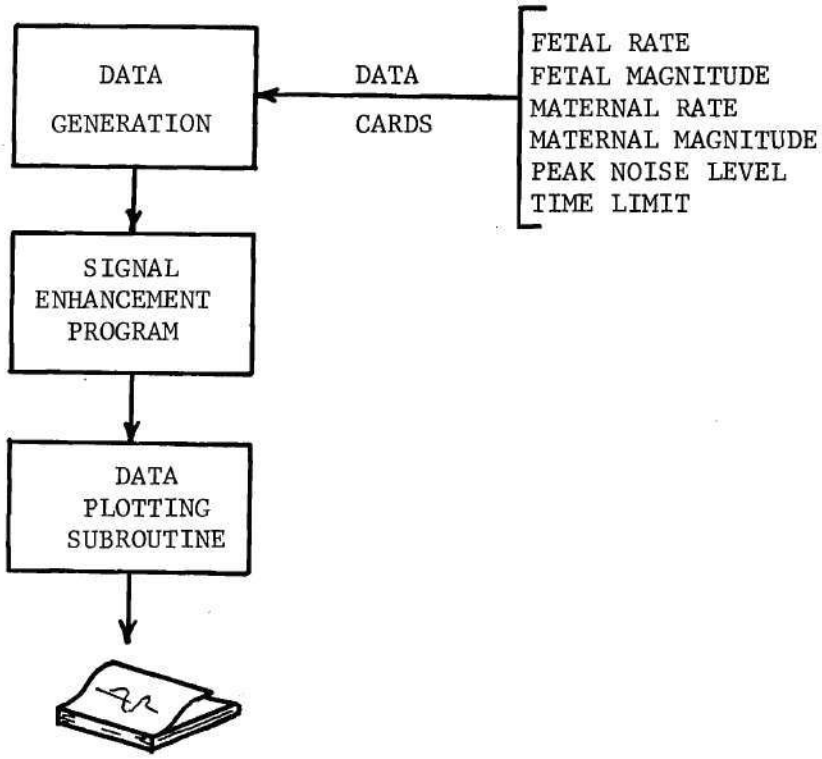

Figure 53. Flow Chart of Simulation Program

level included on the data cards read in by the subroutine. The rates and sizes of the fetal and maternal complexes are changed whenever the time limit on a particular data card is reached and the input factors on the next data card go into effect.

The signal enhancement portion of the program was written to simulate the operation of the SES upon the sequence of data points produced by the data generation subroutine. The various SES functions such as threshold detection, maternal elimination, data storage, and calculation of the averaged waveform, were performed by the program in the same way that the SES would perform them. The enhanced waveform was stored as a sequence of values in an array, just as the SES would store the waveform as a sequence of values within its memory.

The output subroutine plotted the enhanced waveform using an alphabetic page-plotting scheme. The average waveform was plotted each time a new sample of the fetal complex was included in the accumulated average. Thus, the build-up of the fetal signal could be seen.

More complete information concerning this program and its use as a simulation tool can be obtained from the author.

APPENDIX II

THE SPECIAL-PURPOSE CIRCUITS USED BY THE PROTOTYPE

The Delay Line Memory

The specific delay line used was the Computer Devices Corporation Wire Sonic Delay Line, Type MT 762A-3, having a 2000 ± 2 microsecond delay. The bit rate was set at one million bits per second, providing for the storage of 2002 bits. In order to minimize the noise radiated by the delay line driving circuit, this portion of the delay line circuitry was mounted directly on the delay line, thus making the leads carrying the driving pulses as short as possible. Also, a single-stage amplifier was mounted directly at the output terminals. This amplified the output pulses prior to threshold detection within the prototype.

The driving circuit for the delay line is shown in Figure 54. The input data is sent to the line in the RZ (return-to-zero) mode, with each one-bit represented by a narrow pulse and each zero bit represented by the absence of such a pulse. The flip-flop shown in Figure 54 transforms the serial input data to this form. This flip-flop is reset every time the clock signal, T_B, goes positive, and if the data input is a one-bit, the flip-flop is set by the falling edge of the same clock pulse.

When the flip-flop is set, its output drops to zero volts. This change in voltage is coupled through an R-C differentiation circuit into the buffer amplifier, producing a narrow positive spike that turns on the driving transistor. This introduces a narrow current pulse into the in-

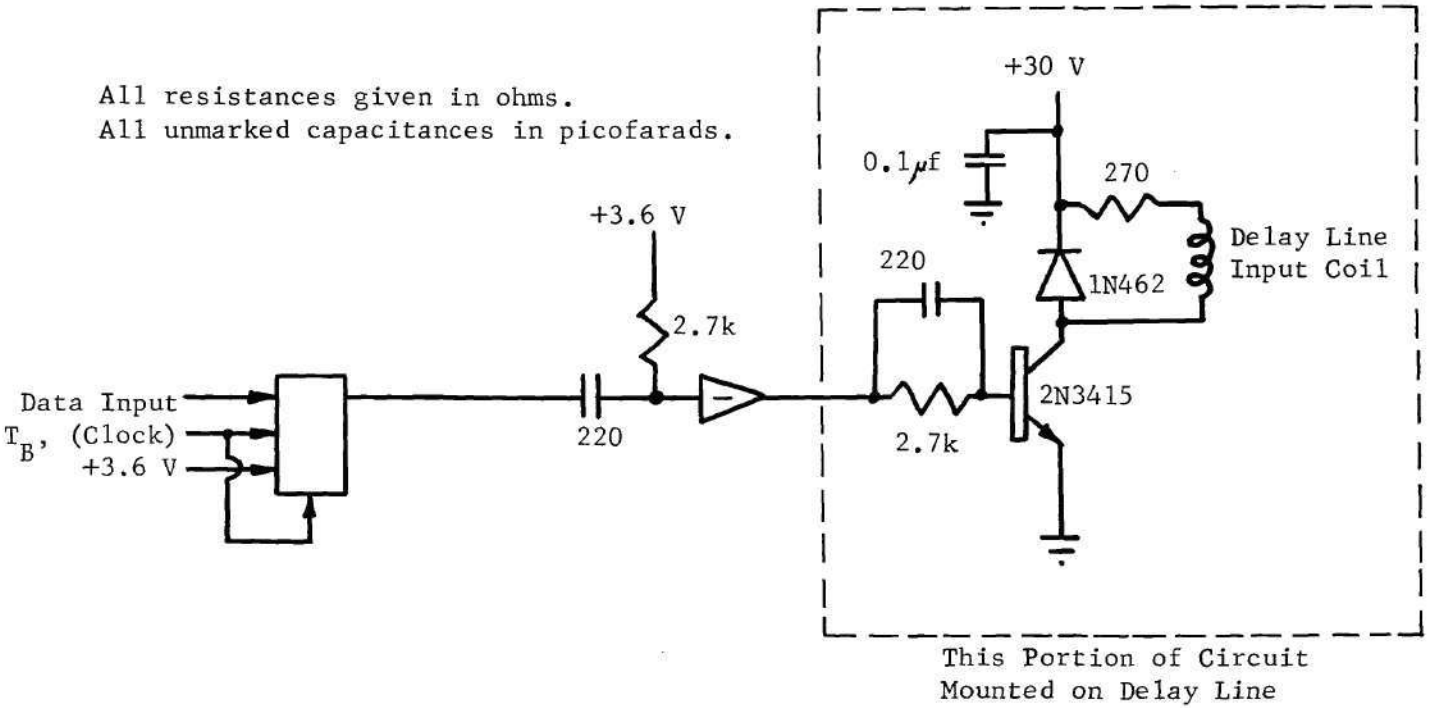

Figure 54. Delay Line Driving Circuitry

put coil of the delay line. The reverse-biased diode placed across the delay line shorts out the reverse voltage spikes that are associated with turning off the current pulse flowing through the inductive driving coil.

The current pulse at the input produces a magnetic deflection of the wire delay line. This deflection propagates along the line and, two milliseconds later, induces a small voltage pulse in the output sensing coil. This output pulse has an amplitude of approximately twelve millivolts. The output sensing circuitry amplifies this output signal and then, by using an analog comparator, determines whether the output was a logical one (a pulse is present) or a logical zero (no pulse present). This output sensing circuitry is shown in Figure 55. The threshold used by the analog comparator is adjusted for reliable operation of the delay line memory prior to the use of the prototype.

The output information is resynchronized with the bit-time clock by the output flip-flop. This information is then recirculated through the delay line for storage.

The Ladder Decoder

The circuit diagram of the ladder decoder that is used for digital-to-analog conversion by the prototype is shown in Figure 56.

The Crystal-controlled Clock Oscillator

The circuit diagram of the crystal-controlled clock oscillator that is used by the prototype is shown in Figure 57.

The Sample-and-hold Circuit

The circuit diagram of the sample-and-hold circuit that is used in

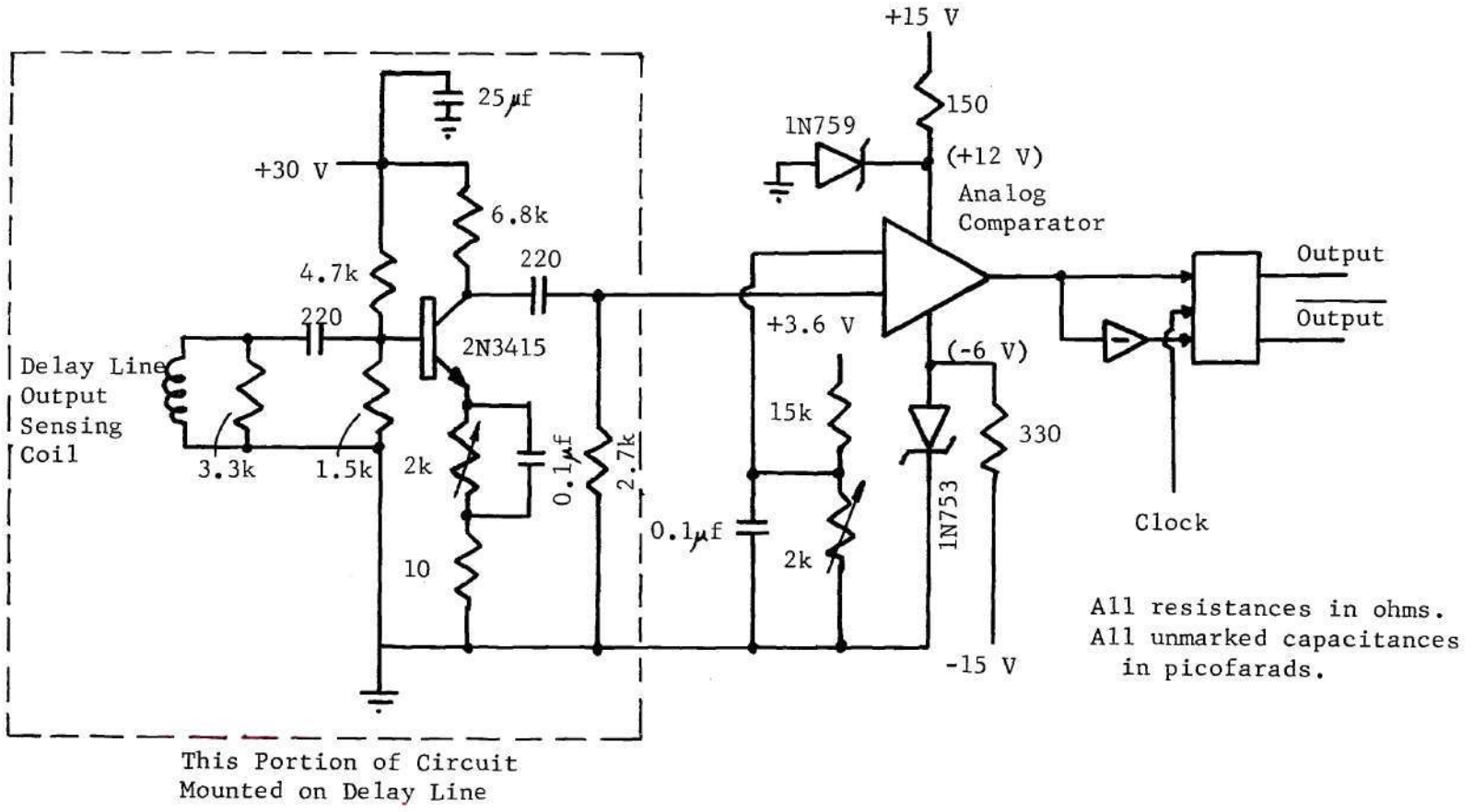

Figure 55. Delay Line Sensing Circuitry

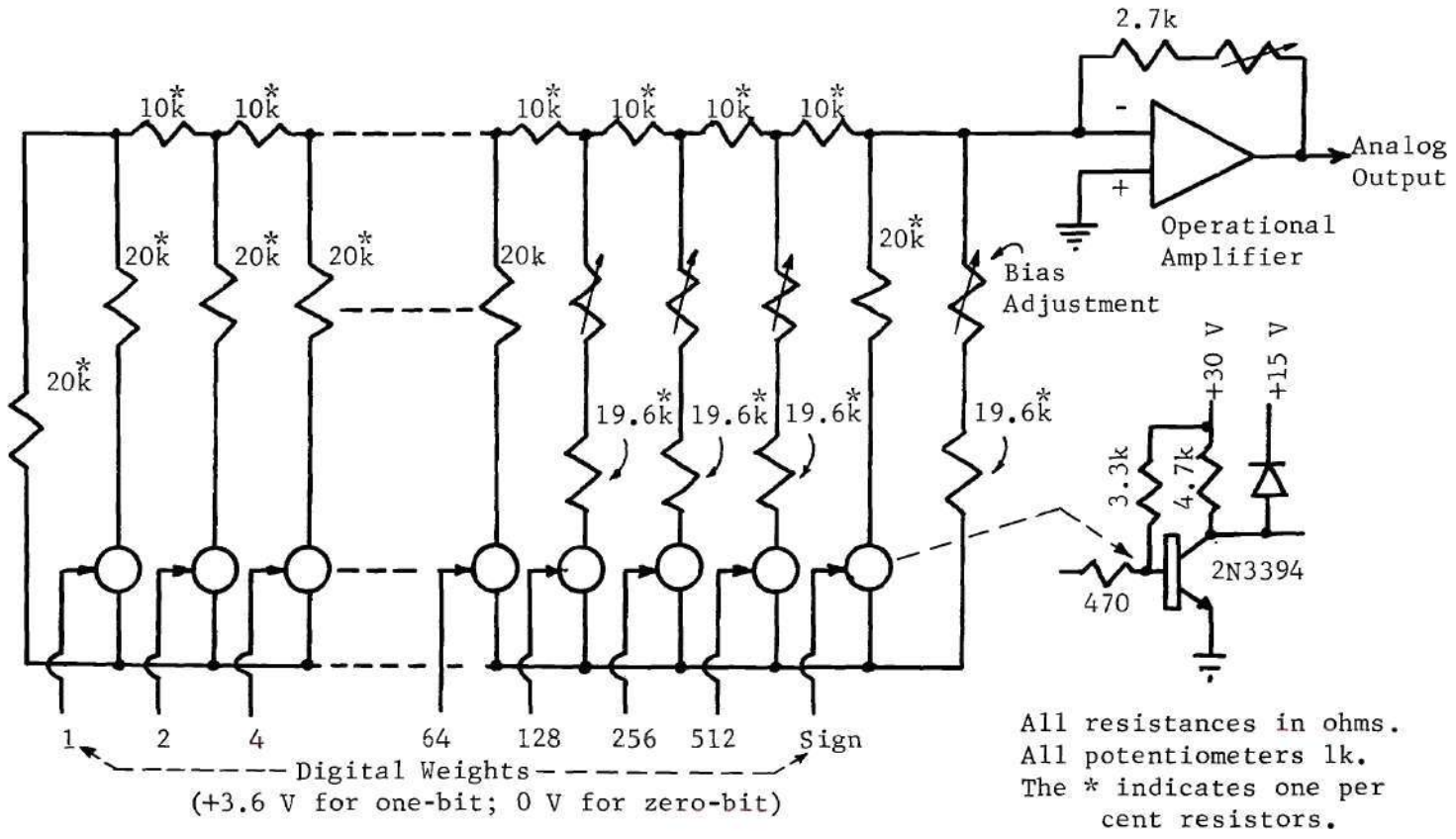

Figure 56. Circuit Diagram of the Ladder Decoder

All resistances in ohms.
All unmarked capacitances in picofarads.

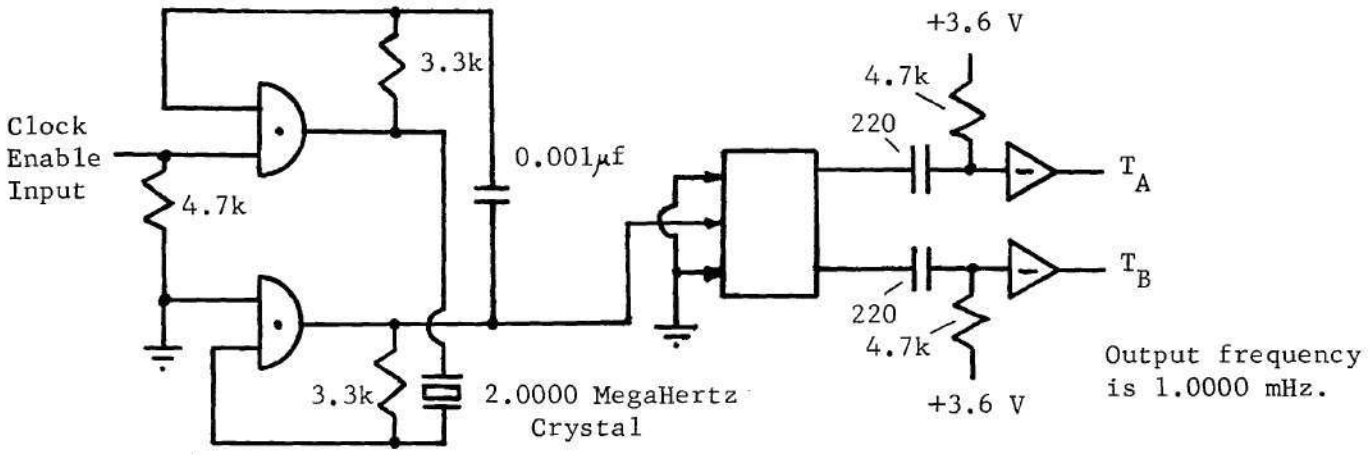

Figure 57. Circuit Diagram of Crystal-controlled Clock Oscillator

the output display portion of the prototype is shown in Figure 58.

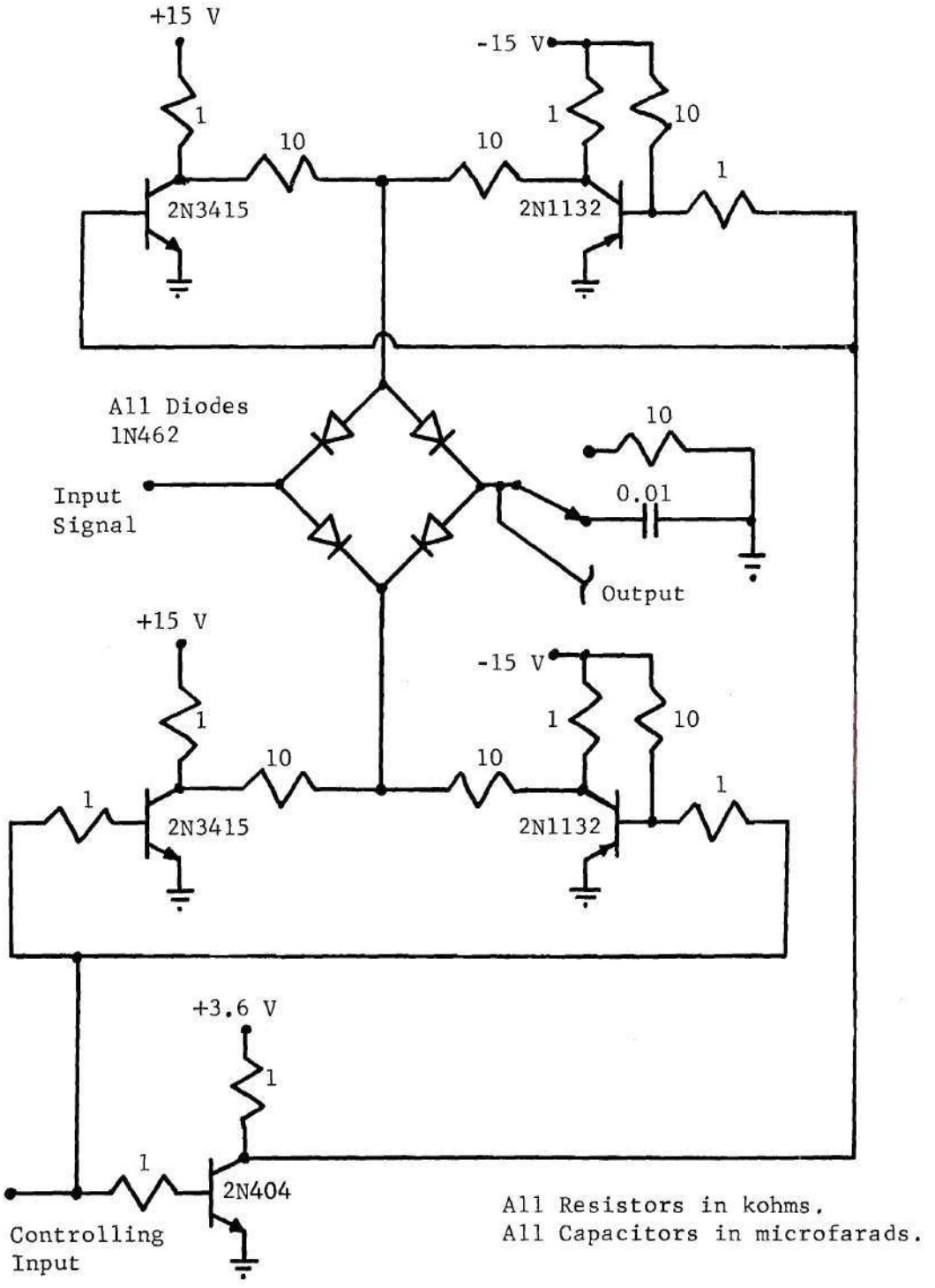

Figure 58. Sample-and-hold Circuit used by the Prototype

BIBLIOGRAPHY

Literature Cited

1. S. D. Larks, "Electronic Aids to the Service of Obstetrics: Electrohysterography and Fetal Electrocardiography," IRE Wescon Convention Record, Part 5, pp. 216-229, 1958.

2. S. D. Larks, and Golda Larks, "Normal Fetal Electrocardiogram, Statistical Data and Representative Waveforms," American Journal of Obstetrics and Gynecology, Vol. 90, No. 8, pp. 1350-1354, December 15, 1964.

3. S. D. Larks, Personal communication, May 11, 1967.

4. Edward H. Hon, "Noise Reduction in Fetal Electrocardiography. III. Instrumentation Problems," Medical Arts and Sciences, Vol. 18, pp. 63-66, 1964.

5. Edward H. Hon, and O. W. Hess, "Instrumentation of Fetal Electrocardiography," Science, Vol. 125, pp. 553-554, March 22, 1957.

6. Graham Schuler, "An Additive Fetal ECG," Proceedings of the 17th Annual Conference on Engineering and Biology, Vol. 6, p. 121, 1964.

7. C. Sureau, and R. Trocellier, "Quelques problèmes techniques d'electrocardiographie médicale," Digest of the 1961 International Conference on Medical Electronics, p. 3, 1961.

8. Edward H. Hon, "Fetal Electrocardiography," Anesthesiology, Vol. 26, No. 4, pp. 477-486, July-August, 1965.

9. Andrew G. Favret, and Alfred F. Caputo, "Evaluation of Autocorrelation Techniques for Detection of the Fetal Electrocardiogram," IEEE Transactions on Bio-medical Engineering, Vol. BME-13, No. 1, pp. 37-43, January, 1966.

10. E. H. Hon, and S. T. Lee, "Averaging Techniques in Fetal Electrocardiography," Medical Electronics and Biological Engineering, Vol. 2, pp. 71-76, March, 1964.

11. Franklin Offner, and Brian Moisand, "A Coincidence Technique for Fetal Electrocardiography," AJOG, Vol. 95, No. 5, pp. 676-680, July 1, 1966.

12. D. C. Amoss, et. al., "Modified Method for On-line Extraction of Fetal Electrocardiograms," Proc. of 19th Ann. Conf. on Eng. in Med. and Bio., November 17, 1966, p. 250.

13. J. H. van Bemmel, and H. van der Weide, "Detection Procedure to Represent the Foetal Heart Rate and Electrocardiogram," IEEE Tran. on Bio-med. Eng., Vol. BME-13, No. 4, pp. 175-182, October, 1966.

14. William A. Welch, "Matched Filter Processing of Fetal Electrocardiograms," Electrical Engineering Research Review, Catholic University of America, No. 4, pp. 46-48, June, 1965.

15. E. H. Hon, and S. T. Lee, "The Signal-to-noise Ratio in Fetal Electrocardiography," Proc. of 16th Ann. Conf. on Eng. in Med. and Bio., pp. 130-131, 1963.

16. Alan R. Kahn, and Stephen Koller, "Effects of the Fetal-Maternal Interface on the Fetal Electrocardiogram," Proc. of 19th Ann. Conf. Eng. in Med. and Bio., p. 136, November, 1966.

Other References

Bodo, Joseph, "Real-time Improvement of FECG Signals," Proc. of 16th Ann. Conf. on Eng. in Med. and Bio., Vol. 5, pp. 132-133, 1963.

Favret, A. G., "Autocorrelation Techniques Applied to the Fetal Electrocardiogram," Digest of the 1961 International Conference on Medical Electronics, p. 5, 1961.

Favret, A. G., "Fetal Signal Enhancement Through Successive Computer Processing," Proc. of 16th Ann. Conf. on Eng. in Med. and Bio., Vol. 5, pp. 128-129, 1963.

Favret, A. G., "Waveforms of the Fetal Electrocardiogram from Abdominal Leads," Proc. of 18th Ann. Conf. on Eng. in Med. and Bio., Vol. 7, p. 139, 1965.

Favret, A. G., and A. F. Caputo, "Application of Computer Techniques to the Fetal Electrocardiogram," Biomedical Sciences Instrumentation, Vol. 1, pp. 317-320, 1963.

Goddard, B. A., et. al., "A Clinical Foetal Electrocardiograph," Medical and Biological Electronics, Vol. 4, No. 2, p. 159, March, 1966.

Hon, E. H., and S. T. Lee, "The Fetal ECG. I. The Electrocardiogram of the Dying Fetus," AJOG, Vol. 87, pp. 104-109, 1963.

Hon, E. H., and S. T. Lee, "The Fetal ECG. II. Measuring Techniques," Obstetrics and Gynecology, Vol. 24, No. 1, pp. 6-12, 1964.

Hon, E. H., and S. T. Lee, "The Fetal ECG. III. Display Techniques," AJOG, Vol. 91, pp. 56-60, January 1, 1965.

Kahn, Alan R., "Transmission Characteristics in Fetal Electrocardiography," Proc. of 16th Ann. Conf. on Eng. in Med. and Bio., Vol. 5, pp. 134-135, 1963.

Kendall, Benjamin, and David Farell, "Uses of Fetal Electrocardiography," American Journal of Nursing, Vol. 64, No. 7, p. 75, July, 1964.

Larks, Saul David, Fetal Electrocardiography, Charles C. Thomas, Publisher, Springfield, Illinois, 1961.

Lee, Y. W., Statistical Theory of Communication, John Wiley and Sons, Inc., New York, 1960.

Lepeschkin, Eugene, Modern Electrocardiography, Williams and Wilkins Co., Baltimore, 1951.

Mattingly, R. F., and S. D. Larks, "The Fetal Electrocardiogram, a New Research Tool," Journal of the American Medical Association, Vol. 183, No. 4, pp. 245-248, 1963.

Schmidt, D. A., et. al., "Evaluation of Fetal Electrocardiography," AJOG, Vol. 83, No. 4, pp. 464-469, 1962.

Shubeck, Frank, "Fetal Electrocardiography: A Survey," The University of Michigan Medical Center Journal, Vol. 30, No. 1, pp. 19-20, January-February, 1964.

Walden, W. D., and S. J. Birnhaum, "Fetal Electrocardiography and Cancellation of Maternal Complexes," AJOG, Vol. 94, pp. 596-598, February 15, 1966.

Whitfield, Charles R., "A Source of Diagnostic Error in Fetal Electrocardiography," AJOG, Vol. 95, pp. 669-675, 1966.

VITA

Vernon Thomas (Tom) Rhyne, the son of Vernon and Elizabeth Rhyne, was born in Gulfport, Mississippi, on February 18, 1942. He attended La Marque High School, La Marque, Texas, graduating in June, 1959. He then entered Mississippi State University, receiving a B.S. in Electrical Engineering with Special Honors in June, 1962. He married Glenda Ruth Pevey of Brookhaven, Mississippi, in June, 1961.

Following his graduation, he was employed as an AeroSpace Technologist in the Data Systems Branch of the National Aeronautics and Space Administration's Langley Research Center, Hampton, Virginia. While at Langley, he earned an M.E.E. from the University of Virginia under the Langley Advanced Training Program. In September, 1965, he took educational leave from NASA to begin graduate studies at Georgia Institute of Technology, where he worked as a graduate teaching assistant and an Instructor in the School of Electrical Engineering. He also was a consulting engineer to the Lockheed-Georgia Research Center, providing assistance in the digital design of automated psychological testing equipment. In 1966 Mr. Rhyne received his Professional Engineering Registration. Following his graduation, he will be employed as an Assistant Professor at Texas A and M University.